UNIVERSITA' DEGLI STUDI DI VERONA

DEPARTMENT OF
Biotechnology

GRADUATE SCHOOL OF
Natural Sciences and Engineering

DOCTORAL PROGRAM IN
Biotechnology

CYCLE XXIX

TITLE OF THE DOCTORAL THESIS

Characterization of plant carbonic anhydrases involvement in nitric oxide production from nitrite and NO-regulated genes during hypersensitive cell death

S.S.D. AGR/07

Coordinator: Prof. Massimo Delledonne

Tutor: Prof. Diana Bellin

Doctoral Student: Ruitao Liu

Abstract

Since the discovery that NO plays a crucial role in mediating plant defense response in the late nineties, extensive research over the past 20 years revealed that NO is acting as a mediator in plant growth and development, as well as coping with biotic and abiotic stresses. However, both NO biosynthesis and NO downstream signaling during the hypersensitive response triggered by an avirulent pathogen still need further clarification.

Two routes for NO production in plants are known, the oxidative pathway and the reductive pathway. To date, the reductive route from nitrite is the most firmly described. NR can produce NO from nitrite but the physiological relevance of this activity is unclear. Furthermore, exogenous nitrite supply to an NR deficient mutant demonstrates that other routes for NO production from nitrite should exist in plants. Interestingly, it was reported that bovine carbonic anhydrase II, an alpha type CA, can convert nitrite to NO. Moreover, additional literature reports suggested the involvement of carbonic anhydrases belonging to the beta family of plant CAs in immunity. Therefore, the first aim of this work was to explore the possible involvement of plant carbonic anhydrase enzymes in nitric oxide synthesis during the HR. Firstly, we tried to explore the NO producing activity of AtαCA2, an Arabidopsis enzyme belonging to the same family as the bovine CA, which expression was induced by pathogen. We found that this protein requires glycosylation for its activity and localizes to plant thylakoids. Unfortunately, the transient expression in plant system, which yielded a properly glycosylated protein, led to low protein expression not enough to verify its NO production activity. Alternative production system should be eventually considered. Two representatives of β and γ type carbonic anhydrases were also cloned, expressed and purified. As expected, tobacco βCA1 showed high carbonic anhydrase activity, and Arabidopsis γCA2 showed no detectable carbonic anhydrase activity. However, these proteins were not able to catalyze the nitrite conversion to NO.

In the second part of this work, we enquired the NO downstream signaling, focusing on transcriptomic changes associated to NO induced cell death. A massive

transcriptomic rearrangement was found to be associated to the NO induced plant cell death. The functional class response to stimuli was strongly enriched in the differentially expressed genes modulated by NO. Moreover, we found a large modulation in signaling and transcription factors. Genes encoding for proteins involved in protein degradation or metabolism of nucleic acids were induced, while genes involved in anabolic processes were down-regulated. Importantly we confirmed that NO treatment leads to a massive metabolic reprogramming, which specially affects lipid metabolism. Finally, among induced genes the enrichment in genes previously found to be involved/associated to cell death confirmed that chosen conditions were adequate to select for genes involved in cell death activation and execution during the HR.

Abbreviations

aa Amino acid
ARC Amidoxime Reducing Component
bp Base pairs
BSA Bovine serum albumin
℃ Degree Celsius
CA Carbonic anhydrase
cDNA Complementary DNA
cGMP Cyclic guanosine monophosphate
DMSO Dimethylsulfoxid
DEGs Differentially expressed genes
EDTA Ethylendiaminetetraacetic acid
ETI Effector-triggered immunity
Endo H Endoglycosidase H
GSNO S-nitrosylated glutathione
GSNOR GSNO reductase
H_2O_2 Hydrogen peroxide
HR Hypersensitive response
kDa Kilo dalton
l Liter
M Molar
MAPKs mitogen-activated protein kinases
mg Milligram
min Minute
mL Milliliter
mM Millimolar
MW Molecular weight
µL Microliter
µM Micromolar
NO Nitric oxide
NOS Nitric oxide synthase
NR Nitrate reductase
NiR Nitrite reductase
$ONOO^-$ Peroxynitrite
ORF Open reading frame
PAMPs Pathogen-associated molecular patterns
PCR Polymerase chain reaction
PR Pathogen-related protein
PRRs Pattern recognition receptors
PTI PAMP triggered immunity
ROS Reactive oxygen species
rpm Rotations per minute

sec Second
SDS Sodium dodecyl sulfate
sGC Soluble guanylate cyclase
SNP Sodium nitroprusside
O_2^- Superoxide
TE Tris-EDTA

Index

1. Introduction

1.1 The plant immunity system

Plants are engaged in a continuous struggle with their pathogens to survive. Plant pathogens include a variety of microbes such as bacteria, fungi, oomycetes, nematodes and aphids (Jones and Dangl, 2006; Dodds and Rathjen, 2010). According to their lifestyles, phytopathogens can be classified as biotrophs, hemi-biotrophs and necrotrophs (Glazebrook, 2005). Biotrophic pathogens feed on living host tissues to get nutrients, while the necrotrophic pathogens take nutrients from dead or dying cells. Hemi-biotrophs, can be biotrophic or necrotrophic pathogens, depending on the stages of their life cycle or infection process. Among hemi-biotrophs is the bacterial pathogen *Pseudomonas syringae* (Glazebrook, 2005; Xin and He, 2013). The interactions between *Arabidopsis thaliana* / *Pseudomonas syringae* have been widely used as a model for characterizing plant / pathogen interactions and deciphering the molecular mechanisms of plant disease resistance and pathogen virulence (Quirino and Bent, 2003). Plant-pathogen interactions can be classified as compatible or incompatible interactions. Compatible interactions take place in susceptible hosts which are not able to recognize the pathogen effectors. In this case the pathogen is virulent. By contrast, incompatible interactions involve recognition of pathogen effectors by resistance genes, in this case the pathogen is called avirulent pathogen (Glazebrook, 2005).

The first layer of defense against microbes is a passive defense constituted of constitutive defense systems. Plants can defend themselves from pathogen by preformed physical barriers such as the cuticle, and inhibit pathogen growth by production of antimicrobial compounds. The cuticle which is composed of cutin and waxes is the outer structures of the epidermis of the land plants (Yeats and Rose,2013). Usually, constitutive defense can defeat the invasion of the majority of pathogens, however, few successful pathogens can reach extracellular space by natural openings such as stomata or wound sites (Melotto et al., 2008).

Plants, unlike mammals, lack specialized mobile immune cells and a somatic adaptive immune system. However, they have the capability of establishing innate immunity, and launching systemic acquired immunity responses upon perception of signals from local infection sites (Gohre and Robatzek, 2008). The classical view of plant innate immunity is depicted by the so-called zigzag model introduced by Jones and Dangl (2006). This model proposes two lines of active defense. The first line of active plant defense is triggered by pattern recognition receptors (PRRs), cell surface receptors that recognize highly conserved molecules within a class of microbes, called pathogen-associated molecular patterns (PAMPs), and activate the so-called PAMP triggered immunity (PTI). Successful pathogens are able to overcome PTI by means of secreted effectors that suppress PTI responses. Pathogenic bacteria typically inject such effectors directly into the host cytoplasm through their type III secretion machinery. During evolution, plants have responded to these effectors with the development of cytoplasmic R-proteins that recognize single effector thus activating a second line of active, much stronger and robust plant defense response, the so called effector-triggered immunity (ETI), which often involves the hypersensitive response (HR), a type of programmed cell death.

However, we should also mention that accumulating evidence shows now that not all microbial defense activators conform to this distinction between PAMPs and effectors, thus this classical division has become hazy (Thomma et al., 2011). Therefore, the classical two layer model of plant immunity is recently evolving to a much modern view in which there is rather a continuum between PTI and ETI. ETI and PTI could be both robust or weak, depending on the specific interaction and possibly also environmental conditions. In a recent review an attempt of classifying R-proteins activating defense according to different mechanisms has also been provided (Kourelis et al., 2018)

1.1.1 PAMP-triggered immunity

According to the classical view of the plant innate immunity, the first line of active defense involves recognition of the conserved microbial elicitors called pathogen associated molecular patterns (PAMPs) by plasma membrane-localized pattern recognition receptors (PRRs). PAMPs are typically essential conserved components of whole classes of pathogens, such as lipopolysaccharides, bacterial flagellin and fungal chitin (Boller and Felix, 2009, Macho and Zipfel, 2014). PRRs include transmembrane receptor kinases and transmembrane receptor-like proteins (Zipfel et al.,2008). There are 610 receptor kinase genes and 57 receptor-like proteins in *A.thaliana* (Dodds and Rathjen, 2010) in contrast to the situation in animals, which own 12 Toll-like receptors (Gay and Gangloff, 2007). This huge number of PRRs in plants greatly enhanced the adaptation ability of plants to biotic stress. One of best characterized PRRs is the *A.thaliana* receptor kinase FLAGELLIN SENSING 2 (FLS2) (Figure 1, Dodds and Rathjen, 2010), which directly binds flagellin (step a). After perception of flagellin, FLS2 rapidly forms a complex with the leucine rich repeat (LRR) receptor kinase BRASSINOSTEROID INSENSITIVE 1-ASSOCIATED KINASE 1(BAK1) (step b). The interaction of FLS2 and BAK1 results in phosphorylation of both proteins (step c).

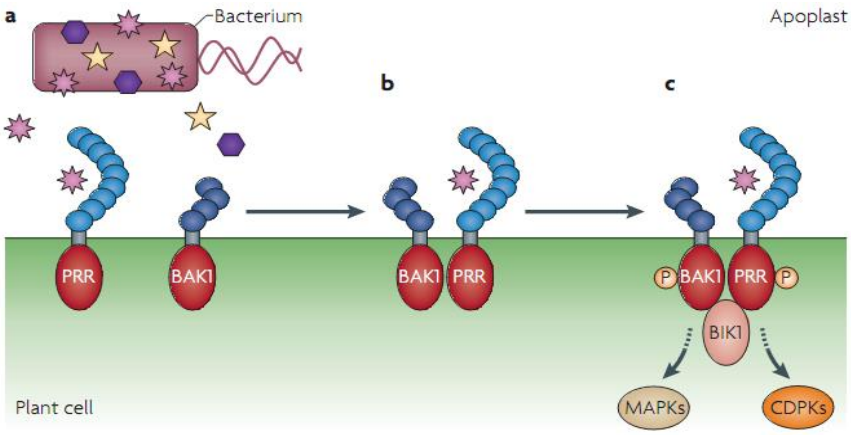

Figure 1. Model of recognition of flagellin by pattern recognition receptor (FLS2). Adapted from Dodds and Rathjen, 2010

The cytoplasmic protein kinase BOTRYTIS INDUCED KINASE 1(BIK1) , BAK1 and FLS2 form FLS2-BAK1-BIK1 complex, and transduce downstream signals by mitogen-activated protein kinases (MAPKs) or calcium-dependent protein kinases (CDPKs) (step c). The recognition of PAMPs by PRRs induces PAMP-triggered immunity (PTI). Its downstream responses include ion fluxes, oxidative burst, MAPK cascades, hormone signaling, transcriptional reprogramming, callose deposition,and stomatal closure (Nicaise et al.,2009, Bigeard et al.,2015).

1.1.2 Effector-triggered immunity

Adapted pathogens can deliver effectors into host cells to interfere with PTI, and promote pathogen virulence on susceptible plants. However, in resistant plants, the immune system uses Resistance (R) proteins to recognize the presence of specific pathogen effector proteins in host cells and induce a robust resistance response (Jones and Dang, 2006, Cui et al., 2015). Most R genes encode nucleotide-bingding leucine-rich repeat (NB-LRR) proteins, and there are about 160 R genes in Arabidopsis genome. Plant NB-LRRs are composed of a variable N terminus, a central nucleotide binding pocket (NB-ARC domain), and a C-terminal LRR domain. Most NB-LRRs can be classed into coiled-coil (CC) NB-LRR and Toll-interleukin-1 receptor (TIR) NB-LRR based on their N-terminal domain. The N-terminal domain decides the requirement for distinct downstream signaling components (Feys and Parker, 2000; Elmore et al., 2011). Enhanced Disease Susceptibility 1 (EDS1) and Non-race specific Disease Resistance 1 (NDR1) are required for activation of TIR-NB-LRRs and CC-NB-LRRs-mediated immune responses, respectively (Aarts et al.,1998). The best characterized NB-LRRs include *Arabidopsis* R-proteins RPM1, RPS2 and RPS5 , which specifically recognize *P. syringae* effectors AvrRpm1/AvrB, AvrRpt2 and AvrPphB, respectively. In most case, recognition of effectors by NB-LRR is not relied on direct interaction between NB-LRR and effector molecule but by an indirect mechanism (Shao et al.,2003, Axtell and Staskawicz,2003; Mackey

et al.,2002,2003., Chisholm et al.,2006). One of the best characterized effectors is Arabidopsis AvrRpm1 (in Figure 2). Plant pathogenic *Pseudomonas syringae* deliver effectors AvrB or AvrRpm1 into the host cells by type III secretion system (TTSS) encoded by hrp (hypersensitive response and pathogenicity) (Step 1). The presence of AvrB or AvrRpm1 is perceived by RIN4 and thus induces phosphorylation of RIN4 (Step 2). The Arabidopsis CC-NB-LRR protein Rpm1 monitors phosphorylation state of RIN4, and activates resistance reactions called ETI (Step 3) (Liu et al 2011, Li et al., 2014).

According to the classical view of plant immunity, the ETI response is quantitatively more prolonged and robust than PTI (Tsuda et al., 2010) and is often referred as hypersensitive response (HR). Importantly, one of the most visible phenotype in ETI is the rapid and localized programmed cell death triggered upon pathogen recognition at the infection site which aims to restrict pathogen growth and spread.

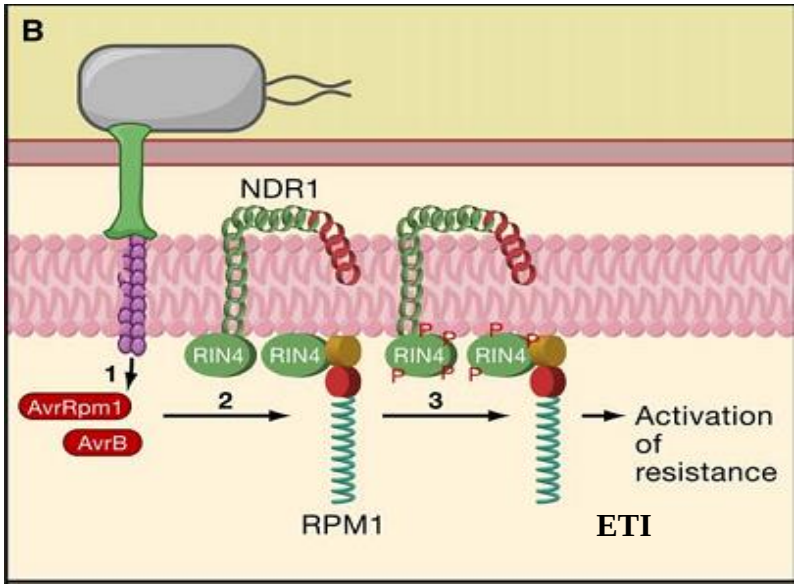

Figure 2. Model for AvrB/AvrRpm1 induced ETI.
Adapted from Chisholm, S.T et al., 2006

1.1.3 The hypersensitive response

The HR is typically triggered upon recognition of pathogen-encoded avirulence (Avr) protein by a cognate plant resistance (R) protein (Figure 3) and is often associated with a rapid localized programmed cell death at the site of infection in few hours following the pathogens infection (Mur et al.,2008; Coll et al.,2011). Besides, the HR is accompanied by the induction of a myriad of defence genes and the production of anti-microbial secondary metabolites such as phytoalexins finally triggering systemic acquired resistance (SAR) (Dangl and Jones,2001; Dixon, 2001; Truman et al.,2006). Depending on different plant-pathogen interactions, the outcome of HR can vary greatly in phenotype and timing at both macro and microscopic scales (Holub et al., 1994; Christopher-Kozjan and Heath, 2003; Krzymowska et al., 2007). Such variations are related with different infection strategies employed by the various types of pathogen, and reflect differences in underlying mechanism(s) of HR cell death. In any case it has been demonstrated that the occurrence of HR is dependent on active metabolism and protein synthesis (Belenghi et al., 2003, Mur et al.,2008).

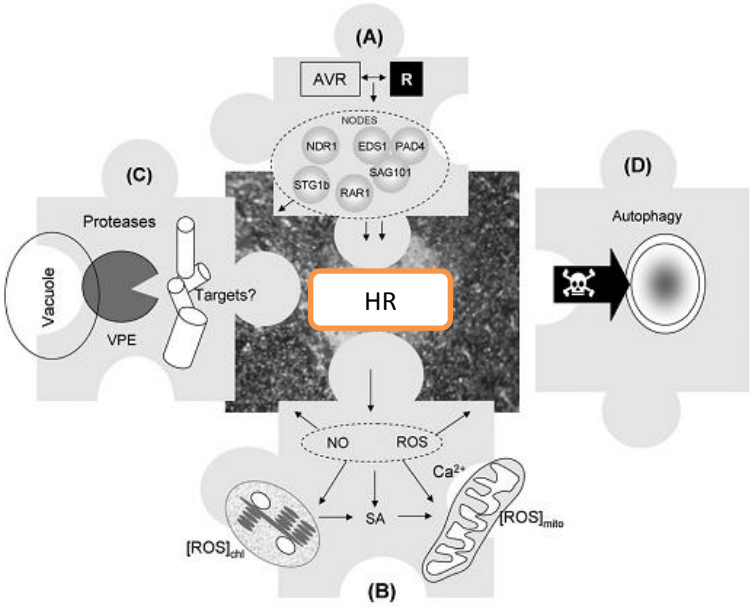

Figure 3. Jigsaw model of the hypersensitive response.
Adapted from Mur et al., 2008

A symphony of cytosolic signaling molecules (including $Ca^{(2+)}$), reactive oxygen species and nitric oxide among others) have been suggested as early components of HR signaling (Figure 3). However, specific interactions among these cytosolic messengers and their roles in the signal cascade are still unclear.

A leading signal following successful Avr and R proteins interaction is Ca^{2+}influx. A persistent rise in cytoplasmic calcium ($[Ca^{2+}]_{cyt}$) was observed indeed in Arabidopsis and cowpea during HR (Xu and Heath,1998; Grant et al.,2000) and application of calcium channel blocker, $LaCl_3$ suppressed avirulent bacteria induced cell death in soybean cultures (Levine et al.,1996). Moreover, application of the cyclic nucleotide gated channel (CNGC) blocker suppressed HR also in Arabidopsis and the Arabidopsis mutant *defense no death* (*dnd1*), mutated in CNGC showed abolished HR, demonstrating that a crucial role of calcium in HR cell death triggering (Clough et al., 2000; Ali et al., 2007).

Another typical signature during the early stages of many forms of HR is the triggering of an oxidative burst due to accumulation of reactive oxygen species (ROS) including superoxide (O_2^-) and hydrogen peroxide (H_2O_2) (Lamb and Dixon, 1997; Heath, 2000). Many studies reported involvement of NADPH oxidase activity for production of H_2O_2 in plant defence (Pugin et al., 1997; Simon-Plas et al., 2002; Torres et al., 2002; Torres and Dangl, 2005). Plant NADPH oxidases (RBOH) catalyse the reduction of dioxygen to O_2^- from the oxidation of NADPH. Then generated O_2^- is rapidly catalysed to H_2O_2 either enzymatically via superoxide dismutase (SOD) or/and non-enzymatically. *A.thaliana* genome contains 10 Rboh forms A-J (respiratory burst oxidative homologues), whose products are closely related to gp91phox homologues in mammalian phagocytes. Torres et al., (2002) reported that in *A. thaliana*, RbohD and RbohF are essential for the accumulation of ROS and for resistance during incompatible plant pathogen interaction. However, further evidences also showed the potential involvement of peroxidases or alternative systems including amine, diamine, and polyamine oxidases in the generation of H_2O_2

during the oxidative burst (Bolwell and Wojtaszek, 1997, O'Brien et al., 2012). The oxidative burst, however, depends both on ROS generation and degradation. Indeed to control ROS homeostasis, plant cells make use of an array of protective enzymatic and non-enzymatical mechanisms, as unwanted injuries may lead to cell death execution (Montillet et al., 2005; Van Breusegem et al., 2006; Laloi et al., 2006). H_2O_2 can be catabolized enzymatically either directly by catalases or/and indirectly by ascorbate peroxidases, peroxiredoxins, glutathione peroxidases and by heterogeneous group of guaiacol peroxidases (Dat et al., 2000). Moreover, non-enzymatic antioxidant molecules such as ascorbate, glutathione, tocopherol and carotenoids are also involved in adjusting intracellular content of ROS to harmless level (Dellapenna et al., 2006). The oxidative burst plays several roles in plant hypersensitive disease resistance response. H_2O_2 contributes to limit the pathogen colonization by acting directly on the pathogen as antibiotic agent (Peng and Kuc, 1992), or indirectly by helping to strengthen the cell wall via oxidative cross-linking of cell wall glycoproteins and/or by participating in the cell-signalling cascade leading to cell death (Lamb and Dixon, 1997; Bolwell et al., 1995). In support, Delledonne et al., (2001) reported that H_2O_2 (not O_2^-) plays a central role in potentiating pathogen-induced cell death during HR. Moreover, a reactive oxygen species contribution to establishment of the systemic acquired resistance has also been reported and studied (Wang et al., 2014).

Nitric oxide (NO) is another early signal molecule accumulating during HR (Delledonne, 1998, Chen et al., 2014). Transgenic plants expressing either bacterial nitric oxide dioxygenases or flavohaemoglobins showed reduced NO level and delayed HR, suggesting that NO plays a key role in the development of the HR (Zeier et al.,2004; Bocarra et al.,2005). During avirulent pathogen infection, the NO production in host cells is stimulated in a biphasic manner as was first demonstrated in a study done in tobacco and soybeans cells infected with incompatible *P. syringae* pv. *glycinea* and further confirmed in additional studies (Delledonne et al., 1998, Gupta et al., 2013, Chen et al., 2014). The first NO burst is short and happens in 1

hour after infection whereas the second burst lasting longer occurs at later stage of infection i.e. 4-8 hours after infection (Delledonne et al., 1998, Chen et al., 2014). The main source for NO production during plant defence response, however, is still largely unknown. Moreover, likewise ROS the NO burst also depends on enzymes involved in its homeostasis (paragraph 2.3). As previously mentioned, synergistic NO and H_2O_2 are required for the initiation of cell death (Delledonne et al., 2001; De Pinto et al., 2002). NO is an highly reactive molecule. Once produced it participates to signalling through its reactivity. Indeed, NO also affects signaling through direct reaction with proteins resulting in post-translational modifications which modulate protein function. Several studies addressed this and many examples of NO mediated post-translational modification leading to modulation of plant protein function and signaling during the HR have been now elucidated (see paragraph 3). Interestingly, it has been recently reported that NO also mediates post-translational modification of a bacterial effector protein and modifies its activity, thus also directly targeting and disarming pathogen effector proteins beside targeting and modulating plant proteins activity during the HR (Ling et al., 2017). Finally NO can induce plant defence gene expression such as phenylalanine ammonia lyase (PAL) and pathogenesis-related 1 (PR1) and therefore modulate plant gene expression and act through the activation of second messengers such as cGMP and cyclic ADP ribose (cADPR) (Durner et al., 2001; Vandelle et al., 2016).

Beside the described early signaling events HR implies execution related process (Figure 3). Plants lack close caspase homologs, but several studies using caspase-specific peptide inhibitors suggested the presence of caspase-like protease activities during plant HR (Lam et al.,2000; Rojo et al., 2004; Hatsugai et al.,2004, 2009). Plant metacaspases are thus suggested to be the ancestors of metazoan caspases, and plant metacaspases have previously been shown to be original cysteine proteases which auto-process in a manner similar to that of animal caspases. Their involvement in plant cell death execution during pathogen infection has been demonstrated. Indeed AtMC1, a type I *Arabidopsis* metacaspase containing a

conserved LSD1-like zinc finger motif interacts with LSD1, and is a positive regulator of cell death as its caspase-like activity is required for both superoxide-dependent cell death and HR mediated by an intracellular nucleotide-binding-leucine-rich repeat receptor (Coll et al., 2010). AtMC2 was also shown to positively regulate cell death (Watanabe and Lam, 2011). The vacuolar processing enzyme VPE in *Nicotiana benthamiana* and its homology VPE gamma in Arabidopsis show caspase-1-like activity during HR (Rojo et al., 2004; Hatsugai et al.,2004). VPE activity can lead to tonoplast rupture and thus cell death. However, the mechanism of activation of VPEs and their proteolytic targets are still unclear. Interestingly it was also shown that autophagic components contribute to HR cell death, but only to EDS1 dependent HR cell death conditioned by Toll/Interleukin-1(TIR)-type immune receptors (Hofius et al.,2009).

1.1.4 Nitric oxide functions during the HR

The first evidence showing NO production in plant cell and its involvement in plant immunity was reported by Delledonne et al., (1998). This work demonstrated that ROS are necessary but not sufficient to trigger host cell death and, as previously mentioned, that nitric oxide (NO) is produced during HR in a biphasic manner and cooperates with ROS in the activation of hypersensitive cell death. In a following study indeed it was demonstrated that a balance production of NO and H_2O_2 is required for the initiation of cell death (Delledonne et al., 2001). Furthermore, Durner et al., (1998), showed that NO once produced affects molecular responses during plant defence and therefore participates in plant disease resistance. More in detail they demonstrated that a high level of NOS-like activity is found in resistant tobacco plants under pathogen attack and they reported the induction of defence genes through NO. Accordingly, genetic approaches to scavenge NO in transgenic plants compromised the HR (Zeier et al.,2004; Bocarra et al.,2005).

Since then, several studies have addressed the key point of revealing how NO is produced and then translates its functions during the HR. An overview of the outcome of these studies concerning either the mechanisms involved in NO production during the HR, or its detailed signalling following its accumulation will be provided in the following paragraph 1.2 and paragraph 1.3. However, despite all these efforts, the NO production mechanism in plant during HR remains elusive and some aspects of NO signalling during HR also expect further elucidation.

1.2 Routes for NO synthesis during the HR

The first demonstration that plant cell can produce NO was that previously mentioned in the field of plant immunity. However, NO is produced by plant cell in many contexts and is widely recognized now as a key molecule in various plant physiological processes (Corpas and Barroso, 2015). Still, how NO is synthesized in plant cell in the different context is partially elusive and a better understanding of these mechanisms would greatly benefit our studies on NO functions in plant growth, development and defense against adverse environmental conditions (Corpas and Barroso, 2015). Biochemically, two routes for NO production can be considered, an oxidative pathway and a reductive pathway (Moreau et al., 2010).

1.2.1 The oxidative pathways for NO synthesis

In animal cells, NO is mainly produced by the oxidative pathway even though the existence of a reductive pathway has been also recently reported (Maia and Moura 2015). In the oxidative NO production pathway, the amino acid arginine is oxidized by nitric oxide synthase (NOS) into citrulline and NO in an oxidoreductase reaction using NADPH as an electron donor, O_2 as a co-substrate, and (6R-)-5,6,7,8-tetrahydrobiopterin (BH4), FAD, FMN, and calmodulin (CaM) as

cofactors (Forstermann and Sessa, 2012). The existence of NOS in plant, however, is still an unsolved mystery. Experimental evidences support the existence of arginine-dependent NO production activity in plants (Corpas et al., 2009). Indeed, first evidence of NO involvement in plant disease resistance and in defense gene induction relied on the application of mammalian NOS inhibitors such as PBITU (S,S0-1,3-Phenylene-bis (1,2-ethanediyl) -bis-isothiourea, L-NAME (NG-Nitro-L-arginine methyl ester), L-NMMA (NG-Mono-methyl-L-arginine) (Delledonne et al., 1998; Durner et al., 1998). However, we know today that these inhibitors which are mainly arginine analogs competing for the active site of the enzyme suffer of not high specificity (Astier et al., 2017). Nevertheless, arginine-dependent NOS-like activity assay detected a NOS-like activity in various plant tissues and organelles such as mitochondria, chloroplasts, peroxisomes and was suggested to be involved in plant development and response to abiotic and biotic stresses (Corpas et al., 2006; Rodriguez-Serrano et al. 2006; Besson-Bard et al. 2008; Wang et al., 2009; Besson-Bard et al. 2009; De Michele et al.2009; Asai and Yoshioka 2009;). These studies strongly indicated that plants may have a NOS-like enzyme (Corpas et al., 2009). However, it is worth noting that plant cell extracts, differently from animal extracts, contain another arginine-dependent activity that could convert arginine to arginosuccinate. Therefore, a reliable NOS activity assay in plants should always include the verification of citrulline production and NO production (Tischner et al.2007).

During the past two decades, great efforts have been put in searching plant NOS. The first reported pathogen-inducible nitric oxide synthase (iNOS) was a variant isoform of the P protein of the glycine decarboxylase complex, isolated through the biochemical purification of a NOS-like activity from kilograms of tobacco leaves (Chandok et al., 2003). Unfortunately, the NOS activity of this iNOS enzyme was not further confirmed in following studies and finally the publication was retracted (Klessig et al., 2004). Meanwhile, through sequence similarity to a hypothetical snail NOS, Guo and colleagues (2003) retrieved a putative Arabidopsis NOS gene, the

corresponding mutant of which, *AtNOS1,* was defective in NO accumulation. However, it was later shown that the AtNOS per se don't produce NO directly but might affect the NO accumulation and or induction. Indeed, AtNOS encodes a circularly permuted GTPase, not a true NOS, therefore, AtNOS was renamed as AtNOA1 (NO-associated protein 1) (Moreau et al.,2008). AtNOA1 belongs to a family of circularly permuted GTPase containing RNA/ribosome binding domains and can hydrolyze GTP to GDP. Overexpression of the AtNOA1's bacterial homolog YqeH complemented the phenotype defect of *atnoa1* mutant and suggested that AtNOA1 function by binding RNA/ribosomes and is required for ribosome functioning (Gas et al., 2009). Therefore, defective NO production in loss-of-function mutants is an indirect effect of interfering with normal plastid functions demonstrating that plastids play an important role in regulating NO levels in plant cells (Moreau et al.,2008). Nevertheless, this mutant is widely used in studies of NO function in plant. In addition to these unsuccessful reports about plant NOS, a study based on a proteomic approach to identifying NOS proteins using mammalian NOS antibodies as indicator obtained candidate proteins that displayed no similarities with animal NOS and no NOS activity (Butt et al., 2003).

However, much recently, in the unicellular marine alga *Ostreococcus tauri*, an OtNOS has been finally characterized with sequence similarity to human NOSs (Forest et al., 2010). OtNOS has the oxygenase and reductase domains of mammalian NOS and could bind all the cofactors of typical mammalian NOS including heme, H4B, NADPH, FMN and FAD (Foresi et al., 2010). The activity of OtNOS can be inhibited by mammalian NOS inhibitor like the inactive Arg analog L-NAME and the Ca^{2+}/CaM was not necessary for enzymatic activity of OtNOS (Foresi et al., 2010). As bacterial NOS-like proteins, both pterin tetrahydrofolate (THF) and H4B can be used by OtNOS as cofactors *in vitro* and *in vivo*. So OtNOS possibly use THF as cofactor in plant instead of H4B which is not present in plant cells (Foresi et al.,2015). The transgenic OtNOS plants, in which *OtNOS* gene expression was under the control of a abiotic stress responsive promoter, accumulated higher NO level compared with the

empty vector transformants and showed enhanced abiotic stress tolerance and increased stomatal development (Foresi et al.,2015). However, this first discovery of a canonical NOS from the plant kingdom in algae, was not followed by the discovery of similar NOS in land plants. Remarkably, a recent work aiming to search for transcripts encoding NO-like proteins using data set generated by the 1000 plants (1kP) international consortium and publicly available plant genomes database highlighted 15 complete sequences presenting enough similarity to be identified as NOS, all belonging to algal species. However, this study failed to identify a canonical NOS sequence from land plants. Therefore, it is likely that the NOS gene was transmitted from a common ancestor to plant and was later lost in land plants, the NOS from algae being the remaining testimony of these events (Jeandroz et al., 2016; Santolini et al., 2017).

Alternative NO production via oxidative pathway includes polyamines and hydroxylamine-mediated NO formation (Gupta et al., 2010). Arginine can be used as substrate for synthesis of polyamines, such as spermine and spermidine. Increased supply of these polyamines to Arabidopsis seedlings rapidly provoked NO production in the elongation zone of root tip and the veins and trichomes of primary leaves (Tun et al., 2006). The arginase enzyme can regulate arginine concentration in plant cells, and a reduction in arginase activity increased NO production and *vice versa* (Flores et al., 2008). Furthermore, NO production in plants was recovered when spermine was exogenously provided, suggesting the polyamine may be involved in the NO synthesis (Yamasaki and Cohen, 2006). Recently, an higher arginase activity impacting the arginine pool was found to be responsible for the impaired NO production and developmental phenotype observed in the *A. thaliana* mutant for the copper amine oxidase 8 (CuAO8), an enzyme involved in polyamine (PA) catabolism (Gross et al., 2017). All these findings support the relevance of the oxidative pathway for NO production in plant. Besides, significant increase in NO emission was detected in NR-deficient tobacco cells supplied with exogenous hydroxylamine under aerobic conditions, supporting the possibility that hydroxylamine can be converted to NO

(Rumer et al.,2009) , but NO emission rate is much lower than that triggered from NR and mitochondrial electron transport chain (Gupta et al., 2010). However, the biochemical mechanisms by which polyamines and hydroxylamine-mediate NO production are unclear, and their physiological significance in context of hypersensitive response awaits further exploration.

1.2.2 The reductive pathways for NO synthesis

Nitrite is currently considered as the main source for NO production in plants by the reductive pathways for NO synthesis (Santolini et al., 2017). First of all, reduction of nitrites to NO can occur non-enzymatically in particular conditions, such as low pH or highly reducing environments, when high concentrations of nitrate are present, but these conditions are rarely encountered (Bethke et al.,2004). Furthermore, several enzymes or cellular complex components have been identified as sources for NO production using nitrite as substrate (Gupta et al., 2010; Moreau et al., 2010).

1.2.2.1 Nitrate reductase

The cytosolic enzyme nitrate reductase (NR) catalyzes the reduction of nitrate to nitrite using NADH as electron donor. Besides that, NR can also catalyze the conversion of nitrite to NO *in vitro* and *in vivo* through the side-reaction $NADH+3H_3O^+ +2NO_2^- \rightarrow NAD^+ +2NO +5H_2O$ (Yamasaki and Sakihama, 2000; Rockel et al., 2002). However, *in vivo* the efficiency of NR catalyzed nitrite reduction to NO is estimated to be only 1% of its nitrate-reducing activity (Rockel et al., 2002; Plantchet et al., 2005). However, this reaction can be promoted by specific conditions such as anoxic or acidic environments. Arabidopisis has two homologous genes (*Nia1* and *Nia2*) encoding NR (Wilkinson and Crawford, 1993). The NR-deficient *nia1nia2* double knock-out mutants showed reduced levels of both nitrite and NO, while the nitrite reductase (NiR) antisense tobacco lines accumulated higher level of nitrite and NO (Modolo et al., 2006; Morot Gaudry-Talarmain et al., 2002). However, due to

reduction of nitrite to ammonia by the plastidic NiR, the nitrite concentration is usually low in contrast to nitrate under normal growth conditions. In addition, nitrate is a potent competitive inhibitors of the nitrite reductase activity of NR, and the Km of NR for NO_2^- is relatively high compared to NO_3^- (Yamasaki and Sakihama, 2000). All this suggest that the nitrite reductase activity of NR is very low compared to its nitrate reductase activity (Meyer et al.,2005). Nevertheless, nitrite based NO production was shown to be involved in various physiological processes and environmental stimuli (Gupta et al., 2010). Moreover, exogenously supplied nitrite to Arabidopsis mutant *nia1nia2* rescues its compromised NO production and disease resistance phenotype, suggesting that other routes than NR for NO formation from nitrite in plants should exist (Modolo et al. 2006; Oliveira et al. 2009). Interestingly, in *Chlamydomonas reinhardtii*, the Amidoxime Reducing Component (ARC) protein and NR have been recently shown to constitute a dual enzymatic systems (Chamizo-Ampudia et al 2016, 2017). In this systems, ARC displays a high affinity for NO_2- and reduces NO_2- to NO *in vitro* and *in vivo* by using electrons supplied by the diaphorase activity of NR. Because this complex can function in the presence of high NO_3^- concentrations and in normoxia, differently from NR alone, the presence and formation of this complex also in higher plants could possibly explain the contradictory findings about NR activity and its involvement in NO production through the reductive pathway and deserve therefore further investigation.

1.2.2.2 Alternative enzymes for nitrite-dependent NO production

In addition to plant NR, a plasma membrane (PM)-bound nitrite:NO reductase can reduce nitrite to NO. This activity reported in membrane fraction of tobacco roots showed to be comparable the NO producing ability of NR, but was insensitive to cyanide and anti NR-IgG. Thus, it is expected to be due to an independent enzyme different from PM-NR and may produce NO from nitrite in apoplastic space (Stohr et al.,2001; Stohr and Stremlau 2006). However, this activity was only found in roots,

while was not reported in leaves (Stohr et al.,2001) and appears therefore not relevant for the NO production in HR.

Mitochondrial electron transport chain is also capable of reducing nitrite to NO by the nitrite reducing activity of complex III and IV. Indeed, nitrite-dependent NO formation can be prevented by mETC inhibitors in algae and tobacco. However, this activity only occurs under hypoxia/anoxia (Tischner et al., 2004; Planchet et al. 2005). Moreover, additional Moco-containing enzymes, namely xanthine oxidases (XOs), aldehyde oxidases (AOs), and sulfite oxidases (SOs), have been shown also to possess a nitrite reducing activity *in vitro* which leads to NO. However, they all can only work in anaerobic conditions (Planchet et al. 2005, Maia and Moura 2015, Wang et al., 2015).
Therefore, all these routes are not relevant to plant hypersensitive response which occurs in leaves under normoxic condition.

Recently, Aamand et al (2009) reported that bovine alpha carbonic anhydrase II, similarly as the previous described enzymes can catalyze nitrite conversion to NO both *in vitro* and *in vivo*. Interestingly they suggested a possible dismutation mechanism ($2NO_2^- + 2H^+ \leftrightarrow 2HNO_2 \leftrightarrow H_2O + N_2O_3$, $N_2O_3 \leftrightarrow NO + NO_2$) for this reaction and demonstrated that this reaction can also occur under normoxic conditions. However, the possible conservation of this mechanism in plant carbonic anhydrases and the relevance of this described mechanisms for the plant hypersensitive response were not enquired so far.

1.2.3 NO turnover

NO homeostasis reflects the balance of NO production and NO turnover or conversion into other reactive nitrogen species (RNS). Concerning the consumption of synthesized NO, more mechanisms can be considered.

First of all, NO can react with glutathione (GSH) to produce S-nitrosylated glutathione (GSNO), that is considered to act as a reservoir for NO and which provides the NO signal for nitrosylation of proteins. The enzyme GSNO reductase (GSNOR) tightly controls GSNO levels by reducing GSNO to oxidized glutathione (GSSG) and ammonia (NH_3) (Liu et al., 2001). This cytosolic enzyme functions in the control of GSNO levels, and thus of the nitrosylation of proteins. In turn, NO produced from nitrate assimilation inhibits GSNOR by nitrosylation, preventing the scavenging of GSNO (Frugillo et al., 2014). *A. thaliana gsnor* knockout mutants accumulate high levels of NO and *S*-nitroso species, and have been widely used to study NO/GSNO functions in different biological contexts, including HR (Feechan et al., 2005; Holzmeister et al., 2011; Rusterucci et al 2007; Yun et al., 2011)..

NO can be scavenged by reacting with reactive oxygen species (ROS). Indeed, NO can react promptly with O_2^- in a diffusion-limited reaction leading to the production of peroxynitrite ($ONOO^-$), a potent oxidizing and nitrating species which, nevertheless, is not cytotoxic in plants (Delledonne et al., 2001; Vandelle and Delledonne, 2011). The non-enzymatic biosynthesis of $ONOO^-$ is tightly controlled by the (enzymatic) formation of its precursors. The availability of O_2^- can modulate the NO burst (and *vice versa*) integrating NO/H_2O_2 signaling during the HR according to the so-called balance model (Delledonne et al., 2001).

Finally, NO can be converted into NO_3^- by the NADPH-dependent NO dioxygenase activity of plant hemoglobins (Perazzolli et al., 2004). The overexpression or silencing of this protein did not affect NO levels or the HR cell death in response to avirulent pathogens in an early study (Perazzolli et al., 2004). More recently, the overexpression of AtHb1 has been shown to compromise NO accumulation in response to avirulent pathogens, associated with a reduction in HR-mediated PCD, whereas AtHb1 silencing enhances the resistance and the modulation of hormones involved in defense. Interestingly, the AtHb1 expression is also rapidly downregulated in response to infection with the avirulent bacteria *Pseudomonas syringae* pv. *tomato*,

suggesting the existence of a mechanism regulating NO turnover to potentiate the NO burst during the HR (Mur et al., 2012).

1.3 Nitric oxide downstream signaling during the hypersensitive response

NO signal transduction involves a highly amplified and integrated signaling system. This mainly relies on NO unique chemical features and reactivity, directly or indirectly affecting a large number of different protein targets ultimately triggering immunity (Leitner et al., 2009; Bellin et al., 2013). Indeed, NO directly modify protein functions by reacting with protein associated transition metals or through specific protein post-translational modifications, like *S*-nitrosylation and nitration, of specific amino acid residues, allowing the transduction of NO signals. Furthermore, NO extensively cross-talks with other signaling pathways like ROS signaling, hormone signaling, downstream mitogen activated protein kinase cascades, second messengers such as Ca^{2+} and cGMP or fatty acids. Ultimately, NO triggers an extensive modulation of gene expression during the HR.

1.3.1 The second messenger cGMP

In animals, the main mediator for NO signaling is the second messenger cGMP. In this pathway, NO binds to heme ferrous iron of soluble guanylate cyclase (sGC) to activate it, thus inducing cGMP production (Martinez-Ruiz et al.,2011). In plants, cGMP increases upon pathogen challenge in NO dependent manner (Meier et al., 2009; Hussain et al., 2016) and exogenous cGMP treatment induced defense related gene expression (Duner et al., 1998). More recently, it was shown that constitutive high cGMP level in transgenic lines overexpressing a rat soluble guanylate cyclase abolish transient cGMP accumulation and compromise SAR establishment, thus confirming a role for cGMP in downstream NO signaling also in plant (Hussain et al.,

2016). Even though several enzymes and kinases with a guanylate cyclase domain have been reported (Turek and Gehring, 2016, Gehring and Turek, 2017), there is still no conclusive evidence for a parallel NO-dependent soluble guanylate cyclase mediating NO signaling in plants during the HR.

1.3.2 Protein S-nitrosylation

S-nitrosylation refers to the covalent addition of an NO moiety to the sulfhydryl group of cysteine residues in a protein (Stamler et al.,2001). Several proteomic studies have revealed numerous S-nitrosylated proteins in plants (Lindermayr.,2005; Abat et al., 2008; Romero-Puertas et al., 2008; Abat and Deswal, 2009). These proteins are involved in many cellular processes including primary and secondary metabolism, photosynthesis, genetic information processing, cellular architecture, and response to biotic and abiotic stresses (Astier et al.,2012). Although numerous plant S-nitrosylated proteins have been identified *in vitro* and/or *in vivo*, the impacts of NO on acitivity, structure, and function of target protein are still limited. The best characterized S-nitrosylated proteins are involved in plant immunity (Astier et al.,2012). The *A. thaliana* AtRBOHD, involved in pathogen induced ROS production, was shown to be *S*-nitrosylated during the HR triggered by the avirulent *Pseudomonas syringae* pv. *tomato* DC3000 AvrB. *In silico* structural modeling indicated that the *S*-nitrosylation of Cys^{890} would disrupt the side chain position of Phe^{921} , which is required to bind FAD, thus explaining the loss of activity (Yun et al., 2011). The NO-dependent regulation of AtRBOHD would help to fine tune NO/ROS cross talk in the HR, thus preventing the generation of excess ROS and allowing to the induction of HR-PCD. NPR1, a transcriptional activator involved in salicylic acid-mediated signal transduction is also subjected to *S*-nitrosylation. In unchallenged cells, NPR1 is present as an oligomer with intermolecular redox-sensitive disulfide bridges and the complex is sequestered in the cytoplasm. Redox changes induced by pathogens and the accumulation of salicylic acid cause a reduction and monomerization of the

protein and, consequently, the monomers are translocated to the nucleus, inducing the induction of specific resistance genes (Mou et al., 2003). The *S*-nitrosylation of NPR1 at the predicted oligomerization interface favors the formation of disulfide bonds that promote oligomerization (Tada et al., 2008) and is required to maintain NPR1 oligomer/monomer homeostasis, thereby facilitating the steady supply of monomeric protein to support salicylic acid-dependent gene expression. Likewise for the NADPH oxidase AtRBOHD and (NPR1), the S-nitrosylation functional consequences for other protein involved in immunity including peroxiredoxin II E (PrxII E), salicylic acid-binding protein 3 (SABP3), the transcription factor TGA1, the GAPDH and the metacaspase AtMC9 were studied. These analyses indicate that S-nitrosylation of critical Cys residues promotes or inhibits the formation of disulphide linkages bounds, induces changes in protein conformations, and impacts the binding of cofactors, thus modifying protein activities or localizations.

1.3.3 Protein nitration

As previously mentioned, NO can react with O_2^- in a diffusion-limited way to form peroxynitrite (ONOO-), a potential reagent for protein tyrosine nitration modification. Therefore, the accumulation of ONOO- occurring during the HR causes an increase in nitrated proteins (Romero-Puertas et al., 2008). Indeed, while $ONOO^-$ promotes PCD in animals, it does not appear to fulfil a similar role in plants and is instead emerging as a potential signaling molecule that acts by selectively nitrating tyrosine residues (Vandelle & Delledonne, 2011). This post-translational modification involves the addition of a nitro-group to the *ortho*-position of the aromatic ring of tyrosine residues, forming 3-nitrotyrosine (Radi, 2004). There is preliminary evidence that protein nitration in plants can achieve selective activity inhibition and can trigger selective proteasome mediated degradation of targets which would be involved in signaling, although this has not been demonstrated in the context of defense responses thus far (Castillo et al., 2015). No clear functional role for protein nitration has been

elucidated in the context of the HR, but some important immunity-related candidate proteins can be nitrated *in vitro* and the potential role in defense and immunity (Begara-Morales et al., 2015; 2014; Chaki et al., 2013; Holzmeister et al., 2015). Interestingly, Peroxiredoxin II E (PrxIIE), which detoxify ONOO-, is inactivated by S-nitrosylation during the HR, thus enhancing the nitrated protein formation and signaling (Romero-Puertas et al.,2007).

1.3.4 NO-mediated gene expression modulation

While the regulation of protein function and signaling by NO through post-translational modification has been well established, there is a substantial lack of information about the inductive or repressive effects of NO on gene expression. Transcriptional changes related to NO action could play a significant role in NO-mediated cellular responses. A preliminary analysis of transcripts profiles of *A.thaliana* leaves infiltrated with NO donor sodium nitroprusside (SNP) by cDNA-amplification fragment length polymorphism (AFLP) technique revealed 71 differentially expressed genes involved in signal transduction, disease resistance, reactive oxygen species production and turnover, photosynthesis and cellular transport (Polverari et al., 2003). Following this pioneer study, further transcriptomic studies have been applied to characterize genes differentially expressed due to NO, mainly based on the application of NO donors. Microarray analysis of Arabidopsis roots treated with different concentration of SNP resulted in the differential expression of 422 genes including 342 up- and 80 down-regulated genes (Parani et al., 2004). Much recently, in an RNASeq study involving Arabidopsis roots and leaves, GSNO mediated transcriptome analysis showed the differential expression of 3263 genes (Begara Morales et al., 2014). Further transcriptional analyses on plant response to NO using different techniques or NO donors have identified thousands of NO-responsive genes, most of them functioning in plant defense and oxidative stress response, hormone signaling, or developmental processes (Huang et al., 2002; Grun et

al.,2006; Ahlfors et al; 2009; Besson-Bard et al.,2009). Further bioinformatics analysis identified several transcription factors binding sites (TFBS) enriched in the promoters of these responsive genes, such as WRKY, GBOX and octopine synthase element-like sequence typically involved in stress responses (Palmieri et al., 2008). However, these data should be interpreted with caution, as these results were obtained by the exogenous application of NO donors, for which both problems in controlling of application timing, as well as side effects associated to the pharmacological treatments, cannot be avoided. As an alternative, a transcriptome study was also performed in transgenic Arabidopsis plants constitutively expressing the rat neuronal NOS (nNOS), leading to increased *in vivo* NO content (Shi et al., 2014). Transcriptome analysis revealed several drought stress related genes and related pathways significantly modulated in nNOS plants. Among genes regulated both by NO and ABA treatment, two ABA receptor were included which were further subjected to functional analysis (Shi et al., 2014). Very recently, genes transcriptionally regulated by NO were identified by using a high-throughout RNA-Seq-mediated transcriptomic approach in leaves infiltrated with 1 mM S-nitrosocysteine (CysNO). Changes in the expression of 6436 genes (2988 down-regulate and 3448 up-regulated) was found, indicating a massive reprogramming of transcription at 6 h post treatment. Increasing cellular NO levels affected many important groups of genes, including metal-containing enzymes, such as peroxidases and catalases, various protein kinases, receptors, and transcription factors. Therefore, NO regulates several physiological pathways through intricate translational and transcriptional controls (Hussain et al., 2016). Lately, a further work focused on the differentially expressed genes emerged in this study encoding for transcription factors, both through *in silico* analyses and by the *in vivo* characterization of the knockout mutants of three among these differentially expressed transcription factors, *ddf1*, *rap 2.6* and *atmyb48* (Imran et al., 2017).

2. Scope of the thesis

Since the discovery that NO plays a crucial role in mediating plant defense response in the late nineties (Delledonne et al.,1998; Durner et al.1998), extensive research over the past 20 years revealed that NO is acting as a mediator in plant growth and development, as well as coping with biotic and abiotic stresses (Bellin et al.,2013; Yu et al., 2014). However, both NO biosynthesis and NO downstream signaling need further clarification.

In animals, NO is mainly produced via nitric oxide synthases (NOSs), which catalyze a two-step oxidation of l-arginine into l-citrulline and NO, using reduced NADPH as the electron donor, oxygen as co-substrate, and (6R-)-5,6,7,8-tetrahydrobiopterin (BH4), FAD, FMN, and calmodulin (CaM) as cofactors. NO production in plants is still not fully understood and remains one of the most challenging issues of the field. It can be schematically achieved via two main routes defined by their chemical properties, one reductive and one oxidative. The reductive pathway, the best characterized pathway for NO production in plant so far, is based on the reduction of nitrite to NO, while the oxidative route relies on the oxidation of aminated molecules, but enzymes involved in this oxidative pathway are not yet defined at least in land plant.

The cytosol enzyme nitrate reductase (NR) primarily catalyzes the nitrate reduction to nitrite. It was demonstrated that it also produce NO from nitrite both in vitro and in vivo, however, the significant occurrence of this reaction in physiological conditions has been questioned (Yamasaki and sakihama, 2000; Rockel et al.,2002: Planchet et al., 2005). Importantly, it has been reported that NO production increases significantly in Arabidopsis NR-defective (*nia1 nia2*) mutant plants challenged with HR-inducing avirulent pathogens when nitrite is supplied exogenously (Modolo et al.,2005; Chen et al.,2014), suggesting that other unidentified routes for NO production from nitrite exist during HR.

Recently, Aamand et al (2009) reported that bovine carbonic anhydrase II can produce

NO from nitrite under normoxic conditions and suggested a possible dismutation mechanism (2NO2- +2H+ ↔2HNO2↔H2O+N2O3, N2O3↔NO+NO2), which raises the question if plant carbonic anhydrases can also convert nitrite to NO particularly during HR.

Carbonic anhydrases (CAs) are zinc metalloenzymes which catalyse the interconversion between CO_2 and HCO_3^- and are ubiquitous in all three kingdoms of life. Several evolutionarily independent CA families with a distinct difference in amino acid sequence and active site structure, but catalyzing the same chemical reaction using similar catalytic mechanisms exist (Hewett-Emmett and Tashian, 1996). The well-studied animal CAs all belong to the α-type carbonic anhydrases containing multiple isoforms with different catalytic activity (Supuran, 2008). In contrast, higher plants CAs are classified in α, β, and γ families (Moroney et al., 2001; Rudenko et al., 2015) which share no significant primary sequence homology but appear to possess a similar catalytic function through the convergent evolution (Hewett-Emmett &Tashian 1996; Tripp et al., 2001). Multiple CA members for each type exist in a single organism, e.g. *Arabidopsis thaliana* has 8 αCA genes, 6 βCA genes and 5 γCA genes (Fabre et al., 2007).

Plant cell αCAs were first reported in the unicellular green alga *Clamydomonas reinhardtti*, and named CAH1 and CAH2 which have periplasmic localization (Fukuzawa et al., 1990; Fujiwara et al., 1990). Interestingly, a third αCA CAH3 in *C. reinhardtii* was a thylakoid membrane-bound protein associated with photosynthesis II (PSII) particles (Karlsson et al., 1998; Moroney et al., 2011). Most αCAs are monomers but the exceptions of multimeric αCAs have already been reported (Moroney et al., 2011; Rudenko et al.,2015). Among the eight αCA genes present in the Arabidopsis genome, only three have a complete expressed sequence tags (ESTs), and the RNA-seq analysis also only reveal very low expression of the other five annotated genes (DiMario et al., 2017). The AtαCA8 contains an early in-frame stop codon is considered as a pseudogene (DiMario et al., 2017). The information on αCA

is rare, possibly due to their very low expression level or organ/tissue expression specificity. Concerning cellular localization, it was found that Arabidopsis αCA1 is a glycoprotein which is targeted to chloroplast via a newly discovered ER to Golgi to chloroplast pathway (Villarejo et al., 2005) and N-glycosylation modification is required for its correct folding and trafficking, and therefore carbonic anhydrase activity (Buren et al., 2011). In addition, Arabidopsis αCA4 was detected in thylakoids membranes proteome by mass spectrometry (Friso et al.,2004). Animal αCAs are involved in many physiological or pathological processes related with pH and CO homoeostasis/sensing, biosynthetic reaction such as lipogenesis, respiration and transport of CO_2/bicarbonate, tumorigenicity (Supuran, 2008, 2016). In Chlamydomonas, the periplasmic CAH1 and CAH2 were suggested to facilitate the diffusion of inorganic carbon from the medium to the plasma membrane, while CAH3 plays a crucial role in inorganic carbon acquisition and supplying CO2 for photosynthesis (Karlsson et al., 1998; Moroney et al., 2011). In Arabidopsis a recent study showed, through mutant characterization, that the αCA2 and αCA4 participate in photosynthetic reaction (Zhurikova et al., 2016). However, the knowledge of physiological roles of higher plant αCAs is still scarce.

By contrast, plants βCAs, the predominating carbonic anhydrase and among the most abundant enzymes in plant leaves after the Rubisco (Badger and Price, 1994), have been much widely characterized given their high expression level (Fabre et al.,2007; DiMario et al., 2017). βCAs are multimers such tetramer, octamers and the fundamental structure unit of βCA is a dimer (Rowlett et al., 2010). βCAs exist in a variety of subcellular compartments including chloroplasts, mitochondria, cytosol, and plasma membrane (Rudenko et al., 2015; DiMario et al., 2016a). Among the six βCAs of Arabidopsis, AtβCA1 and AtβCA5 target to the chloroplast (Fabre et al., 2007; Hu et al., 2015), AtβCA2 and AtβCA3 and AtβCA4.2 are cytosolic (Fabre et al.,2007; DiMario et al., 2016) while AtβCA4.1 localizes to the plasm membrane. AtβCA6, finally, is located in the mitochondria matrix (Fabre et al., 2007; Jiang et al., 2014). Majority of total leaf soluble CA activity is contributed by βCAs (Badger and

Price, 1994). Initially, βCA was assumed to play an important role in CO_2 fixation by Rubisco by facilitating the diffusion of CO_2 into chloroplasts and in regulating pH in chloroplast stroma in response to environmental fluctuations (Everson, 1970; Poincelot, 1972; Werdan and Heldt, 1972, Badger and Price, 1994). However, the antisense transformant tobacco plants with 1%-2% of the CA activity of WT plants didn't show significant differences in CO_2 assimilation rates, Rubisco activity, and chlorophyll content compared to WT plants (Majeau et al.,1994; Price et al.,1994). Furthermore, by using Arabidopsis antisense transformants and knockout lines of βCA1, Ferreira and colleagues (2008) demonstrated that lack of βCA1 reduced seedling survival and the cotyledons have compromised CO_2 assimilation rates. However, if the transformants did survive, the mature plants showed no distinguishing phenotypes with WT plants, suggesting AtβCA1 have no direct effect on photosynthesis in mature plants (Ferreira et al.,2008). More recently the involvement of AtβCA1and AtβCA4 together in stomatal movement and development have been extensively characterized (Hu et al., 2010; Engineer et al.,2014). Importantly, βCAs are involved in defense strategies for coping with challenges from various pathogens (Slaymaker et al., 2002; Restrepo et al., 2005; Jung et al., 2008; Wang et al., 2009; Collins et al., 2010). Silencing of tobacco chloroplast βCA1(SABP3, salicylic-acid-binding protein 3) expression suppresses the Pto:avrPto-Mediated HR in leaves, suggesting tobacco βCA1 is involved in hypersensitive defense response (Slaymaker et al., 2002). Furthermore, S-nitrosylation of Arabidopsis βCA1 suppressed both CA and SA binding activities and abolished plant immunity response (Wang et al., 2009).

Finally, γCAs which have a similar active site as αCA function as a trimer with the active site constituted by histidine residues from two neighboring subunits (Ferry et al.2010). In Arabidopsis there are five γCAs including two γCA-likes and all localize to mitochondria as part of mitochondria complex I (Braun and Zabaleta et al., 2007). They have a role in reproductive development and mitochondrial carbon metabolism to support efficient photosynthesis in the chloroplasts under ambient conditions

(Braun and Zabaleta, 2007; Wang et al.,2012; Fromm et al.,2016a, 2016b). Plant γCAs have active-site residues similar to that found in other bacteria active γCAs (Braun and Zabaleta, 2007). However, no CA activity has been detected from higher plant γCAs (Perales et al.,2005; Braun and Zabaleta, 2007).

Given preliminary data on plant carbonic anhydrase, the first aim of this work was to explore the possible involvement of plant carbonic anhydrase enzymes in nitric oxide synthesis during the HR. To test this hypothesis, three carbonic anhydrases, named AtαCA2, Ntβ-CA1 and AtγCA2 were chosen as representatives of each of the three carbonic anhydrase families in plants. Firstly, we tried to explore the NO producing activity of AtαCA2, an Arabidopsis enzyme belonging to the same family as the bovine CA for which the NO producing activity was reported (Aamand et al., 2009). Moreover, the possible involvement in NO production of the Ntβ-CA1and AtγCA2 was determined using ozone-based chemiluminescense, given the literature report about their involvement in plant disease resistance (Slymaker et al. 2002, Wang et al., 2009).

Signal transduction downstream of NO accumulation mainly relies on chemical NO reactivity. Indeed, NO directly modify protein through specific protein post-translational modifications, like *S*-nitrosylation and nitration, modifying function or cellular localization finally allowing the transduction of NO signals. Besides that, it has been documented that NO triggers extensive modulation of gene expression during the HR. However, while many S-nitrosylation targets have been identified and the consequences of S-nitrosylation on protein function deeply investigated and often clarified, transcriptomic changes induced by NO are much less characterized and there still is a substantial lack of information about the effects of NO on gene expression and how this is triggered. Transcriptomic studies applied so far to characterize genes differentially expressed due to NO accumulation in plant cells mainly rely on the application of NO donors. However, data from pharmacological treatments should be interpreted with caution, as such treatments imply problems in

carefully controlling timing and side effects associated to backbones or additionally released compounds in pharmacological treatments cannot be avoided. Therefore, alternative approaches should be applied to confirm observed transcriptomic changes following these NO treatment. In the second part of this thesis work, we have taken advantage of a fumigation system allowing the treatment of plants directly with gas NO in air with the aim to characterize the transcriptomic changes associated to NO treatment. In more detail, we have characterized transcriptomic changes associated to NO treatment, specifically those associated to treatments leading to cell death. To this aim, we first defined the conditions of exogenous NO fumigation on plants triggering an uniform cell death. Then an RNASeq experiment on samples subjected to this treatment or untreated samples was done to characterize the transcriptome modulation and identify gene functional classes which expression is more affected by the treatment.

3. Materials and Methods

3.1 Materials

3.1.1 Plants

Nicotiana benthamiana and *Arabidopsis thaliana* (Col-0) were grown in growth chamber with a 8 h day/16 h night photoperiod.

3.1.2 Bacteria strains

Bacteria strains	**Growth medium**	**Antibiotics**
Escherichia coli DH5α, DB3.1, BL21	LB	–
Agrobacterium tumefaciens GV3101::pMP90	LB	Rif50+ Gen25
Agrobacterium tumefaciens EHA105	LB	Rif50
Pseudomonas syringae pv. tomato DC3000 carrying avrB	KB	Rif50+Kan50

Rifampicin 50 ug/ml; Gentamycin 25 ug/ml; Kanamycin 50 ug/ml.

3.1.3 Vectors

Vectors	**Purpose**	**Selective antibiotics**
pDONR221	Entry cloning	Kan 50
pENTR/SD/D-TOPO,	Entry cloning	Kan 50
pET28a	Bacterial expression vector	Kan 50
pDEST17	Bacterial expression vector	Carb 50
pGR106	Plant expression vector	Kan 50
pK7WG2	Plant expression vector	Spec 50, Strep 50

Kanamycin 50 ug/mL; Carbenicillin 50 ug/mL; Spectinomycin100 ug/ml; Streptomycin 300 ug/mL.

3.1.4 Reagents

Name	**Company**
Acetosyringone	Sigma
Acetic acid	Merck
Antifoam SE-15	Sigma
Bacterial agar	FORMEDIUM
BSA (Bovine serum albumin)	Sigma
Carbenicillin	Duchefa biochemie
Chloroform	Sigma
Coomassie Brilliant Blue R-250	Sigma
CTAB (Hexadecyl trimethyl ammonium Bromide)	ACROS ORGANIC
DTT (DL-Dithiothreitol)	Sigma
EDTA (Ethylenediaminetetraacetic acid) disodium salt	Sigma
Ethanol	Sigma
Gentamycin	Duchefa biochemie
Glycerol	Sigma
Glycine	Sigma
HCl (Hydrochloric acid)	Sigma
Imidazole	Sigma
Isopropyl alcohol	Sigma
IPTG (Isopropyl β-D-1-Thiogalactopyranoside)	V.W.R
Kanamycin	Duchefa biochemie
KNO_2 (Potassium nitrite)	Sigma
K_2HPO_4 (Potassium phosphate monobasic)	Sigma
KH_2PO_4 (Potassium phosphate dibasic)	Sigma
beta-mercaptoethanol	Sigma
Methanol	Sigma
$MgCl_2$ (Magnesium chloride)	J.T. Baker

$MgSO_4 \cdot 7H_2O$ (Magnesium sulfate heptahydrate)	Applichem
NaCl (Sodium chloride)	Sigma
Peptone water	Sigma
PMSF (Phenylmethanesulfonyl fluoride)	Sigma
Rifampicin	Duchefa biochemie
Spectinomycin	Duchefa biochemie
Streptomycin	Duchefa biochemie
Sucrose	Duchefa biochemie
Tris (Tris (hydroxymethyl) aminomethane)	Sigma
Triton X-100	Sigma
Tryptone	Sigma
Yeast extract	Duchefa biochemie
$ZnCl_2$ (Zinc chloride)	Sigma

3.1.5 Buffers and mediums

TE buffer:

10 mM Tris, 1 mM EDTA, pH 8.0.

CTAB buffer:

2% CTAB, 1.4 M NaCl, 20 mM EDTA, 100 mM Tris, 2% PVP40, pH 8.0.

Potassium phosphate buffer stock:

1 M KH_2PO_4 and 1 M K_2HPO_4, mixed in an appropriate ratio to obtain desired concentration and pH.

Lysis buffer:

50 mM Tris-HCl pH 7.4, 0.5 M NaCl, 10% glycerol, Triton-X100 1%, PMSF 1 mM, DTT 1 mM, 10 mM Imidazole.

Equilibration buffer:

50 mM Tris-HCl pH 7.4, 300 mM NaCL, 10 mM Imidazole.

Wash buffer:

50 mM Tris-HCl pH 7.4, 300 mM NaCL, 20 mM Imidazole.

Elution buffer:

50 mM Tris-HCl pH 7.4, 300 mM NaCL, 80, 100, 200, 400 and 500 mM Imidazole.

Desalting buffer:

phosphate buffer 10 mM, pH 7.2, 10% Glycerol.

4x SDS Protein Sample Buffer:

40% Glycerol, 240 mM Tris/HCl pH 6.8, 8% SDS, 0.04% bromophenol blue, 5% beta-mercaptoethanol.

Coomassie Brilliant Blue R-250 staining solution: 0.1% Coomassie Blue R-250, Methanol (50% [v/v]), Acetic acid (10% [v/v]).

Ponceau S Staining Solution: 0.1% (w/v) Ponceau S in 5% (v/v) acetic acid.

Luria Broth (LB) medium:

for 1 litre 10 g tryptone, 5 g yeast extract, 10 g NaCl, pH 7.0.

King's B (KB) medium:

for 1 litre 10g peptone, 1.5g K_2HPO_4, 1.5g MgSO4 ·7H_2O, 10 mL glycerol, pH 7.2.

3.1.6 Reagent kits

Name	**Company**
dNTP (100 mM) set	Invitrogen, Life technologies
ECL Select Western Blotting Detection Reagent	GE Healthcare
E.Z.N.A.® Plasmid Mini Kit I	OMEGA
GENECLEAN® II Kit	M.P Biomedicals
Platinum Pfx DNA polymerase	Invitrogen, Life technologies
Platinum® SYBR® Green qPCR SuperMix-UDG with ROX	Invitrogen, Life technologies
Restriction enzymes	New England BioLabs
SuperScript II Reverse Transcriptase	Invitrogen, Life technologies
TURBO DNA-free	Ambion, Applied Biosystems

Taq DNA polymerase	Invitrogen, Life technologies

3.1.7 Primers

Name of primers	Sequence (5'→3')
Nt βCA-For (Nde I)	CACCCGCCAGCCATATGGAATTGCAATCATCA
Nt βCA-Rev (EcoR I)	CTCGGCGAATTCGCTTCATACGGAAAGAGA
AtβCA1-For (Nde I)	CACCCGCCAGCCATATGTCGACCGCTCCTCTC
AtβCA1-Rev (EcoR I)	CTCGGCGAATTCGCTCTACAGCTTCCAATG
AtγCA2-For (Ndel I)	GGAATTCCATATGACGTTGATGAATGTGT
AtγCA2-Rev(Hind III)	CTCGGCGAATTCGCTCTACAGCTTCCAATG
AtαCA2-For (Nde I, SP)	CACCCATATGGCGACAGATTATAGAGAAGTTG
AtαCA2-Rev (Sac I, SP)	CGAGCTCTCATAGTGATTTTGGTTTGTATAA
AtαCA2-For (no SP)	AATAGAGGCCATGATATGATGCTG
AtαCA2-Rev (no SP)	AGTAGTAAGTGATCCAATGTAT
AtαCA2-real time-For	CATTGGCATTCTCCCTCTGA
AtαCA2-real time-Rev	CCAGCAATCCGAGAAAAGAAT
AtαCA2-Flag-For	ggggacaagtttgtacaaaaaagcaggcttcATGGCGACAGATTATAGAGAAGTTG
AtαCA2-Flag-Rev	ggggaccactttgtacaagaaagctgggtcTCActtatcgtca tcgtccttgtaatcgctgccgcgcggcaccagTAGTGATTTTGGTTTGTATAA

3.2. Methods

3.2.1 RNA extraction

Total RNA was isolated from leaves using TRIzol reagent (Invitrogen).

Homogenize about 100 mg leaves frozen by liquid nitrogen in a 1.5 ml Eppendorf tube containing glass beads using a power homogenizer.

Add 1 ml of TRIzol reagent and vortex.

After incubation for 5 minutes at room temperature, add 0.2 mL of chloroform and mix them vigorously by hand for 15 seconds.

Incubate for 3 minutes at room temperature and centrifuge at 12,000×g for 15 minutes at 4℃.

Transfer carefully the aqueous phase to a new tube and add 0.5 ml of isopropanol and mix well. Incubate at room temperature for 10 minutes and centrifuge at 12,000×g for 15 minutes at 4℃.

Remove the supernatant and wash the pellet with cold 75% ethanol twice.

Air dry the RNA and dissolve it in RNase free water. Store RNA samples at −80℃.

The concentration of total RNA was measured with NanoDrop-1000 Spectrophotometer (Thermo Scientific). The purity was assessed by optical density (OD) absorption ratio OD 260 nm / OD 280 and OD260 nm /230 nm. The integrity was examined by 1.0 % agarose gel electrophoresis.

3.2.2 Genomic DNA extraction

Preheat the CTAB buffer containing 1% beta-mercaptoethanol to 65 ℃.

Grind 50-100mg frozen leaves into fine power.

Add the 500 μl of pre-warmed CTAB buffer to the tube with samples and incubate at 65 ℃ for 30 min.

Add 500 µl of chloroform and mix well.

Centrifuge at 13,000 g for 5 min and transfer the supernatant to a new tube.

Add 330 µl isopropanol and mix gently and incubate at room temperature for 10 min.

Centrifuge the mixture at 13,000 g for 10 min at 4℃.

Remove the supernatant and suspend the pellet in 1 ml 70% ethanol.

Centrifuge the mixture at 13,000 g for 10 min at 4℃ to remove ethanol.

Air dry the DNA pellet.

Dissolve the DNA pellet in 30 µl TE Buffer with 1 µl RNase solution

3.2.3 Synthesis of first strand cDNA

To eliminate genomic DNA contamination, the RNA samples were treated with TURBO DNase enzyme (TURBO DNA-free kit; Ambion, Inc., Applied Biosystems). First strand cDNA was synthesized using SuperScript™ II Reverse Transcriptase (Invitrogen) with Oligo (dT)15 in 20 µl reaction volume according to the manufacturer's protocol.

3.2.4 Quantitative RT-PCR

Quantitative RT-PCR using gene-specific primers was performed using Platinum® SYBR® Green qPCR SuperMix-UDG with ROX (Invitrogen) on the StepOnePlus Real-Time PCR Systems (Applied Biosystems).

The components in a 25 µl PCR reaction include 12.5 µl Platinum® SYBR® Green qPCR SuperMix-UDG with ROX, 0.25 µl of forward primer and reverse primer (each 20 µM), 7 µl of sterilized H_2O and 5 µl of 10-fold diluted cDNA.

The relative gene expression was calculated by the 2^-ΔΔCt method (Livak and Schmittgen, 2001) using ACTIN2 (At3g18780) as a reference gene.

3.2.5 PCR, PCR product purification, Restriction enzyme digestion and ligation

PCR reaction was performed using Platinum® Pfx DNA Polymerase or Taq DNA Polymerase (Invitrogen).

The DNA fragments in PCR product were purified from agarose gel slices using GENECLEAN® II Kit.

Restriction enzyme digestions and ligations were performed following the manufacturer's instructions.

Ligation reactions were performed by using the T4 DNA ligase according to manufacturer instructions.

3.2.6 Gene cloning

TOPO® Cloning was performed following the protocols provided in TOPO® Cloning Kits.

LR Reaction and BP Reaction were performed using Gateway™ LR Clonase™ II Enzyme Mix and Gateway™ BP Clonase™ II Enzyme Mix, respectively for cloning in gateway compatible vectors. Appropriate amounts of LR Reaction or BP Reaction were used for bacterial transformation.

Alternatively for gene cloning into pET expression system vectors primers with adequate restriction sites were used and traditional restriction digestion and ligations were applied.

3.2.7 Plasmid DNA extraction and purification

Plasmid DNA was isolated from bacteria using E.Z.N.A.® Plasmid Mini Kit I (OMEGA).

1. Grow 3 mL culture overnight in a 13 mL culture tube.
2. Transfer culture into 1.5 ml microcentrifuge tube, centrifuge at 10,000 x g for 1

minute at room temperature and discard the supernatant.

3. Add 250 μl Solution I mixed with RNase A, and vortex to mix thoroughly.

4. Add 250 μl Solution II. Invert and gently rotate the tube several times to obtain a clear lysate. Incubation for 2-3 minutes.

5. Add 350 μl Solution III. Immediately invert several time until a flocculent white precipitate forms. Centrifuge at 13,000 x g for 10 minutes.

6. Insert a HiBind® DNA Mini Column into a 2 mL collection tube.

7. Transfer the cleared supernatant into the HiBind® DNA Mini Column. Centrifuge at 13,000 x g for 60 seconds. Discard the filtrate and reuse the collection tube.

8. Add 500 μl HBC buffer diluted with isopropanol.

9. Centrifuge at 13,000 x g for 60 seconds. Discard the filtrate and reuse the collection tube.

10. Add 700 μl DNA wash buffer diluted with ethanol. Centrifuge at maximum speed for 30 seconds. Discard the filtrate and reuse the collection tube.

11. Repeat step 10.

12. Centrifuge the empty HiBind® DNA Mini Column at 13,000 x g for 2 minutes to dry the column.

13. Transfer the HiBind® DNA Mini Column into a nuclease-free 1.5 ml micro-centrifuge tube.

14. Add 30 μl Elution buffer and incubation at room temperature for 60 seconds. Centrifuge at 13,000 x g for 60 seconds.

15. Store eluted DNA at -20℃.

3.2.8 Electroporation of *E.coli* and *Agrobacterium*

Electrocompetent *E.coli* and *Agrobacterium* cells were electrotransformed with the corresponding plasmids using a Gene Pulser™ apparatus (Bio-Rad).

1. Keep competent cells on ice and chill an electroporation cuvette.

2. Add 1 μl of plasmid (10 - 50 ng) to the competent cells aliquot, mix gently and

transfer to the pre-chilled cuvette.

3. Dry the exterior of the cuvette with a bit of paper and insert in the electroporator.

4. Put the lid on, adjust voltage to 1.8 kV (for *Agrobacterium*) or 2.5 kV (for *E.coli*)., press start and wait till you hear the 'beep'. Immediately take the cuvette and add 200 µl of SOC or LB with no antibiotics.

5. Transfer to a micro-centrifuge tube and rescue for 3-4 h in a shaking incubator at 28 ℃ (for *Agrobacterium*) or for 1 h, 37℃(for *E.coli*).

6. Plate out 25-100 µl in a plate with the appropriate antibiotics and incubate at 28 ℃ for two days(for *Agrobacterium*) or 37℃ overnight (for *E.coli)*.

3.2.9 Recombinant protein expression in *E.coli*

E.coli BL21 (DE3) cells carrying constructs for protein expression were grown as overnight pre-culture in LB at 37℃ with appropriate antibiotics. Then culture was diluted 1 to 100 and grown for further 2 to 3 hours until the OD600 of the culture reached 0.6-0.8. The protein expression was induced with IPTG and 0.1 mM $ZnCl_2$ at optimal temperatures for indicated times. IPTG concentrations and expression conditions were pre-optimized for the different constructs and are given in the respective results sections. Thereafter, cells were harvested by centrifugation and stored at -80℃. Thawed cell pellets were resuspended in lysis buffer and lysed by sonication in a pulse mode (60-70% bursts, 10 cycles of 10s, 20 seconds interval). The resulting homogenate was centrifuged at 10,000×g for 15 min at 4℃.

After centrifugation at 10,000×g for 15 min at 4℃, the pellet, containing inclusion bodies was washed with lysis buffer once and resuspended in the solubilization buffer (50 mM Tris-HCl pH 7.4, 0.5 M NaCl, 8 M Urea, 1 mM β-Mercaptoethanol, 5 mM Imidazole). The mixture was incubated at room temperature for 1 hour and centrifuged at 12,000×g for 15 min at 4℃. Protein expression was tested by antibodies after loading in acrylamide gels.

3.2.10 Recombinant protein purification

The supernatants were filtered with a 0.45 μm syringe filter and used for protein purification by Ni-NTA matrix (Qiagen). Alternatively, inclusion bodies after solubilization were used for protein purification on Ni-NTA resin under denaturing conditions.

PD-10 columns (GE Healthcare) were used for buffer exchange and desalting of the eluate containing most of the recombinant proteins.

3.2.11 SDS-PAGE

Sodium dodecylsulfate-polyacrylamide gel electrophoresis (SDS-PAGE) with Stacking gel (4%) and Resolving gel (10%) was performed using Mini-PROTEIN Tetra Cell (Bio-Rad). The components of SDS-PAGE gel are shown in Table 1 (amount for one gel).

Table 1 SDS-PAGE gel components

Reagent	10% Resolving gel	4% Stacking gel
4x Tris-HCl(1.5 M), pH 8.8	1.25 ml	─
4x Tris-HCl(0.5 M), pH 6.8	─	0.5 ml
Acrylamide: Bis, 40%	1.25 ml	200 μl
APS 10%	50 μl	20 μl
TEMED	5 μl	2 μl
H_2O	2.5 ml	1.2 ml

Protein samples dissolved in 1X protein loading buffer were boiled for 5 min and centrifuged at 10,000×g for 5 min. The resulting supernatant was loaded into the well. After SDS-PAGE, gels were stained with Coomassie Blue R250 staining solution.

3.2.12 Western blot

For Western blotting analysis, SDS-PAGE gels were blotted onto nitrocellulose blotting membrane by using the indicated apparatus and manufacturer instructions (GE Healthcare, Amersham Protran Premium 0.45µm NC). Ponceau S staining was used for checking the transfer efficiency.

After blocking the membrane in TBST buffer with 5% skim milk power overnight at 4℃, the membrane was incubated with the primary antibody diluted in TBST buffer contaning 3% skim milk power at room temperature with agitation for 2 hours. Horseradish peroxidase-coupled anti-His antibody (A 7058, Sigma-Aldrich, 1:60,000) was used to detect His tagged proteins.

For Flag tagged proteins, rabbit-ANTI-FLAG antibody (F 7425, Sigma-Aldrich, 1:2,000) was used as primary antibody. After washing the membrane three times each 10 min with TBST buffer, horseradish peroxidase-coupled secondary antibody anti-rabbit (A 6154, Sigma-Aldrich, 1:5,000) for Flag tag was put on for 2 hours at room temperature.

Signals were detected by chemiluminescence using ECL Select™ Western Blotting Detection Reagent (GE Healthcare) and visualized on ECL film or imaged with the ChemiDoc Touch Imaging System (Bio-Rad).

3.2.13 Transient expression of proteins in *Nicotiana benthamiana* leaves by agroinfiltration

Preparation of Agrobacterium cultures and agroinfiltration of *N. benthamiana* were performed as described by Liu et al. (2003) and Avesani et al. (2014) with some modifications.

Agrobacterium tumefaciens strains GV3101 containing pGR106-AtαCA2, and EHA105 containing pK7WG2-AtαCA2 or pK7WG2-gfp were grown at 28℃ overnight in 3 ml of LB medium containing appropriate antibiotics with shaking at

180 rpm. This overnight culture was inoculated into 25 ml of LB medium with 10 mM MES-K (pH 5.6), 20 μM acetosyringone as well as appropriate antibiotics, and grown overnight at 28℃. Agrobacterium cells were harvested by centrifugation and re-suspended in infiltration buffer (10 mM MgCl2, 10 mM MES [pH 5.6], 100 μM acetosyringone) to a final optical density at 600 nm (OD600) of 0.8. Bacteria were maintained at room temperature for 2-3 h.

Fully expanded leaves of 6 to 7-week-old *N.benthamiana* plants were infiltrated using a syringe without a needle.

3.2.14 Total protein extraction from plant tissue

Leaf discs harvested from infiltrated plants were frozen in liquid nitrogen and then used for protein extraction. Homogenate were produced in 1X Laemmli buffer and then samples were centrifuged for 15min at 15,000g at 4℃. Supernatants of plant extracts were stored at -80℃ freezer.

3.2.15 Endoglycosidase H digestion

Protein samples were dissolved in Glycoprotein denaturing buffer (0.5% SDS,40 mM DTT) and incubated at 95℃for 10 mins. To total reaction volume of 20 μl, 2 μl of 10X G5 reaction buffer , 2 μl Endo H and H_2O were added and incubation was performed at 37℃for 60 mins. The reaction was stopped at 75℃for 10 mins.

3.2.16 Isolation of thylakoids

Thylakoids were isolated from frozen leaves of *N.benthamiana* plants essentially according to Ignatova et al.(2011).

Frozen leaves were homogenized with a mortar and pestle in ice-cold Grinding buffer (0.4 M sucrose, 35 mM K_2HPO_4, 15 mM NaH_2PO_4, 3 mM MgSO4, 10 mM KCl, 20

mM sodium ascorbate, 10 mM $KHCO_3$, and 2 mM EDTA-Na) at a ratio of Grinding buffer to leaves of 40 mL:10 g^{-1} fresh weight (FW).

The homogenate was filtered through nylon cloth and centrifuged at 200×g for 2 min to eliminate cell debris. All centrifugations were performed at 4℃.

The resulting homogenate (H) was centrifuged at 3600×g for 6 min. The pellet obtained was suspended in ten-fold diluted Grinding buffer and incubated on ice for 10 min to break chloroplasts. Thylakoids were harvested at 3600×g for 6 min.

After washed with Washing buffer (0.4 M sucrose, 35 mM K_2HPO_4,15mM NaH_2PO_4, 3 mM $MgSO_4$, 2 mM sodium ascorbate, 1 mM $KHCO_3$, and 0.5 mM EDTA-Na) at least twice, the thylakoids membranes were resuspended in medium with 1 mM PMSF, 50 mM Tris-HCl, 150 mM NaCl, 10 ml glycerol, pH 7.4 and were kept at -80 ℃.

The chlorophyll content in the samples was determined in aceton extracts according to Porra et al., 1989.

3.2.17 Carbonic anhydrase activity assay

CA activity was measured by a modified electrometric method of Wilbur and Anderson (1948). The sample was added into 6 ml of ice-cold 20 mM Tris-HCl buffer (pH 8.3) in a 25ml plastic graduated cylinder with stirring, and the reaction was initiated by adding 4 ml of ice-cold CO_2-saturated water. The time required for the pH drop of the reaction mixture from 8.3 to 6.3 was recorded. The activity was expressed in Wilbur-Anderson (W-A) units per mg of protein or chlorophyll in samples used. W-A units = $2\times(t_0-t) / t$, where t_0 and t are times required for the pH change in control buffer and the test sample, respectively. Bovine CAII purchased from Sigma was used as a positive control.

3.2.18 Detection of NO production by chemiluminescence

Reaction was conducted in the liquid purge vessel with 3 ml of 10 mM phosphate buffer containing appropriate amount of KNO_2 and protein samples. A gas air flow of 0.3 L/min filtered by deNOxer was passed through reaction mixture, and NO concentration of the air flow was monitored and recorded by a chemiluminescence detector (ECO Physics cld 88et,Switzerland, detection limit 0.5ppt).

3.2.19 NO fumigation treatment

A home-made NO fumigation system was used for NO fumigation treatment. Gas from air and NO cylinders (600 ppm) was controlled by mass flow controllers to adjust their flow to get desired NO concentration. An electronic device was linked with the mass flow controllers to set the desired flow speed. The chamber used for NO fumigation was a box-shaped and made of Plexiglas, with an airtight locker to avoid gas leak. The NO concentration was checked by a chemiluminescence based high sensitive NO detector (ECO PHYSICS CLD 70 E). 7-weeks old Arabidopsis wild type plants are fumigated with NO at the different concentrations as indicated in the result section for given times in fumigation chamber with light (30-40 μmol/m^2/s) at room temperature.

Fully expanded leaves from fumigated and un-fumigated plants were harvested for RNA extraction.

3.2.20 Electrolyte leakage assay

Leaf discs were removed from Arabidopsis leaves with a 6-mm punch. After floating on distilled water for 30 min, six leaf discs per genotype from different plants were transferred to a plate containing 2 ml of distilled water and agitated on a shaker (80 rpm/min). Conductivity (μs/cm2) was measured with the B-173 compact conductivity

meter (HORIBA) at interval times as indicated.

3.2.21 Library preparation for RNASeq analysis, sequencing and bioinformatics analysis

Samples from three independent biological replicate for each condition were considered, each obtained by pooling leaves of three independent treated or untreated plants. RNA was extracted from Arabidopsis leaves as described in 3.2.1. The quantity and purity of RNA were quantified by NanoDrop®ND-1000 spectrophotometer. The RNA integrity was examined by Agilent 2100 Bioanalyzer with RNA 6000 Nano Kit I (Agilent). Illumina non directional RNA-Seq libraries were prepared from 3.0 μg of total RNA per sample by using the TruSeq RNA Sample Prep Kit v2 according to the manufacturer's instructions (Illumina Inc.,San Diego, California, USA). The RNA-Seq libraries were size-selected at 350 to 550 bp using the Pippin Prep DNA size selection system (Sage Science). Library quality was determined using the Agilent High Sensitivity DNA kit on the Agilent 2100 bioanalyzer, and the quantity was determined by quantitative PCR using the KAPA Library Quantification kit (KapaBiosystems).

3.2.22 Sequencing for the RNASeq analysis

Libraries were then pooled in equimolar concentrations and sequenced with the TruSeq Sequencing by Synthesis Kit v3-HS and TruSeq Paired End Cluster Kit v3-cBot-HS (Illumina) using an Illumina HiSequation 1000 sequencer according to the manufacturer's instructions to generate 100-bp paired-end reads.

3.2.23 Bioinformatic analysis of RNASeq data

Bioinformatic analysis was performed by Pietro Delfino (unpublished results).

To identify differentially expressed genes, reads (FASTQ data) were trimmed, tested for quality (FastQC software analysis) and aligned against the Arabidopsis genome TAIR 10 by using the HISAT software (Kim et al., 2015). Differential expression analysis was performed by applying the DESeq software (Anders and Huber, 2010) with standard parameters. DEGs were identified by comparing samples treated with 8 h NO 200ppm and untreated samples. As criteria: (log_2FC)>1,5 and (log_2FC)<-1,5 log2(FC) $\geq$ |1,5| was used as threshold. Gene ontology enrichment analysis was performed on differentially expressed genes by using the online AgriGO v2.0 analysis toolkit (Du et al., 2010, Tian et al., 2017) using the Singular Enrichment Analysis and selecting biological processes in the GO slim gene ontologies.

4. Results

4.1 Nitric oxide synthesis during the HR: characterization of plant alpha carbonic anhydrase as candidate enzyme for nitric oxide production from nitrite

4.1.1 Selection of Arabidopsis AtαCA2 protein as candidate for the characterization

Eight genes encoding for αCAs exist in the *Arabidopsis thaliana* genome (Fabre et al., 2007, Table 1). However, in contrast to the well-studied mammalian αCAs, the information on plant αCAs is very poor.

Table 1. The *Arabidopsis thaliana* αCA gene family

	AGI number	**Name**
α CA gene family	At3g52720	AtαCA1
	At2g28210	AtαCA2
	At5g04180	AtαCA3
	At4g20990	AtαCA4
	At1g08065	AtαCA5
	At4g21000	AtαCA6
	At1g08080	AtαCA7
	At5g56330	AtαCA8

All CA proteins belonging to class alpha show similar identity percentage at amino acid level to bovine CAII (about 30%). Multiple amino acid sequence comparison of these proteins with bovine CAII revealed that αCA1-8 all retain the 3 histidine residues which are involved in coordinating the Zn^{2+} ion in the mammalian CAs active site (according to structural characterization of the human isoenzyme II αCA, Swiss Prot accession number P00918, Eriksson et al., 1988). Furthermore, residues that interact with H_2O and assist in charging Zn^{2+} ion with the hydroxyl and residues involved in composing the hydrophobic pocket for CO_2 hydration/ HCO_3^- dehydration are also widely conserved in the plant αCA family (Fabre et al., 2007, Figure 4).

This conservation suggests that Arabidopsis αCAs may possess a similar catalytic capacity like Bovine CAII, including nitrite disproportionation (Amand et al., 2009), and that this could be a shared feature for all family members. However, as small differences exist in the sequences of AtACA 1, AtACA 3, AtACA 4, AtACA 6,

AtACA 8 affecting residues which are involved in hydroxyl binding that could impact on nitrite binding (Nielsen et al., 2015), we didn't select these as main candidates in the family for our biochemical characterization.

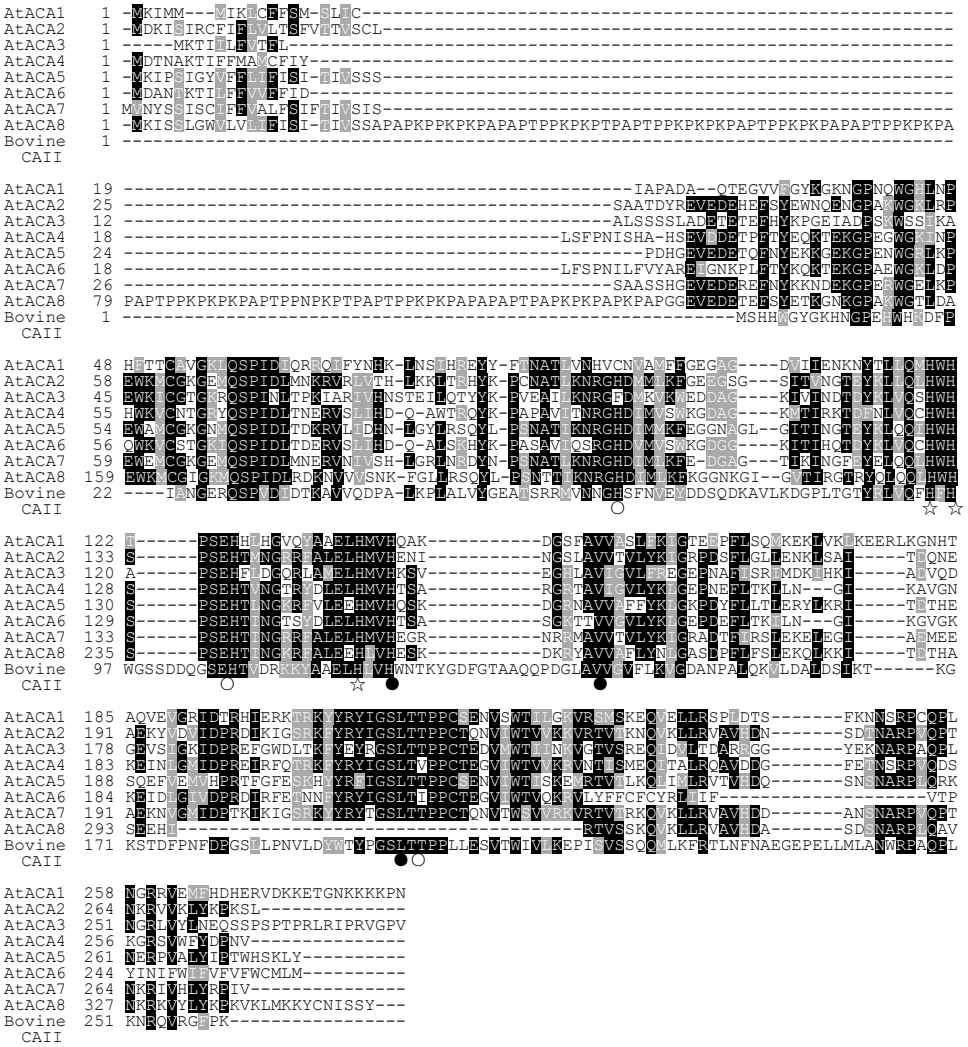

Figure 4. Amino acid sequence alignment of Arabidopsis αCAs with Bovine CAII.
Multiple alignment was processed using Clustal Omega and further formatted using the BoxShade programs. Conserved and similar amino acids are shown with black-shaded and grey-shaded boxes and gaps introduced to maximize the alignment are indicated by hyphens (−). The histidine residues ligated to Zn ion are denoted as stars. Residues that interact with H_2O and assist in charging Zn^{2+} ion with a hydroxyl are marked by white circles. Residues composing the CO_2 hydrophobic pocket are indicated with black circles.

As further information to select the best candidate for our characterization, we decided to explore also gene expression. Transcriptomic data of *Arabidopsis thaliana* Col-0 adult leaves challenged with the avirulent pathogen *Pseudomonas syringae* pv.

tomato (Pst) DC3000 carrying the avirulence gene AvrB (Jingjing Huang unpubblished data) were analysed to retrieve expression information for all alpha CAs family members. We found that among αCAs, *AtαCA1* was the highest expressed gene at basal conditions, followed by *AtαCA2* gene, while all other *αCAs* showed very low expression or no expression (Figure 5). Interestingly, *AtαCA1* was down-regulated following pathogen infection both at 8 and 12 hours post infection, while *AtαCA2* was significantly up-regulated. Therefore, AtαCA2 was selected for our biochemical characterization, to explore the possible involvement of plant αCAs family in NO production from nitrite during pathogen infection.

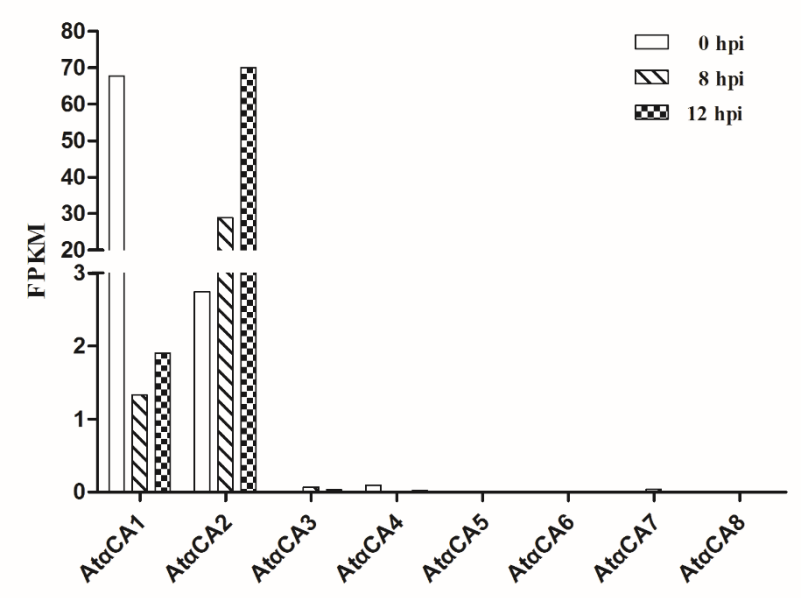

Figure 5. Expression of αCA family members in Arabidopsis leaves infiltrated with avirulent pathogen *Pseudomonas syringae* pv *tomato* carrying AvrB at 0, 8 and 12 hours post infection.
Arabidopsis thaliana Col-0 leaves were infiltrated with $5x10^6$ cfu/ml of *Pst* AvrB. RNASeq libraries were produced from leaves sampled at indicated times after infection. Expression levels as FPKM (Fragments per Kilobase per Million Reads) deduced from these samples (Jingjing Huang unpublished results) are plotted for each AtαCA family member.

4.1.2 Characterization of the recombinant At*α*CA2 produced in *E. coli*

4.1.2.1 Production of the recombinant At*α*CA2

Given the expression profiles previously reported (see paragraph 4.1.1), we decided to clone the *AtαCA2* coding sequence from leaf samples infected with the *Pst* AvrB avirulent pathogen ($5x10^6$ cfu/ml) and harvested at 8 hours post infection.

The coding sequence was amplified from cDNA by using primers designed on the manually refined ORF derived from RNASeq available reads. Moreover, subcellular localization prediction by Target P v1.1 program (http://www.cbs.dtu.dk/services/TargetP/) (Emanuelsson et al., 2007) indicated that the deduced 276 aa protein sequence for AtαCA2 very likely includes a 23 aa secretory pathway signal peptide (Table 2). Amplification primers were thus designed to avoid including the sequence encoding for the signal peptide and are reported in paragraph 3.1.7.

Table 2. Signal pepetide and subcellular location prediction for AtαCA2 by Target P v1.1 program

Name	Len	cTP	mTP	SP	other	Loc	RC	TPlen
AtαCA2	276	0.002	0.032	0.995	0.093	S	1	23

Protein sequence analysis was performed by using the TargetP software (http://www.cbs.dtu.dk/services/TargetP/). cTP: chloroplast transit peptide, mTP: mitochondrial transit peptide, SP: secretory pathway signal peptide, C: chloroplast, M: mitochondria, TPlen: transit peptide length.

The purified PCR product was cloned into a pENTR vector by using the TOPOCLONING system and then transfered by LR reaction (Gateway system, see paragraph 3.2.6) to a pDEST17 vector for expressing in *Escherichia coli*, the recombinant protein was fused to an N-terminal 6x-Histidine tag (Figure 6). This construct was finally transferred to BL21 *Escherichia coli* strain for protein expression.

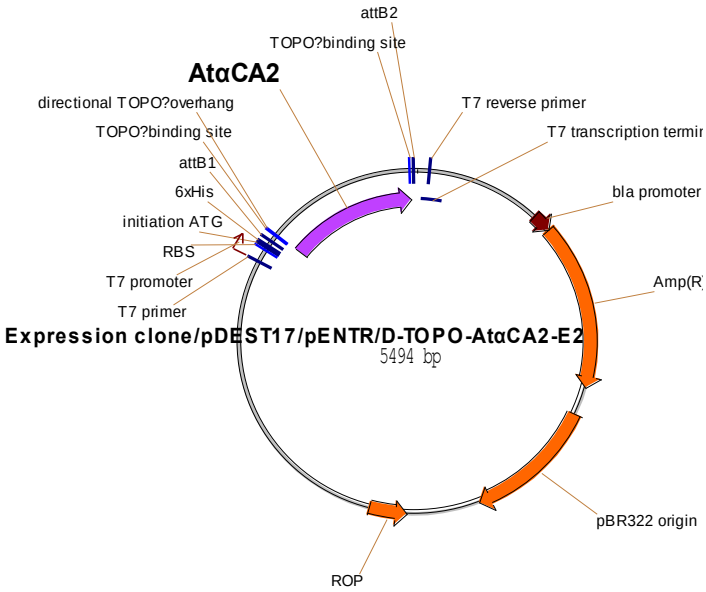

Figure 6. **Map of the pDEST17 construct for expression in heterologous *E. coli* system of the 6x-histidine tagged recombinant AtαCA2**

The coding sequence for AtαCA2 without predicted signal peptide was cloned in the pDEST17 vector for expression in *E. coli* of His-tagged proteins by using the topocloning and gateway cloning system.

Different temperatures (21℃ or 37℃) and different concentrations of IPTG (0.4 mM or 0.05 mM) were tested for the over night induction of the AtαCA2 expression in order to maximize the amount of protein produced in the soluble fraction. Induction of protein expression at 21℃ over night and 0.05 mM IPTG were selected as best conditions (Figure 7). The recombinant 6XHis-AtαCA2 was purified from soluble fraction by affinity chromatography using the Ni-NTA agarose (QIAGEN) (Figure 8) and dialyzed against the elution buffer to remove imidazole. Western blot analysis confirmed that we could successfully produce and purify the histidine tagged AtαCA2. The yield of the recombinant AtαCA2 in our expression system was 0.2 mg per liter of bacterial culture.

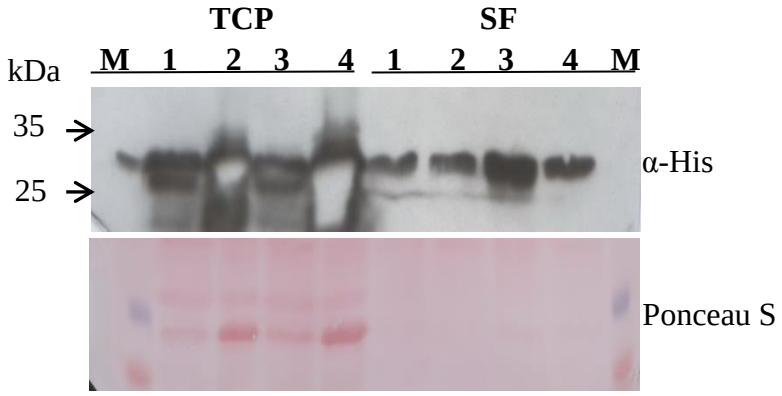

Figure 7. Western blot analysis of recombinant 6XHis-AtαCA2 expressed in *E.coli* under different conditions.

Western blot analysis by using an α-His antibody was performed on total cell proteins (TCP) or soluble protein fractions (SF) recovered from equal volumes of *E. coli* BL21 cell lysate. Protein expression was induced over night by using the following different conditions: 1. 21℃, 0.4 mM IPTG; 2. 37℃, 0.4 mM IPTG; 3. 21℃, 0.05 mM IPTG; 4. 37℃, 0.05 mM IPTG.

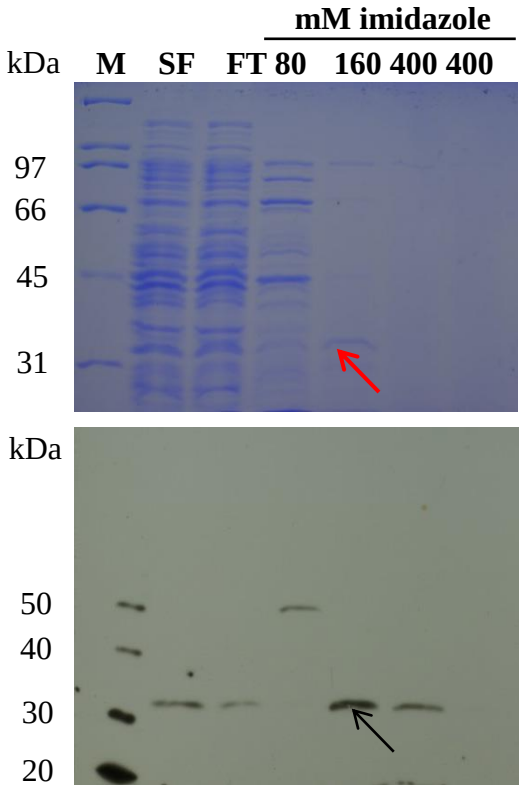

Figure 8. **Purification of the recombinant 6XHis-AtαCA2 protein**.

Equal volume samples for each fraction eluted with buffers at different imidazole concentrations (80, 160, 400 mM) were resolved by SDS-PAGE, stained with Commassie brilliant blue R-250 and analyzed by western blot using the α-His antibody. SF, soluble fraction of *E.coli* cells lysate. FT, flow through.

4.1.2.2 Activity of the recombinant AtαCA2 produced in *E. coli*

The carbonic anhydrase activity of the purified AtαCA2 was measured according to the Wilbur-Anderson method (Wilbur and Anderson, 1948). Unfortunately, no CA activity was detected for the recombinant AtαCA2 produced in *E.coli* (Figure 9).

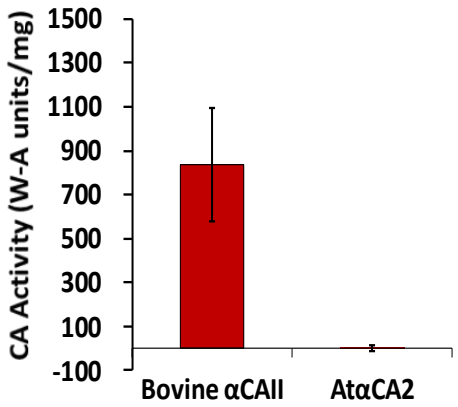

Figure 9. Carbonic anhydrase activity of recombinant AtαCA2 purified from *E.coli*.
Carbonic anhydrase activity was tested by the Wilbur Anderson protocol and plotted as average W-A units for mg of used protein (n=5, ± SD). Commercial bovine αCA II was used as a control.

Interestingly, it was shown in literature that N-glycosylation was necessary for CA activity of AtαCA1 (Villarejo et al., 2005; Buren et al., 2011). The AtαCA2 shares 39% of identity at protein level with AtαCA1. In silico N-glycosylation prediction analysis performed by NetNGlyc 1.0 program (http://www.cbs.dtu.dk/services/NetNGlyc/) indicated that AtαCA2 sequence contains three potential N-glycosylation sites (Figure 10). Thus, we hypothesized that AtαCA2 could be requiring N-glycosylation, which is lacking in *E.coli* expression system, at least for its carbonic anhydrase activity.

Since AtαCA2 protein produced in the *E. coli* expression system was not an active recombinant protein, we decided not to proceed further our analysis to verify the AtαCA2 putative involvement in converting nitrite to NO, and to chose instead an alternative expression system allowing N-glycosylation.

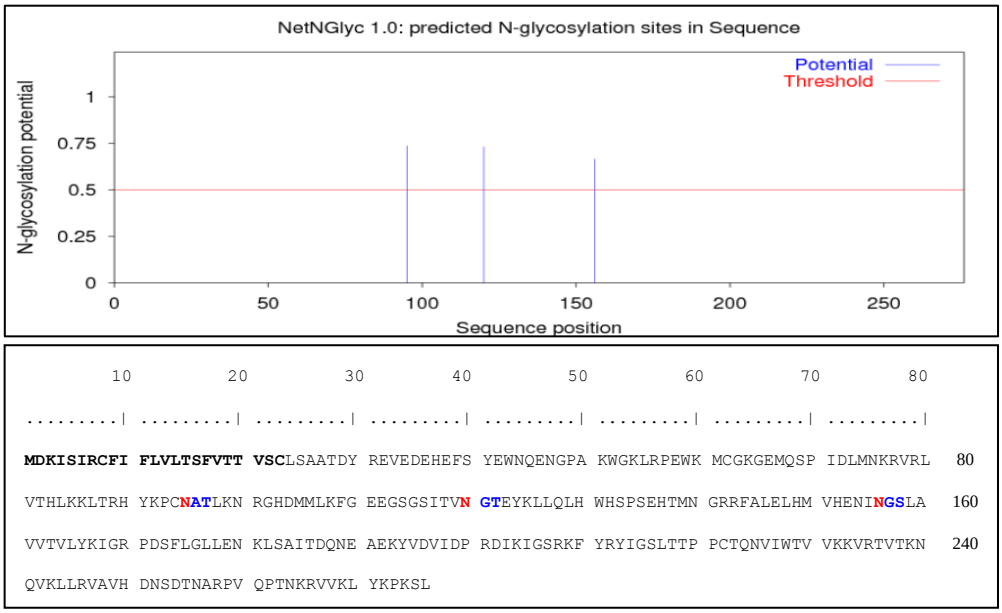

Figure 10. N-glycosylation sites of the deduced amino acid sequence of AtαCA2.
The output of the in silico N-glycosylation prediction analysis performed by NetNGlyc 1.0 program (http://www.cbs.dtu.dk/services/NetNGlyc/) is provided. Predicted signal peptide is reported in bold. Asn-Xaa-Ser/Thr signatures in the AtαCA2 sequence are highlighted in blue and asparagines with N- glycosylation potential higher than threshold are highlighted in red.

4.1.3 Characterization of recombinant AtαCA2 produced in plants

4.1.3.1 Preparation of constructs for expression of AtαCA2 in plants

With the final aim of producing an active AtαCA2 recombinant protein, which possibly requires N-linked glycosylation, to be tested for its involvement in NO production from nitrite, we decided then to try an alternative expression system to *E. coli* which lacks protein N-glycosylation. More in detail, we chose to use the *Nicotiana benthamiana* plant as protein expression system. Two different vectors for expression in plants were chosen to compare protein yields. One was the gateway compatible pGR106new expression construct for protein expression in plants based on the plant virus *Potato virus X* (PVX) system (Angell and Baulcombe, 1997, Cerovska et al., 2004). This vector is similar to the pGR106 binary vector derived from pGreen0000 but carries a gateway cassette cloned in the SalI restriction site of

the polylinker inserted in the coat protein (CP) promoter. The second was the pK7WG2 gateway compatible vector for constitutive expression of proteins in plants (Karimi et al., 2002).

In both cases an Agrobacterium mediated transient transformation system was selected for delivery of the vector. However, the pGR106new vector relies on the PVX virus which should allow an higher level of expression for the foreign gene according to the optimized conditions described in Cerovska et al., 2004.

The full-length coding sequence of AtαCA2 gene including the signal peptide was amplified from cDNA of pathogen infected Arabidopsis leaves by using primers designed on the manually refined ORF derived from RNASeq available reads (see paragraph 3.1.7). This sequence was cloned in the entry vector to create the construct pENTR-AtαCA2-E. The same construct was then used to produce a modified version of the coding sequence including the FLAG and His tags in the C-terminal portion subcloned into the Gateway entry vector pENTR/D-TOPO to create the construct pENTR-AtαCA2-FLAG-His-P which was also verified by sequencing. The entry vector was recombined with the binary vectors pGR106new and pK7WG2 by LR Clonase, to construct the plant expression vectors pGR106- AtαCA2-flag-His and pK7WG2- AtαCA2-flag-His respectively. Finally, the pGR106-AtαCA2-flag-His and pK7WG2- AtαCA2-flag-His plasmids verified by PCR using gene specific primers and restriction enzyme digestion were introduced into *Agrobacterium tumefaciens* strains GV3101. Maps of the prepared constructs are provided in Figure 11.

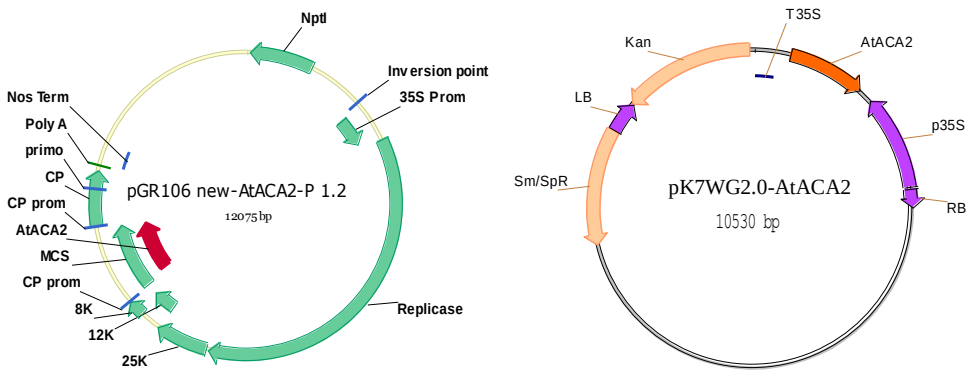

Figure 11. Maps of construct pGR106-AtαCA2-His-Flag and pK7WG2-AtαCA2-His-Flag.

4.1.3.2 Transient expression of AtαCA2 in *N. benthamiana* leaves

The two plant binary expression vectors pGR106new and pK7WG2 described in the previous paragraph were then delivered by agroinfiltration to *N.benthamiana* leaves to induce the transient expression of AtαCA2.

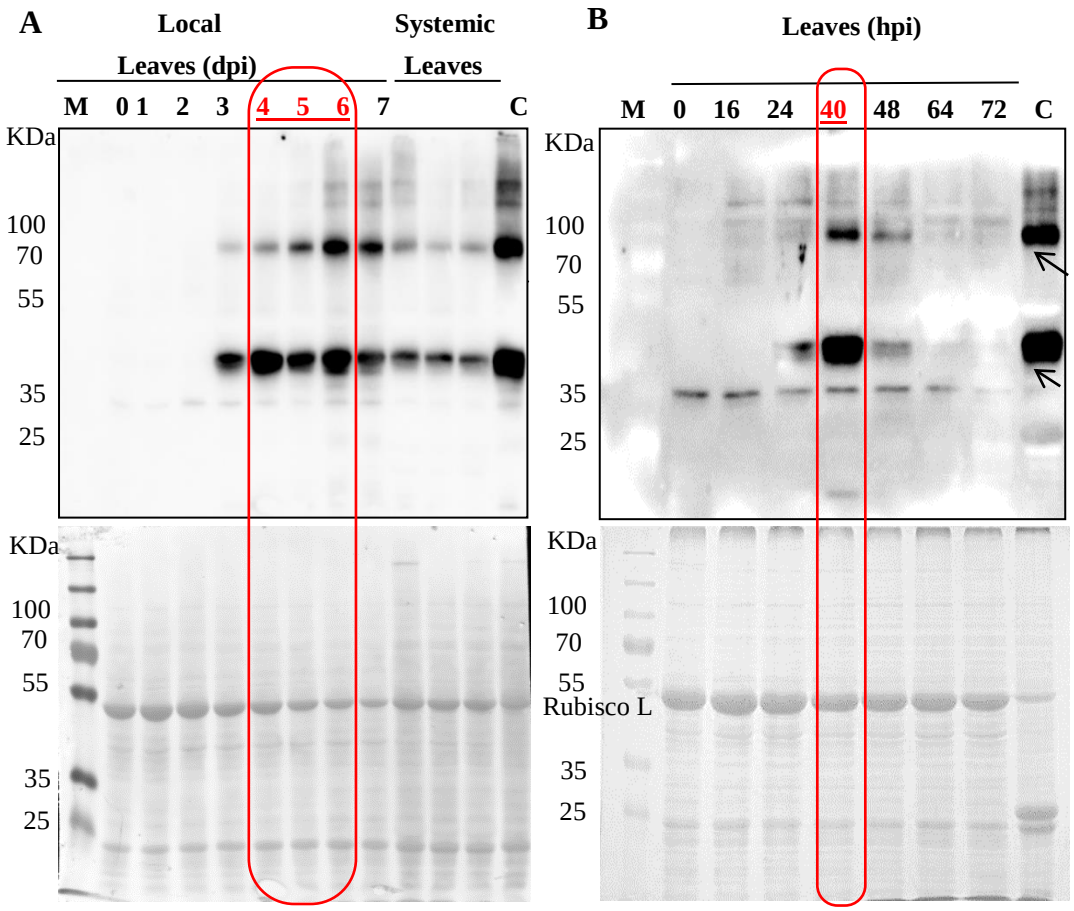

Figure 12. Western blot analysis of transiently expressed AtαCA2 accumulation in *N.benthamiana* leaves.

(A) Time-course of AtαCA2-Flag-His expression in plant analysed by anti-FLAG western blotting. *N. benthamiana* leaves were infiltrated with *Agrobacterium tumefaciens* GV3101 strain carrying the pGR106new binary vector. Samples were harvested from locally infected leaves at indicated times (dpi, day post infection) or from systemic leaves 9 dpi.

(B) Time-course of AtαCA2-Flag-His expression in plant analysed by anti-FLAG western blotting. *N. benthamiana* leaves were infiltrated with *Agrobacterium tumefaciens* GV3101 strain carrying the pK7WG2 binary vector. Samples were harvested from locally infected leaves at indicated times (dpi, day post infection) or from systemic leaves 9 dpi. A sample extracted from systemic leaves wes loaded in both A and B as comparison. Comassie stained gel is provided under western blot as loading control.

RT-PCR analyses were performed to preliminarly test gene expression (data not shown).

Then, in order to identify the best expression system and timing of protein accumulation, protein expression was monitored in a time-course study for both expression systems (Figure 12). When using the pGR106new construct, which relies on the PVX virus mediated expression system, locally infected leaf samples were harvested from 1 to 7 dpi (days post-infiltration). Furthermore, leaf samples were collected from systemic leaves at 9 dpi to test for protein accumulation following the spread of the virus. Alternatively, when using the pK7WG2 vector for protein expression in plant local leaf, samples were collected for 3 days following agroinfiltration.

Equal volumes of total protein extracts were separated on SDS PAGE and western blot analysis by using the anti-FLAG antibody was performed to test AtαCA2-Flag-His expression and accumulation in time. As shown in Figure 12, anti-FLAG immunoreactive proteins of about 40 and 80 kDa (see arrows in Figure 12 A) started to accumulate from 3 dpi (days post-infiltration) in local leaves and maximum accumulation appeared from 4 to 6 dpi when using the vector pGR106new. Morever, systemic leaves showed lower level of protein accumulation compared to local leaves. Highest accumulation of anti-FLAG immunoreactive proteins of similar molecular weight (MW) appeared instead at about 40 hours post-infiltration when using the binary vector pK7WG2 (Figure 12 B).

Comparison of maximum immunoreactive protein accumulation levels in the two systems by densitometric analysis and using same concentrated sample (C) as control showed that maximum levels of protein accumulation were comparable by using the two different expression systems or even stronger when using the pK7WG2 construct for transient expression at 40 hpi (hours post-infiltration).

4.1.3.3 AtαCA2 protein expressed in *N.benthamiana* leaves is N-glycosylated

We observed that the protein expressed in *Nicotiana benthamiana* leaves (Figure 12 A and B) showed an apparent MW higher than the expected MW for full length AtαCA2 including the two C-terminal added tags (34,8 kDa). Indeed the protein showed a MW of 40 kDa. Furthermore, a second immunoreactive band at 80 kDa was also observed. We speculated that the expressed AtαCA2 protein could be thus properly N-glycosylated when expressed in the plant system, leading to the shift from the expected weight of 34,8 kDa to the observed weight of 40 kDa. Furthermore, AtαCA2 could possibly produce dimers, stable in the SDS-PAGE, thus explaining the immunoreactive band at about 80 kDa.

To confirm that the 40 kDa immunoreactive protein corresponded indeed to the N-glycosylated form of AtαCA2-Flag-His proteins, total proteins isolated from leaves infected with Agrobacterium carrying previously described constructs were treated with the endoglycosidase H enzyme, which cleaves within the chitobiose core of high mannose and some hybrid oligosaccharides from N-linked glycoproteins (Figure 13). Interestingly, following Endo H treatment we observed a size shift in the apparent MW of the protein from the 40 kDa to about 35 kDa.

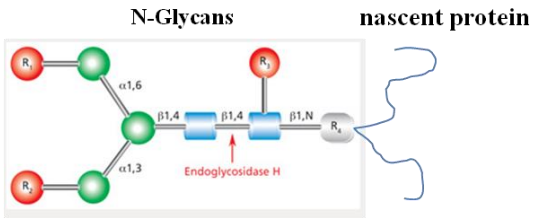

Figure 13. Endoglycosidase H cleavage site on N-glycans bound to nascent proteins

Therefore, as it showed to be sensitive to Endo H digestion, we concluded AtαCA2 was glycosylated when expressed in *N. benthamiana* leaves (Figure 14).

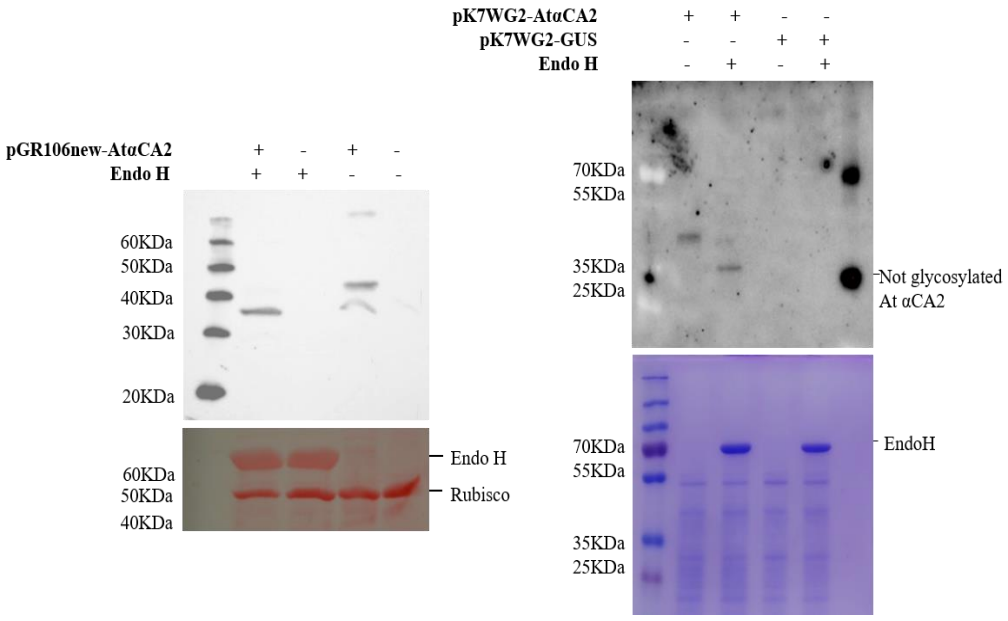

Figure 14. Endo H sensitivity of plant produced AtαCA2

Total protein extracts from *N. benthamiana* leaves agroinfiltrated with pGR106new-AtαCA2 (left panel) or pK7WG2-AtαCA2 constructs (right panel) and harvested respectively 5 dpi or 40hpi were treated with EndoH enzyme, separated on SDS-PAGE and then analysed by western blotting by using an anti-FLAG antibody. Protein extracts from non agroinfiltrated leaves or leaves infiltrated with pK7WG2-GFP (only right panel) are shown as control. Comparison of protein size for EndoH treated and untreated samples is shown for each panel. In the right panel non glycosylated FLAG tagged AtαCA2 (produced in *E. coli*, 32 KDa) is loaded as MW reference. Ponceau stained membrane or Comassie stained gel are provided as equal loading control of samples.

4.1.3.4 Thylakoid fractions prepared from leaves expressing AtαCA2 accumulate N-glycosylated AtαCA2

We previously mentioned that subcellular localization prediction by Target P1.1 program (http://www.cbs.dtu.dk/services/TargetP/) showed that AtαCA2, similarly as AtαCA1, has a secretary pathway signal peptide which would target protein to the endoplasmic reticulum (ER) (see paragraph 4.1.2.1). However, it was demonstrated that AtαCA1, like other glycoproteins such as Rice Plastidial N-Glycosylated NPP1 or Rice a-Amylase, was finally targeted to plastids (chloroplasts) through an ER to Golgi to chloroplast protein transport pathway (Villarejo et al., 2005; Nanjo et al., 2006; Kitajima et al.,2009). Therefore, we expected that AtαCA2 could also target to

chloroplast through a similar pathway. Moreover, considering that the expressed AtαCA2 mainly accumulated in insoluble fractions, we expected that AtαCA2 could be associated with chloroplast membrane system.

We tested first whether the recombinant AtαCA2 was enriched in thylakoids using LHCII, a thylakoid marker protein, for comparison. Indeed, we found that AtαCA2 amount in thylakoids fraction was comparable to AtαCA2 in total homogenates (H), in a similar manner as LHCII, suggesting that recombinant AtαCA2 protein, like LHCII, mainly accumulates in thylakoid fraction of *N.benthamiana* leaves when transiently expressed (Figure 15).

Prepared thylakoid fraction showed very low level of contamination with stroma proteins (Rubisco) (see Comassie in Figure 16A). To further confirm that contamination of thylacoid was very low, a serial dilution of total homogenate was compared for Rubisco content to thylakoids. We could clearly see that in our thylakoids samples Rubisco content was lower than the amount present in total homogenate after 1: 100 dilution (Figure 15B).

Finally, we enquired whether the protein enriched in thylakoid fraction was also N-glycosylated. We extracted and solubilized thylakoid proteins, containg AtαCA2, and showed by western blotting that AtαCA2 present in the thylakoid fraction was Endo H sensitive similarly as previously shown for AtαCA2 from total protein extracts (Figure 16).

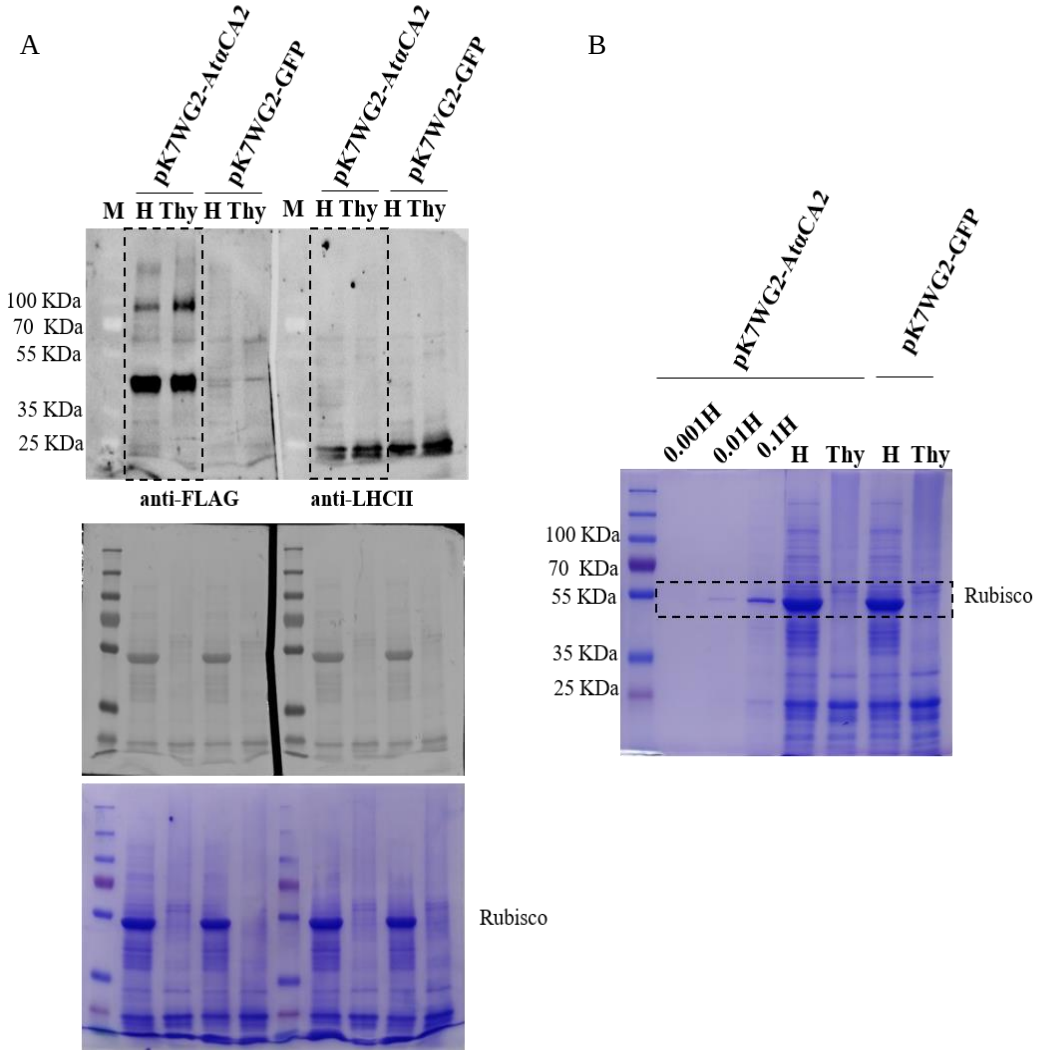

Figure 15. AtαCA2 transiently expressed in plant accumulates in thylakoid fractions

(A) *N. benthamiana* leaves agroinfiltrated with pK7WG2-AtαCA2 construct (or pK7WG2-GFP as negative control) and harvested 40hpi were used for preparing either total protein homogenate (H) or thylakoid fractions (Thy). Samples (1 ug of chlorophyll each) were tested by western blotting using an anti-FLAG antibody or an anti LHCII antibody. AtαCA2 content in thylakoids was comparable to the amount in total homogenate similarly as was for LHCII. Ponceau stained membrane and Comassie stained gel are shown as sample loading control. Rubisco was absent in thylakoid fraction as expected.

(B) Serial dilution of total homogenates (H) demonstrates that thylakoid fraction prepared and used in (A) carries as low as 1/100 of Rubisco protein.

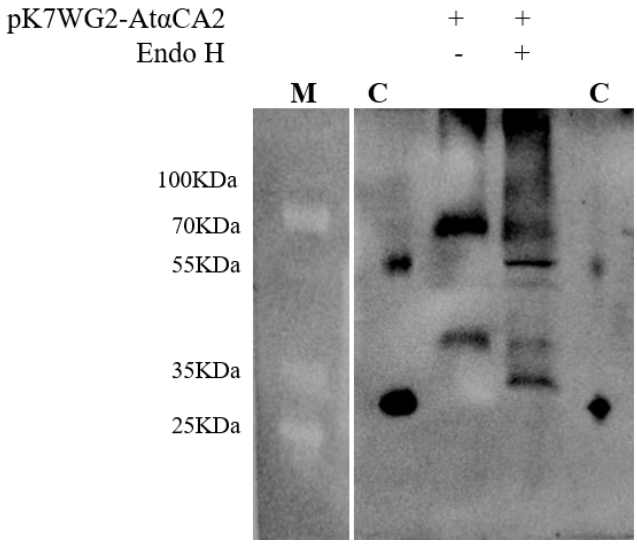

Figure 16. Endo H sensitivity of AtαCA2 in solubilized thylakoid fractions
Solubilized thylakoids (0.1% TritonX-100) prepared from *N. benthamiana* leaves expressing AtαCA2 were either treated or not with Endo H. Comparison of protein size for EndoH treated and untreated samples is shown. Non glycosylated FLAG tagged AtαCA2 (produced in *E. coli*, 32 KDa, 5ng, 2 ng) is loaded as MW reference.

4.1.3.5 Estimation of recombinant AtαCA2 expression in *N.benthamiana* leaves

To evaluate the expression level of the recombinant AtαCA2-FLAG-His in *N.benthamiana* leaves following agroinfiltration, we have first expressed and purified the AtαCA2 protein without signal peptide tagged both with 6xHis and FLAG in *E.coli* to be used as standard.

The same procedure already reported in paragraph 4.1.2.1 was applied to produce the FLAG tagged standard. Briefly, we constructed the *E. coli* expression vector pDEST17 carrying AtαCA2-Flag encoding sequence without signal peptide and expressed the His-AtαCA2-Flag protein in *E. coli* using previously established conditions. Western blotting using both anti-FLAG and Anti-His are given in Figure 17 showing that the tagged recombinant His-AtαCA2-Flag protein (32 kDa)

accumulated mostly in insoluble fraction. The His-AtαCA2-Flag protein was then purified from solubilized inclusion bodies as previously described. Concentration of purified protein was carefully evaluated by densitometric analysis in Comassie stained SDS-PAGE against know amounts of BSA.

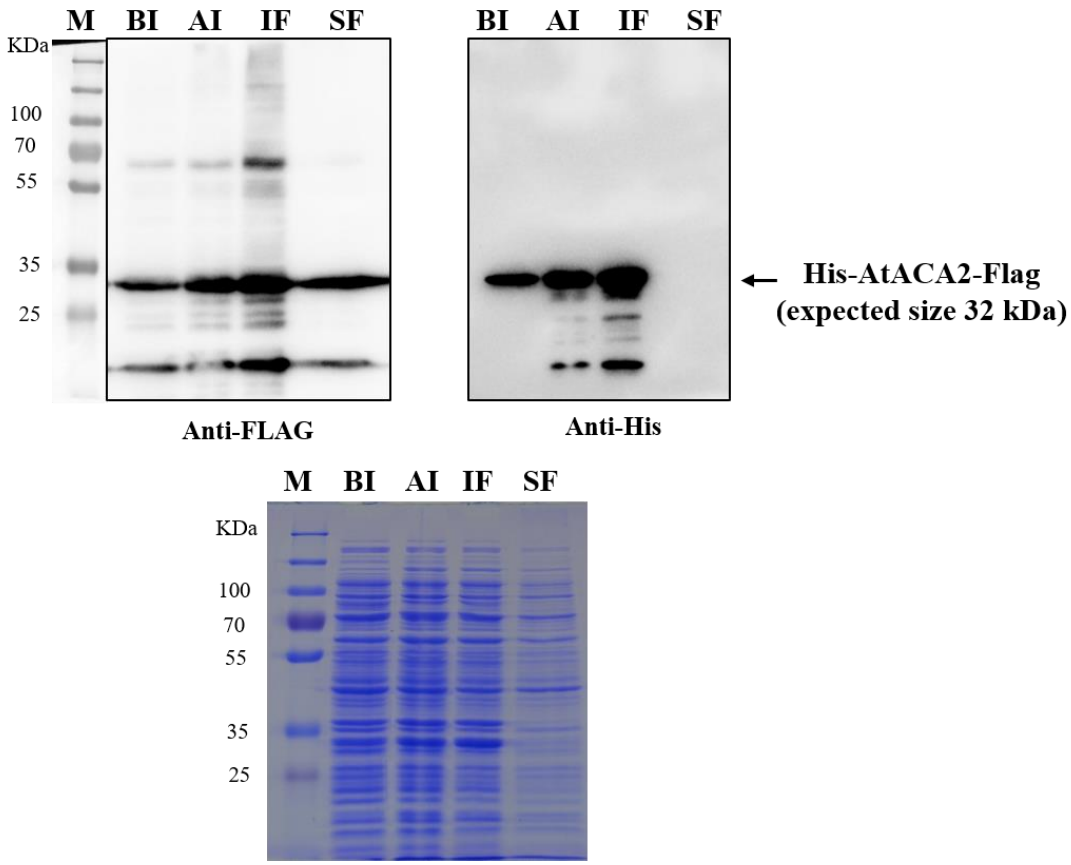

Figure 17. Western blotting of the His/FLAG tagged recombinant AtαCA2 protein expressed in *E.coli* to be used as standard for plant expression quantification

Conditions as reported in paragraph 1.2 were used for protein expression in *E. coli*. Western blotting by using an anti-FLAG antibody (left panel) or anti-His antibody (right panel) on the same stripped membrane are shown. The corresponding Comassie stained SDS-PAGE is shown under. Equal amounts of protein extracts were loaded (BI, total cell proteins before induction; AI, total cell proteins after induction; IF, protein insoluble fraction; SF, protein soluble fraction).

Using purified His-AtαCA2-Flag protein as standard, the expression level of AtαCA2-Flag-His protein expressed in *N.benthamiana* leaves following agroinfiltration was quantified by densitometric analysis of western blotting (anti-FLAG antibody) (Figure 18). According to this quantification, we estimated that about 8.6 ug of AtαCA2 was produced per gram of fresh leaf, when using the pK7WG2 construct for transient plant protein expression.

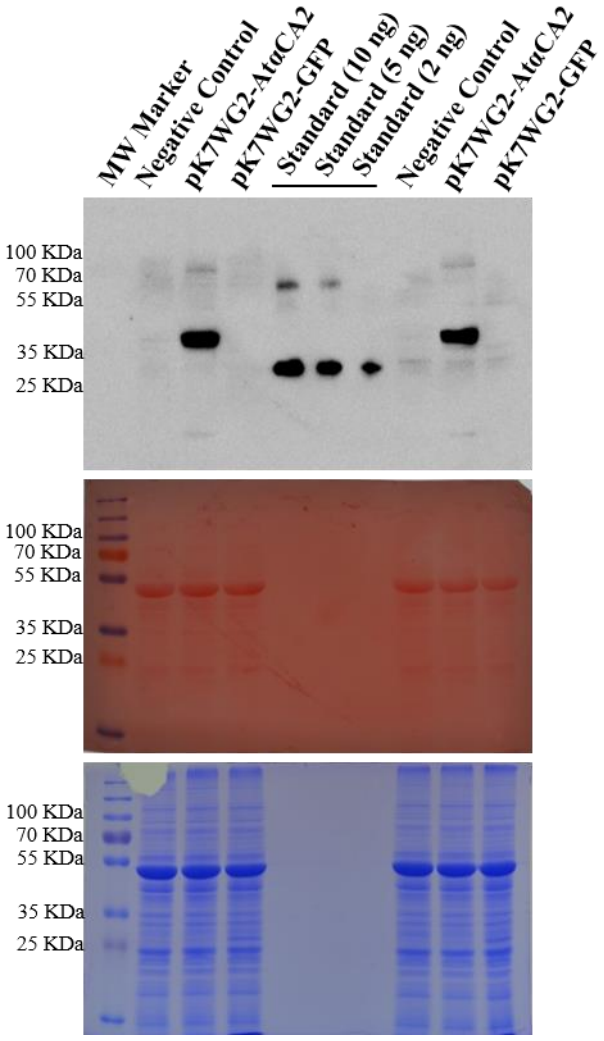

Figure 18. Estimation of protein expression level in agroinfiltrated *N.bethamiana* leaves by using the pK7WG2-AtαCA2 construct

Total protein extracts from *N. benthamiana* leaves agroinfiltrated with pK7WG2-AtαCA2 construct and harvested 40hpi were separated on SDS-PAGE and then analysed by westrn blotting using an anti-FLAG antibody. Protein extracts were also prepared from non agroinfiltrated leaves (negative control) and from leaves infiltrated with pK7WG2-GFP. Two independent experiments are shown. Densitometric analysis was performed to estimate protein expression using FLAG tagged AtαCA2 produced in *E. coli* at known concentration at different dilution as standard.

Quantification of protein level was also performed for samples collected from *N. benthamiana* leaves infiltrated with Agrobacyerium carrying the pGR106new construct by using the same procedure. A comparable amount of protein expression (7,5 ug per gram of fresh weight) was extimated in plant tissue. Moreover, attempts to purify the AtαCA2 protein either from whole plant tissue or purified thylakoids membranes yielded even lower amount of protein (~1.26 ug recombinant AtαCA2 per gram of fresh weight in best cases). As some milligram of recombinant AtαCA2 is required to test its NO production from nitrite by using chemiluminescence, we estimated the amount of expressed protein in plant tissue with this transient system too low and decided no to proceed further with protein purification.

4.2 Nitric oxide synthesis during the HR: characterization of plant beta and gamma carbonic anhydrase as candidate enzymes for nitric oxide production from nitrite

4.2.1 Selection of tobacco NtβCA1, Arabidopsis AtβCA1 and AtγCA2 carbonic anhydrases as candidates for the characterization

In higher plants, differently from mammalian, majority of soluble carbonic anhydrase activity is ascribed to the β-class of carbonic anhydrases (β-CAs), a class of independently evolved enzymes with CA activity (Majeau et al., 1994; Price et al.,1994). This class is constituted of six genes in *Arabidopsis thaliana* (Table 3). Encoded proteins show distinct primary amino acid sequences compared to bovine CA, but partially conserved residues in the catalytic domain (Figure 19, Kimber and Pai, 2000; Rowlett, 2010). Among genes in this class, litterature data provided indication about the involvement of the tobacco and Arabidopsis carbonic anhydrase enzyme SABP3s (respectively NtβCA1 and AtβCA1) in immunity. Indeed, these genes were required for hypersensitive cell death and/or immunity response (Slaymaker et al.,2002; Wang et al.,2009). Therefore, even if AtβCA1 was down-regulated by avirulent pathogen infection (Figure 20), these two gene were selected according to literature to test the possibility that enzymes belonging to β-class of carbonic anhydrases are responsible for nitrite to nitric oxide conversion expecially in the HR, similarly as shown for bovine alphaCA.

Table 3. The *Arabidopsis thaliana* βCA gene family

	AGI number	**Name**
β CA gene family	At3g01500	AtβCA1
	At5g14740	AtβCA2
	At1g23730	AtβCA3
	At1g70410	AtβCA4
	At4g33580	AtβCA5
	At1g58180	AtβCA6

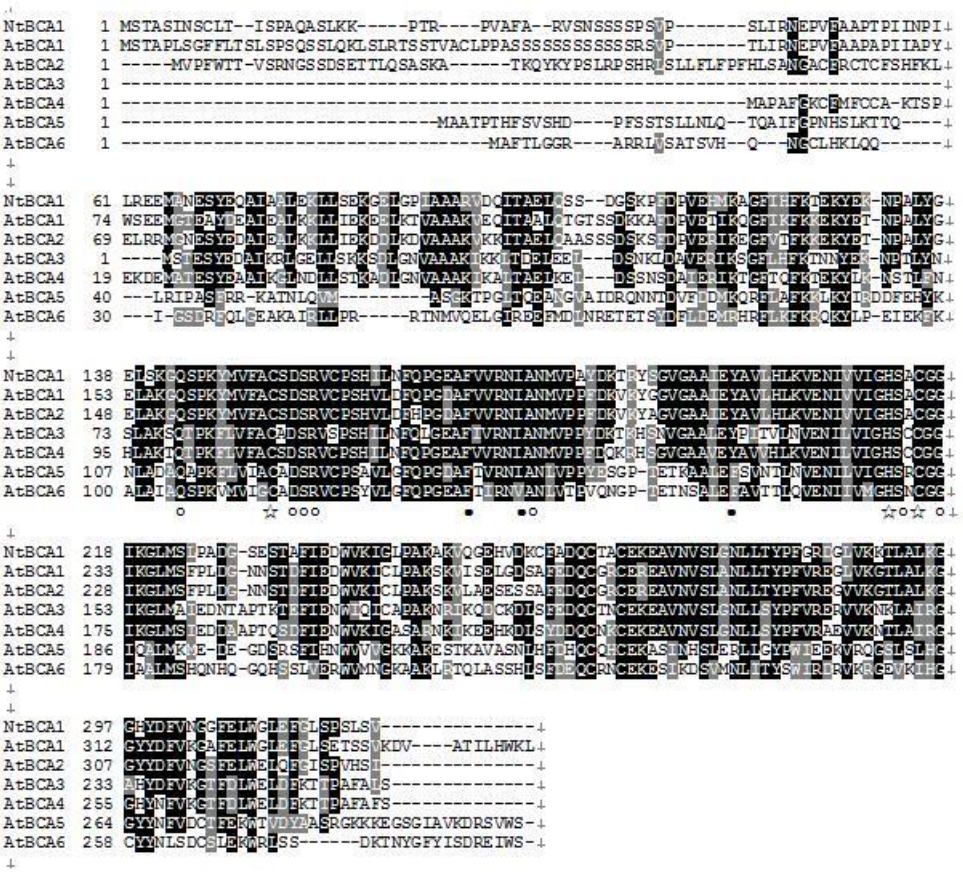

Figure 19. Amino acid sequence alignment of Arabidopsis βCAs and tobacco NtβCA.
Multiple alignment was processed using Clustal Omega and further formatted using the BoxShade programs. Conserved and similar amino acids are shown with blank-shaded and grey-shaded boxes and gaps introduced to maximize the alignment are indicated by hyphens (−). The cysteine and histidine residues ligated to Zn ion are denoted as stars. Residues that interact with H_2O and assist in charging Zn ion with a hydroxyl are marked by white circles. Residues composing the CO_2 hydrophobic pocket are indicated with black circles.

In plant, a further family of carbonic anhydrases exists, the γCA gene family (Parisi et al.,2004). However, no real carbonic anhydrase activity was shown so far for proteins belonging to this family, even though residues for zinc coordination are found in γCAs (Kisker et al., 1996. Figure 21). These proteins are mainly targeted to the mitochondria and are supposed therefore to have structural function.

In Arabidopsis, there are three genes encoding γCA and two genes encoding γCA-like proteins (Table 4). γCAs are more similar to each other at the amino acid sequence level (Figure 21) , even though they show no similarity with bovine αCAs. All γCAs and γCA-likes were up-regulated by avirulent pathogen infection (Figure 20).

Recombinant AtγCA2 protein was already expressed in several studies and showed higher induction following pathogen infection (Perales et al.,2005; Sunderhaus et al., 2006; Villarreal et al.,2009). Therefore, we selected AtγCA2 as a representative of plant γCA for our characterization.

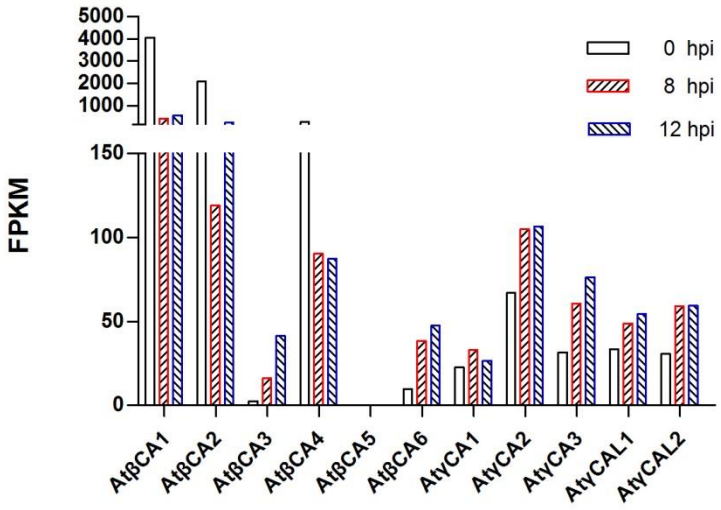

Figure 20. Expression of βCA and γCA gene family members in Arabidopsis leaves infiltrated with avirulent pathogen *Pseudomonas syringae* pv *tomato* carrying AvrB at 0, 8 and 12 hours post infection.

Arabidopsis thaliana Col-0 leaves were infiltrated with $5x10^6$ cfu/ml of *Pst* AvrB. RNASeq libraries were produced from leaves sampled at indicated times after infection. Expression levels as FPKM (Fragments per Kilobase per Million Reads) deduced from these samples (Jingjing Huang unpublished results) are plotted for each CA family member.

Table 4. The *Arabidopsis thaliana* γCA gene family

	AGI number	**Name**
γCA gene family	AT1G19580	AtγCA1
	AT1G47260	AtγCA2
	AT5G66510	AtγCA3
	AT5G63510	AtγCAL1
	AT3G48680	AtγCAL2

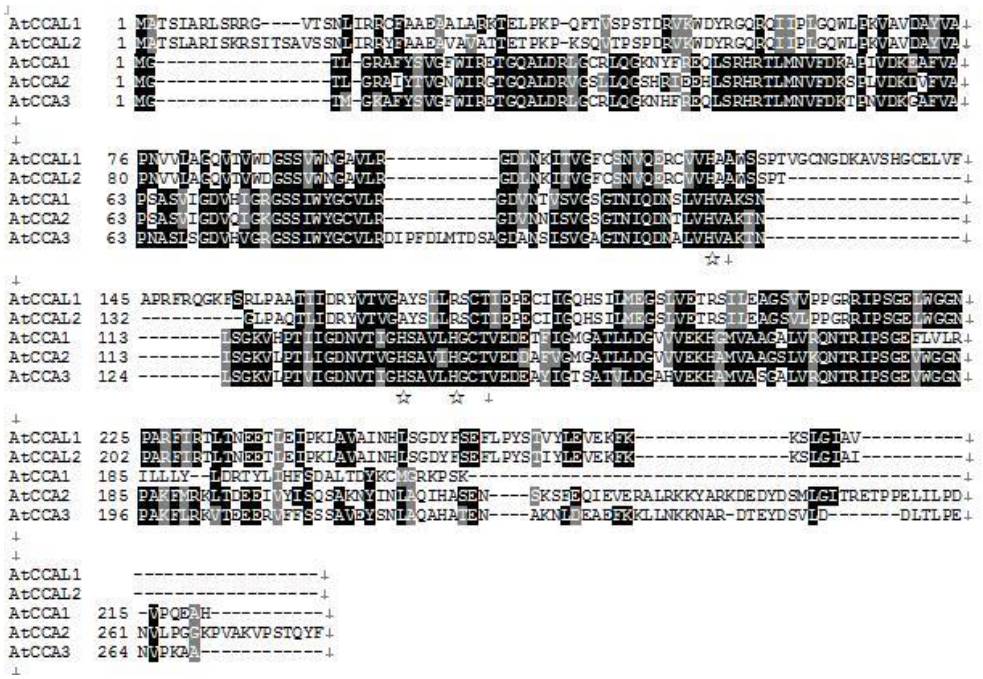

Figure 21. Amino acid sequence alignment of Arabidopsis γCAs and γCALs.

Multiple alignment was processed using Clustal Omega and further formatted using the BoxShade programs. Conserved and similar amino acids are shown with blank-shaded and grey-shaded boxes and gaps introduced to maximize the alignment are indicated by hyphens (−). The histidine residues ligated to Zn ion are denoted as stars.

4.2.2 Production of recombinant beta and gamma carbonic anhydrases

The coding sequences of selected genes NtβCA1, AtβCA1 and AtγCA2 without the predicted signal peptide (Table 5) were cloned into the expression vector pET28a to produce in-frame fusion proteins with the 6xHis tag.

The expression of the recombinant His-NtβCA1, His-AtβCA1 or His-AtγCA2 in *E.coli* BL21 cells containing pET28a-NtβCA1, pET28a-AtβCA1or pET28a-AtγCA2 constructs was induced by using different temperatures and induction times in order to identify best conditions for accumulation of proteins in soluble fractions. More in detail, the recombinant His-NtβCA1 was expressed in both insoluble and soluble fractions of *E.coli* cells after induction for 4 h at 21 ℃ (Figure 22, expected size 26k Da). The recombinant His-AtβCA1 was instead mainly expressed in insoluble fraction (Figure 23, expected size 31 kDa) and this was independent of time and temperature

conditions used for induction. Finally, the recombinant His-AtγCA2 was mainly expressed in soluble fraction after induction for 18 h at 21 ℃ (Figure 24, expected size 21 kDa).

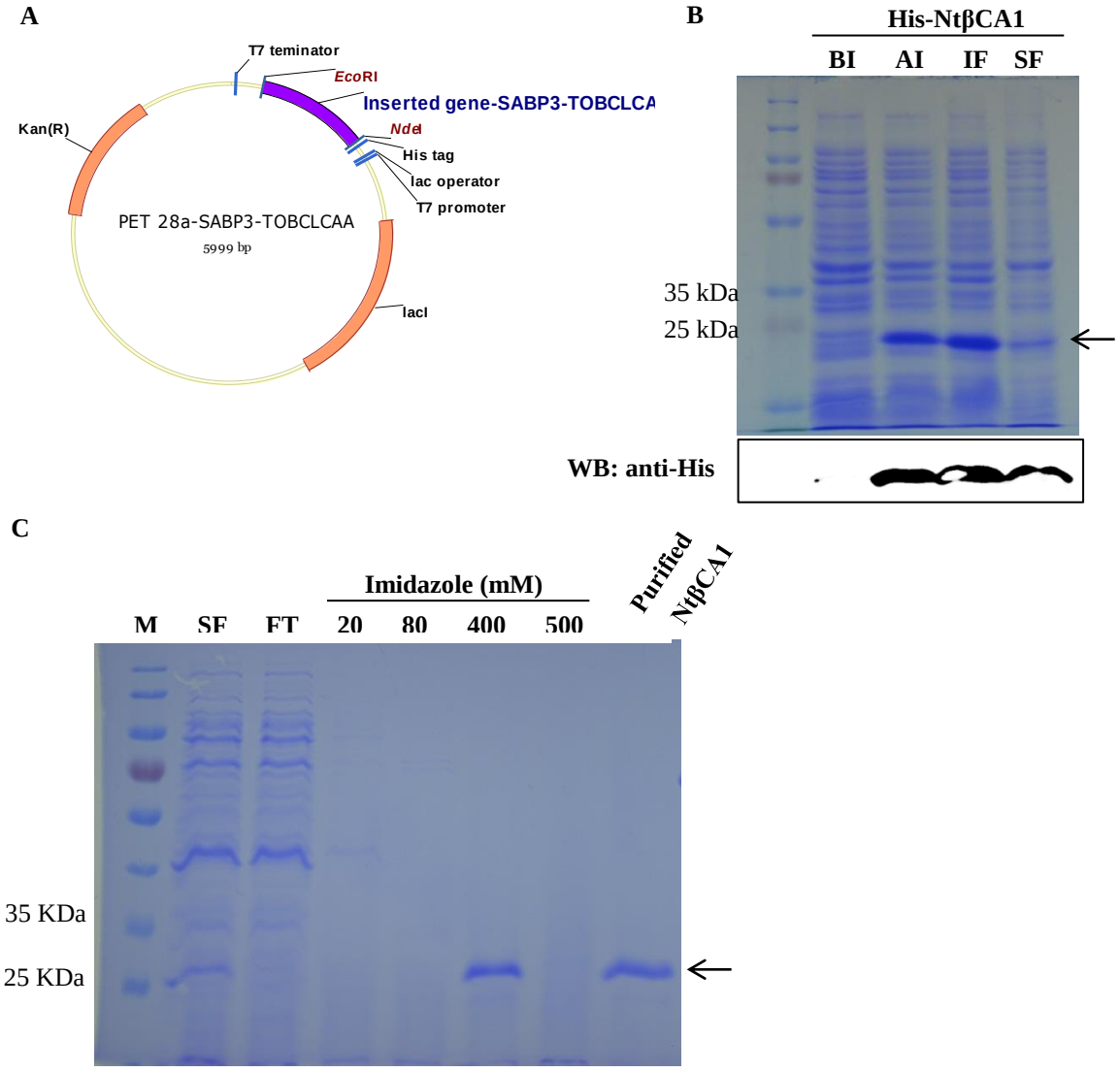

Figure 22. Production of the recombinant NtβCA1 in *E.coli*

A. Map of the construct pET28a-NtβCA1 prepared for the expression of the His tagged recombinant protein in *E. coli*.

B. Expression of the recombinant protein in *E.coli*. Comassie stained gels and Western blot, by using an α-His antibody, for total cell proteins before induction (BI) or after induction (AI) and insoluble or soluble protein fractions (IF, SF) derived from equal volumes of *E. coli* BL21 cell lysate are shown. Protein expression was induced for 4h at 21 ℃.

C. Purification of recombinant NtβCA1. Fractions were collected from Ni-NTA agarose resin washed with elution buffer containing different concentrations of imidazole as indicated. Imidazole was removed from elution fraction with most of recombinant NtβCA1 through buffer change. SF, soluble fraction. FT, flow through.

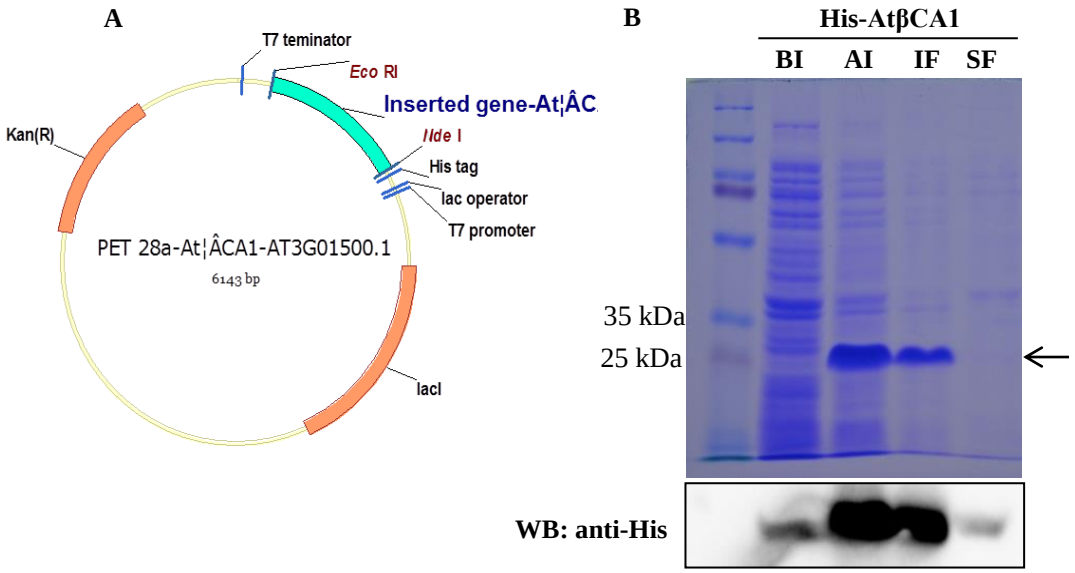

Figure 23. Production of the recombinant AtβCA1 in *E.coli*

A. Map of the construct pET28a- AtβCA1 prepared for the expression of the His tagged recombinant protein in *E. coli*.

B. Expression of the recombinant protein in *E.coli*. Comassie stained gels and Western blot, by using an α-His antibody, for total cell proteins before induction (BI) or after induction (AI) and insoluble or soluble protein fractions (IF, SF) derived from equal volumes of *E. coli* BL21 cell lysate are shown. Protein expression was induced here for 4h at 21 ℃. Induction for longer times (18 h) either at 21 ℃ or 16 ℃ did not improve the amount of protein in the soluble fraction.

Table 5. Signal pepetide and subcellular location prediction for selected β and γ CA by Target P v1.1 program

Name	Len	cTP	mTP	SP	other	Loc	RC	TPlen
NtβCA1	321	0.966	0.052	0.015	0.036	C	1	62
AtβCA1	347	0.977	0.044	0.005	0.013	C	1	47
AtγCA2	278	0.038	0.921	0.008	0.210	M	2	43

Protein sequence analysis was performed by using the TargetP software (http://www.cbs.dtu.dk/services/TargetP/). cTP: chloroplast transit peptide, mTP: mitochondrial transit peptide, SP: secretory pathway signal peptide, C: chloroplast, M: mitochondria, TPlen: transit peptide length.

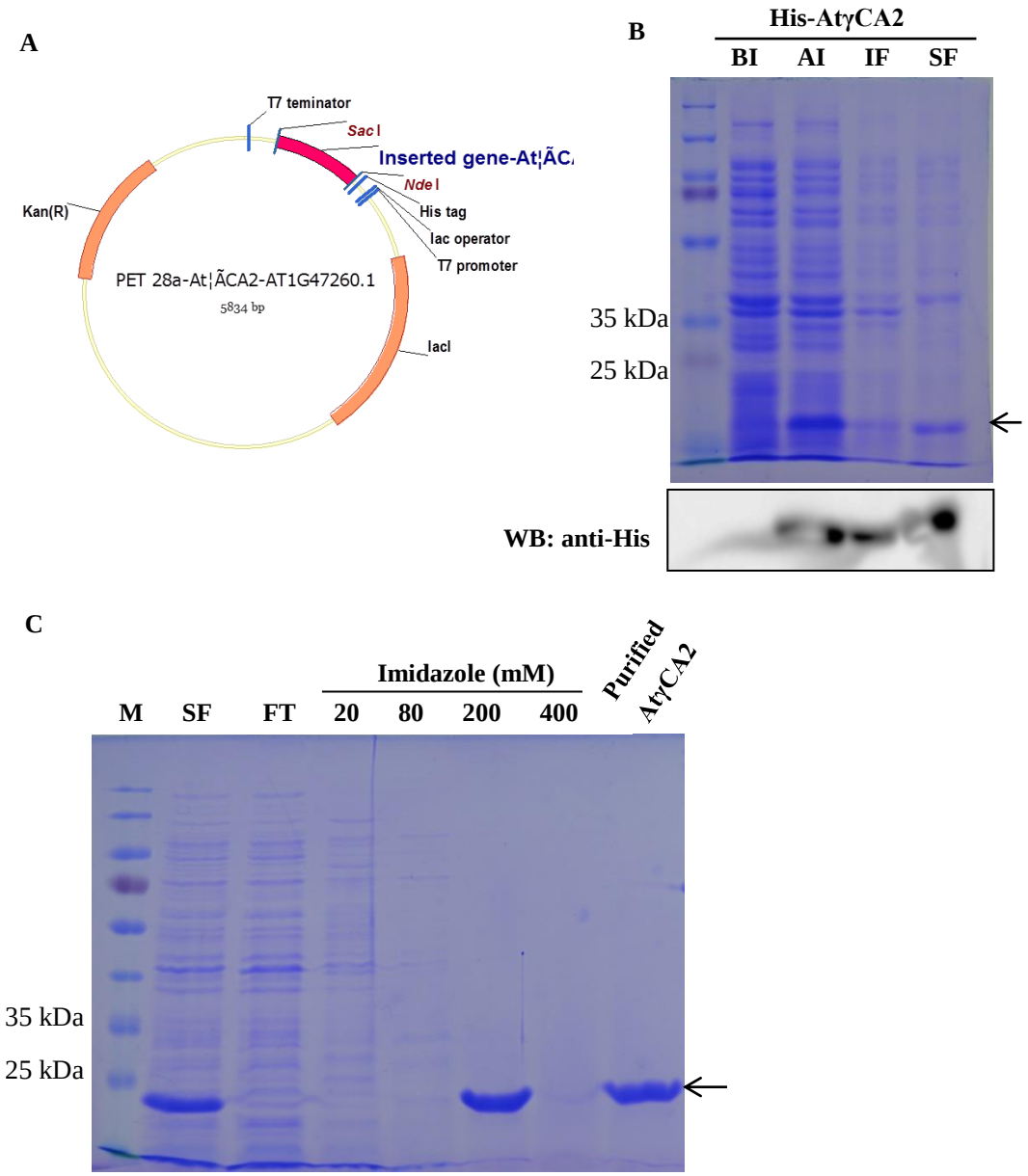

Figure 24. Production of the recombinant AtγCA2 in *E.coli*

A. Map of the construct pET28a- AtγCA2 prepared for the expression of the His tagged recombinant protein in *E. coli*.

B. Expression of the recombinant protein in *E.coli*. Comassie stained gels and Western blot, by using an α-His antibody, for total cell proteins before induction (BI) or after induction (AI) and insoluble or soluble protein fractions (IF, SF) derived from equal volumes of *E. coli* BL21 cell lysate are shown. Protein expression was induced for 18h at 21 ℃.

C. Purification of recombinant AtγCA2. Fractions were collected from Ni-NTA agarose resin washed with elution buffer containing different concentrations of imidazole as indicated. Imidazole was removed from elution fraction with most of recombinant AtγCA2 through buffer change. SF, soluble fraction. FT, flow through.

Soluble fractions containing respective recombinant proteins were used for purification of His-NtβCA1 and His-AtγCA2. Since recombinant His-AtβCA1 was instead mainly expressed in insoluble fraction, we did not proceed with protein purification for this. The elution fraction with the highest amount of recombinant proteins was subjected to buffer exchange to remove imidazole. The purity of the purified His-NtβCA1 or His-AtγCA2 was high as shown in SDS-PAGE analysis (Figures 22 and Figures 24). Estimated yield was about 4 mg/liter for His-NtβCA1 and 3 mg/liter for His-AtγCA2.

4.2.3 Carbonic anhydrase activity of recombinant NtβCA1 and AtγCA2

To verify that recombinant proteins were produced in their active form, the carbonic anhydrase activity was first determined.

As expected (Slaymaker et al.,2002), the purified NtβCA1 showed carbonic anhydrase activity (Figure 25), indicating that NtβCA1s have the correct active conformation and can be used for further analysis. Consistent with previous results (Perales et al.,2005), no carbonic anhydrase activity was detected instead for the AtγCA2 recombinant protein produced in *E.coli*, even if sequence comparison and computer modeling would support a possible carbonic anhydrase activity for AtγCA2.

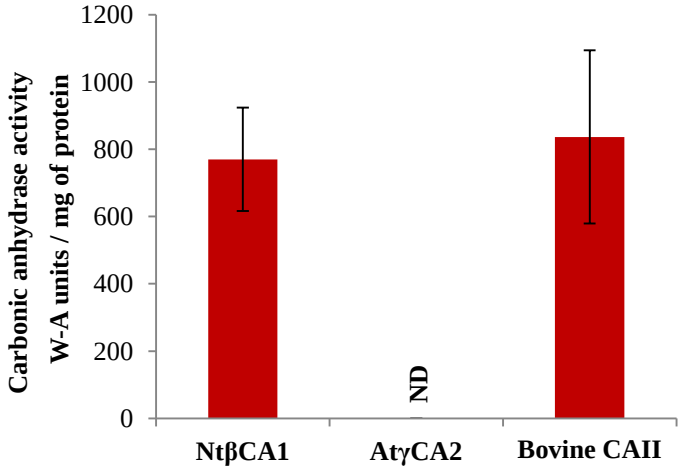

Figure 25. Carbonic anhydrase activity of recombinant NtβCA1 and AtγCA2 purified from *E. coli.*

Carbonic anhydrase activity was tested by the Wilbur Anderson protocol and plotted as average W-A units for mg of protein (n=5, ± SD). Commercial bovine αCA II was used as a control.

ND: not detected

4.2.4 NO production from nitrite by recombinant NtβCA1 and AtγCA2

Both proteins were then used for testing their ability to produce NO from nitrite. NO was measured by using a chemiluminescence based NO detector (CLD88E Ecophysics) coupled to a glass vial for reactions in solution fluxed with air. The bovine CAII, as expected, gave a clear NO signal. However, no NO signal could be detected for recombinant NtβCA1 and AtγCA2 proteins in our experimental conditions (Figure 26).

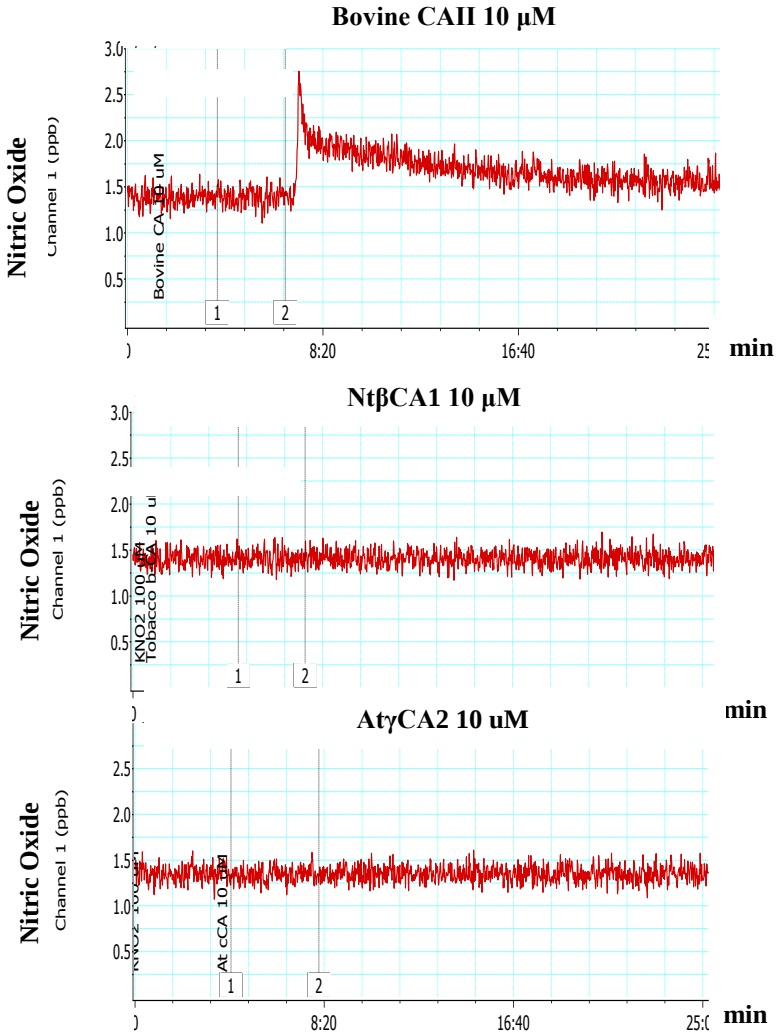

Figure 26. NO production activity of recombinant NtβCA1 and AtγCA2 from nitrite measured by chemiluminescence.

Reaction was performed in 3 ml final reaction volume in 10 mM phosphate buffer in a glass vial coupled to the NO detector. 100 uM KNO_2 was first added and then protein was injected to provide a final concentration equal to 10uM (Aamand et al., 2009). Bovine CAII was used as a positive control. Recorded NO traces content in air along time are shown (Ppb: parts per billion of NO in air gas).

4.3 Nitric oxide signaling during the HR-cell death: transcriptomic changes associated to NO induced cell death

4.3.1 Establishing NO fumigation conditions triggering cell death in Arabidopsis plants

Beside working on possible mecchanisms involved in NO production during the HR, we were also interested in investigating the downstream NO signaling following the NO burst induced by the pathogen recongnition and in particular the signaling involved in the cell death triggering. To this aim, we decided to set up an experimental approach, based on transcriptomic analysis, to identify transcriptomic changes associated the NO burst and more specifically to the NO triggered cell-death.

NO accumulation in the HR is well documented (Delledonne et al., 1998; Chen et al., 2014). This burst usually lasts a few hours after pathogen recognition and is required for the development of cell death associated to the HR. We decided to take advantage of a fumigation system, which was previously established in our lab, to treat plants with know amount of NO triggering cell death, to mimic this burst without pathogen infection, thus focusing specifically on the transcriptomic changes associated to the NO burst and consequent cell death development.

Conditions triggering cell death on four-weeks-old *Arabidopsis thaliana* Col-0 plants were previously established (Zahra Imanifard, PhD thesis). Here, we applied the same NO treatment (200 ppm for 8 hours) to six-weeks-old Arabidopsis Col-0 plants and showed that such treatment was leading to HR also in older plants. In Figure 27, visual cell death symptoms 48 hours after fumigation on plants treated with NO can be observed. As comparison, we lowered either the time for NO fumigation or the NO concentration and found that no obvious cell death was observed in leaves fumigated for 3 hours with NO at 100 ppm or for 4 hours with NO at 200 ppm. Partial cell death was triggered instead in leaves fumigated for 6 hours with NO at 200 ppm.

To validate these observations, cell death visual symptoms were correlated with the results of a test for quantitative assessment of cell death on leaf discs, the ion leakage

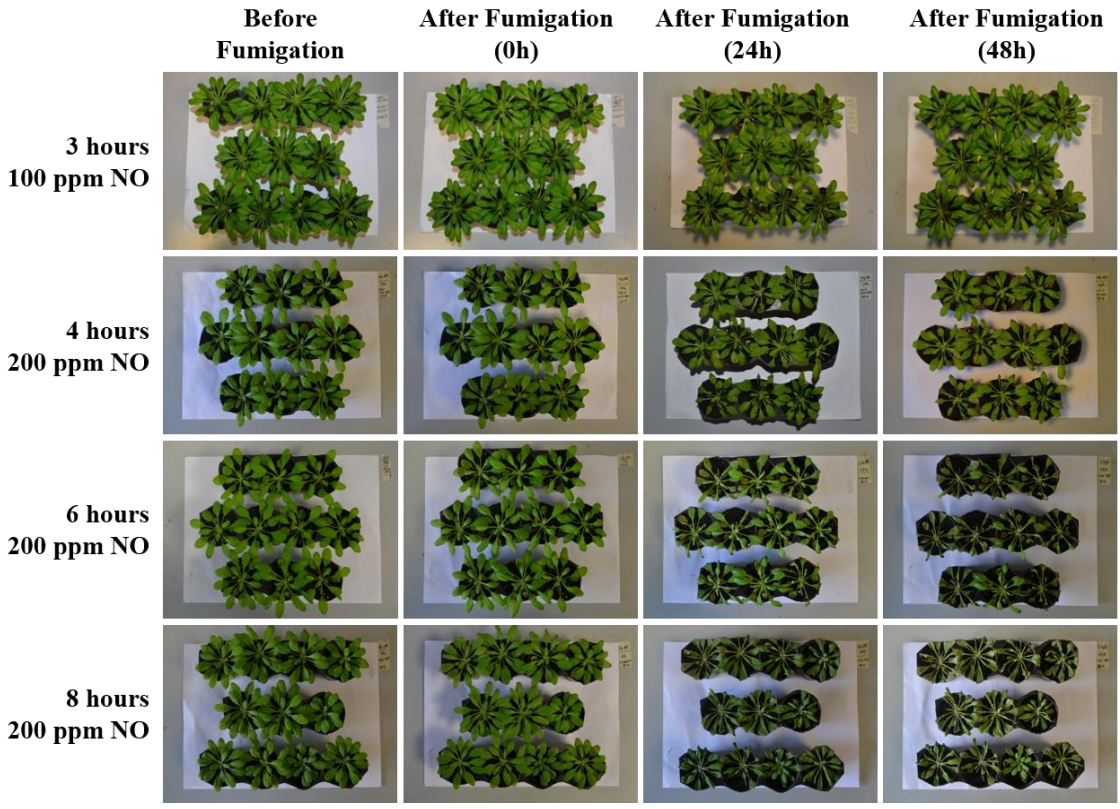

Figure 27. Visual sympthoms of NO fumigation-induced cell death in six-week-old Arabidopsis Col-0.

Six weeks old Arabidopsis plants were treated with NO by using a fumigation chamber system for time indicated and with indicated amounts of NO (ppm of NO in air). Photos were taken before fumigations, immediately after fumigation and then after 24 hours and 48 hours.

assay. Indeed, the cell death in plant tissues is accompanied by the loss of electrolytes from dying cells due to membrane injury and measurement of ion leakage from plant tissues allows to evaluate cell death. Therefore, leaf disks were produced from leaves subjected to the different NO treatments previously described, and release of ion in solution was then quantified along time. As shown in Figure 28, no significant difference in ion leakage was found between tissues fumigated either for 3 hours or 4 hours with NO at 100 ppm or 200 ppm and untreated tissues. However, 6 hours or 8 hours of NO fumigation at 200 ppm strongly increased the ion leakage, indicating that cell death was triggered by both treatments, even thought the careful inspection of visual symptoms indicated a much uniform cell death in tissues for the 8 hours treatment with NO.

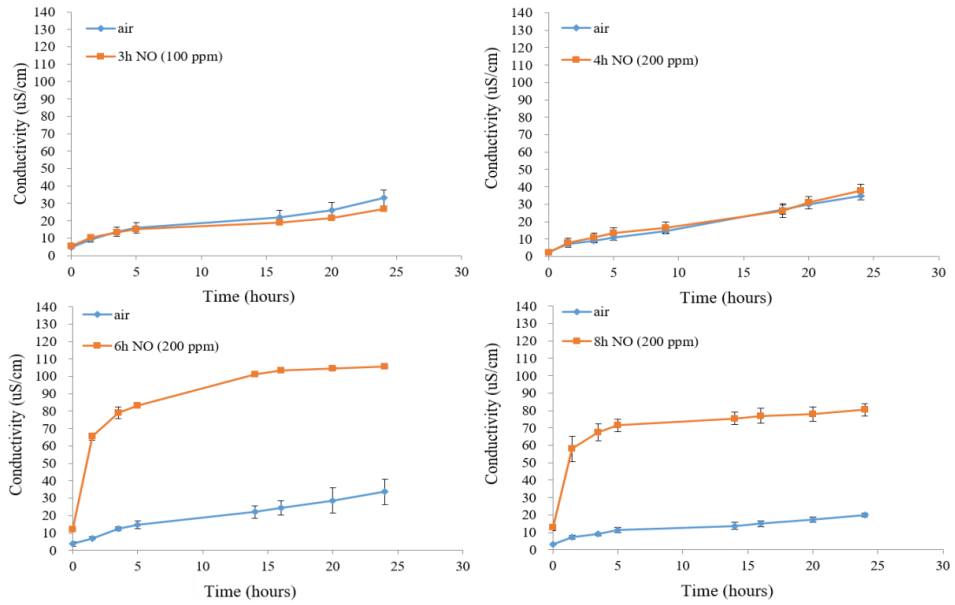

Figure 28. **Ion leakage assays to assess cell death in Arabidopsis adult leaves triggered by different NO treatment conditions**.

Different NO fumigation conditions were applied to 6 weeks old Arabidopsis plants Col-0 as indicated in legends. After fumigation leaf discs from fully expanded leaves were used for the ion leakage assay to quantify cell death. Conductivity (uS/cm) in water is measured along time. Values are average of n=3 ± SD. The experiment was repeated twice.

4.3.2 Transcriptomic changes triggered by NO fumigation conditions inducing cell death

Once conditions for the uniform NO-triggering of cell death were established, a gene expression analysis by RNASeq was performed to identify genes induced or repressed by the treatment and therefore possibly involved in NO mediated cell death. Fully expanded Arabidopsis leaves were harvested for RNA extraction immediately after NO fumigation for 8 h with NO (200 ppm). Untreated plants were used as control sample. For each condition, three independent samples were harvested as biological replicates.

Sequencing library were prepared for each sample in collaboration with the Functional Genomic Centre at the University of Verona and sequenced with an Illumina sequencer. Untreated and NO fumigated samples provided complexively 145045586 and 58841352 paired-end 100 bp reads, respectively.

Table 6. Statistics of RNASeq sequencing. For each sample total number of reads obtained as well as mapped (unique position or multi mapped) and unmapped reads are indicated.

Sample name	Treatment	Replica	Total reads	Unique Mapped	Multi mapped	Unmapped
NO_untreated	Untreated	1	24287344	22082550 (90.922%)	1425800 (5.87055%)	778994 (3.20741%)
	Untreated	2	50287688	47162438 (93.7853%)	1027025 (2.0423%)	2098225 (4.17244%)
	Untreated	3	70470554	65699523 (93.2298%)	997326 (1.41524%)	3773705 (5.35501%)
NO_8h200ppm	200ppmNO_8h	1	23871782	22402371 (93.8446%)	492732 (2.06408%)	976679 (4.09135%)
	200ppmNO_8h	2	16295289	15164743 (93.0621%)	501350 (3.07666%)	629196 (3.86121%)
	200ppmNO_8h	3	18674288	17586864 (94.1769%)	341601 (1.82926%)	745823 (3.99385%)

Up to 93.79% and 94.18% mapped on genome by using *A. thaliana* TAIR10 reference genome. Even though the full number of reads was different in untreated samples and NO treated samples, samples could be properly distinguished as seen in Figure 29.

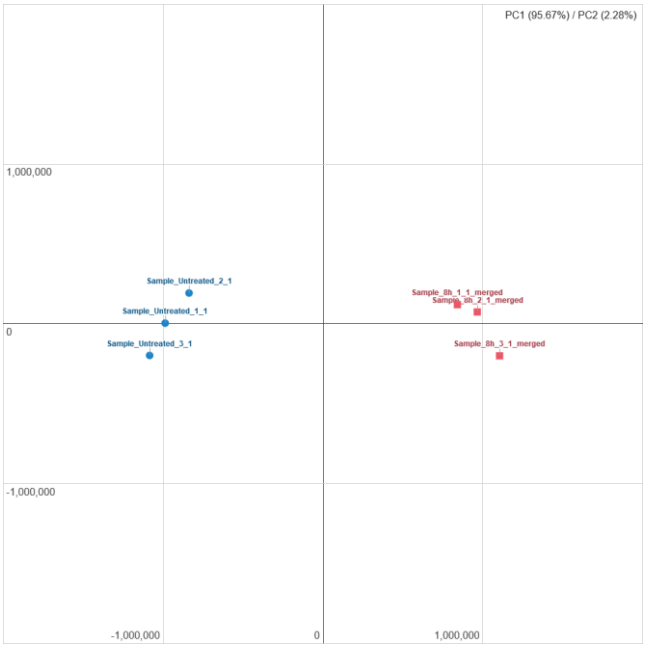

Figure 29. Principal Component Analysis (PCA) on normalized gene expression values. X- and Y-axes show the PC1 and PC2 (amount of variance explained by each component in parenthesis). Each point represents a sample, dots of the same colors are replicates of a same experimental group.

Differential gene expression analysis was performed by using the DESeq2 software. This analysis revealed that among 18690 expressed genes, 15416 were significantly differentially expressed in NO fumigated Arabidopsis leaves compared with untreated leaves, thus revealing a major transcriptome modulation upon NO treatment.

By setting as threshold (log_2FC)>1,5 and (log_2FC)<-1,5, we focused on the 4678 most upregulated and 5960 most downregulated genes.

Gene enrichment analysis on the most upregulated genes showed the functional class "response to stimulus" as the most enriched one (Figure 30). This included in more detail genes involved in response to endogenous as well as extracellular stimuli and genes involved in abiotic and biotic stress responses. These genes encoded mainly transcription factors and proteins involved in signaling, including receptors, kinases and phosphatases. Many genes commonly involved in plant response to pathogens or hormones, as well as redox or other stresses were included. Interestingly, genes encoding for marker proteins for HR or autophagy related, senescence associated, or involved in cell death were found in these enriched classes as well. Enrichment in functional classes associated to ongoing "cellular and biological processes" and its regulation were also found. This included again many genes involved in cellular communication and signal transduction. Furthermore, we found enrichment in functional classes for "cellular metabolic processes" which included genes encoding for proteins involved in proteins modifications, mainly phosphorylation or ubiquitination, and in modification of nucleobase containing compounds, which included beside transcription factors also genes involved in the modulation and processing of nucleic acids. Finally, our enrichment analsyis of upregulated genes highlighted an enrichment also in functional classes for "establishment of localization", "transport" or "catabolic processes" and "cell death".

Gene enrichment analysis on the most downregulated genes showed that several of the functional classes enriched in the most upregulated genes were represented in the most downregulated genes too, thus confirming the relevant NO effect on genes belonging to these functional classes (Figure 31). In particular, we found again an

enrichment in the functional class “response to stimulus” including genes involved in response to abiotic or endogenous stimulus encoding for hormones receptors, other receptors, kinases and transcription factors.

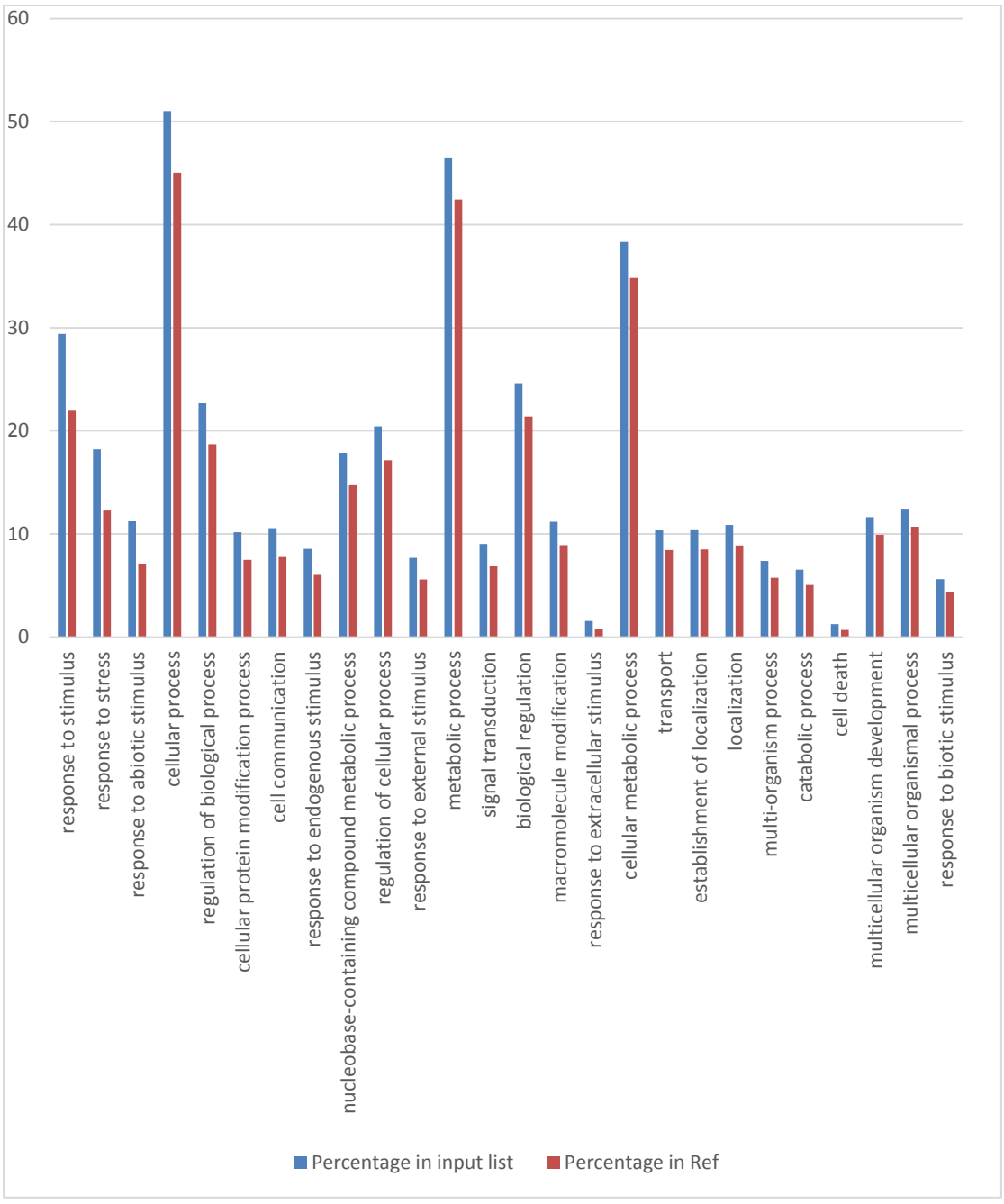

Figure 30. **Gene enrichment analysis of gene ontologies functional classes in genes upregulated by the NO treatment**

Percentage of genes belonging to each enriched gene ontology functional class (biological process, GO slim annotation) was plotted beside the percentage of genes belonging to the same class in the reference annotated genome (TAIR10). Enrichment analysis was performed by the on-line AgriGO software version 2.0 (http://bioinfo.cau.edu.cn/agriGO/).

Furthermore, we found the functional class “regulation of cellular processes”, which was also found enriched in upregulated genes, including similar kind of genes. However, the enriched functional class “metabolic and cellular processes” included different genes compared to the genes found in the corresponding class in upregulated genes. Indeed, we found an enrichment in genes involved in photosynthesis and energy precursors, as well as genes involved in carbohydrates and lipids metabolism.

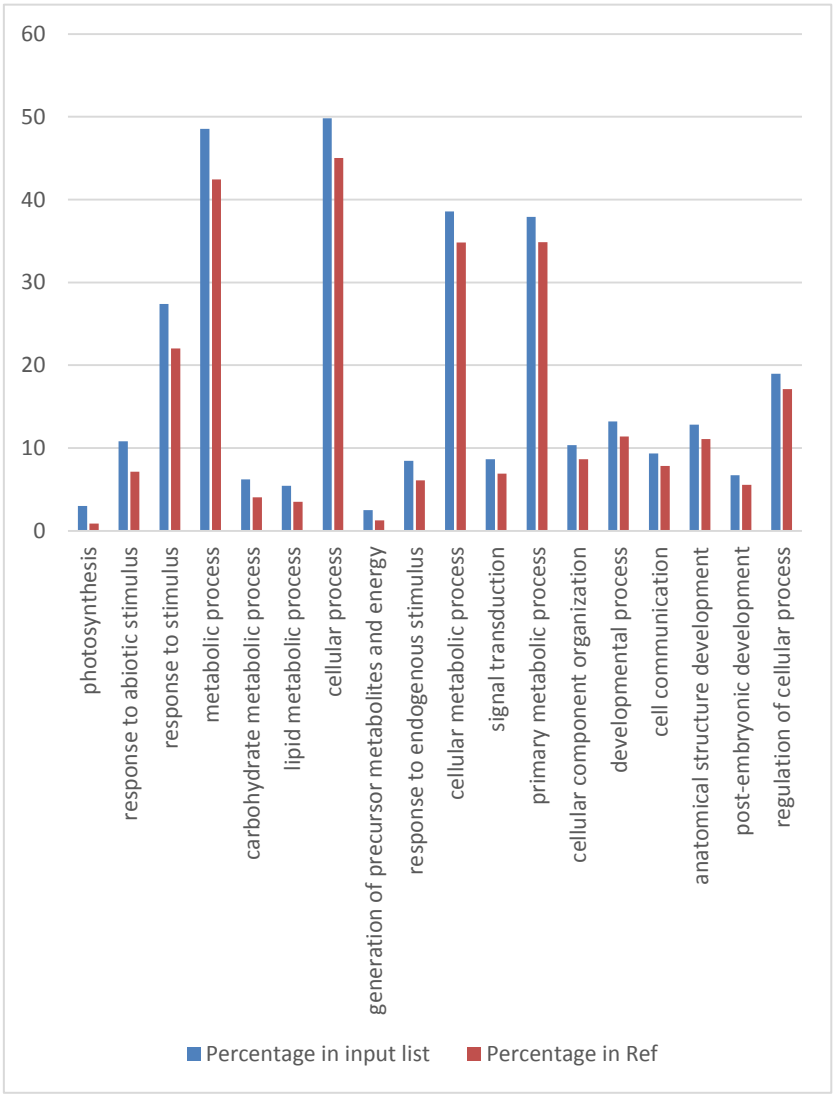

Figure 31. Gene enrichment analysis of gene ontologies functional classes in genes downregulated by the NO treatment

Percentage of genes belonging to each enriched gene ontology functional class (biological process, GO slim annotation) was plotted beside the percentage of genes belonging to the same class in the reference annotated genome (TAIR10). Enrichment analysis was perfomed by the on-line AgriGO software version 2.0 (http://bioinfo.cau.edu.cn/agriGO/).

Interestingly, genes involved in lipid metabolism were mainly related to fatty acid synthesis, steroid metabolism and synthesis and metabolism of phospholipids.

Finally, we also found an enrichment in the functional class “development” including again many genes involved in the cellular communication, but also genes involved in development of specific anatomic structure and related to post-embrionic development.

Differently from up regulated genes, we did not find an enrichment in genes involved in cell death regulation in genes downregulated by NO treatment. The complete list of DEG genes upregulated by the cell death inducing NO treatment belonging to the functional class “cell death” is provided as Supplemental table 1. The full list includes 93 genes which have been related to cell death processes. Moreover, among these, 57 genes showed a Log_2FC higher than 1,5.

5. Discussion

Nitric oxide is a gas molecule which is crucial as signaling molecule in hypersensitive cell death (Yu et al.,2014). Since its first discovery in plants during plant pathogen interaction in the late nineties (Delledonne et al., 1998), many studies have focused on this signaling molecule, attempting to clarify its production and function in plant pathogen interaction but also in several additional contexts, like seed germination, plant development, flowering or response to abiotic stresses, to name a few. Despite intensive studies, NO production in plants is still not fully understood and remains one of the most challenging issues of the field. NO synthesis in plants can be schematically achieved via two main routes defined by their chemical properties, one reductive and one oxidative. The reductive routes concern the reduction of nitrite. To date, this reductive route is the most firmly described and evidenced synthesis pathway for NO in plants. However, the first discovered NO production activity in plant was through the oxidative pathway (Corpas et al., 2004), but still after many years no enzyme involved in this activity could be found by any of the several approaches applied (Jeandroz et al., 2016, Santolini et al., 2017). Moreover, the enzymes specifically involved in the reductive pathway are still largely questioned. While the NR can definitely catalyse the NO production from nitrite as side reaction, the relevance of this reaction in *in vivo* plant cell conditions is still under debate. Furthermore, additional enzymes which could catalyse this reaction mainly work under anaerobiosis and thus their relevance in the frame of the plant pathogen interaction is also unclear.

Recently, it was reported that bovine carbonic anhydrase II can produce NO from nitrite under normoxia conditions and this activity is enhanced by CA activity inhibitors (Aamand et al., 2009). Applying CA inhibitor dorzolamide slightly increased NO production during potato - *P. infestans* incompatible interaction at 3hpi, suggesting a possible functional link between CA and NO production in plants (Floryszak-Wieczorek and Arasimowicz-Jelonek, 2017). This prompted us to explore if plant carbonic anhydrases can directly produce NO from nitrite, especially during HR.

The bovine carbonic anhydrase II enzyme belongs to α-type carbonic anhydrase, while there are three types of carbonic anhydrases in higher plants (Moroney et al.,2001). The model plant Arabidopsis genome contains eight genes encoding for αCA (Fabre et al., 2007). However, only AtαCA1-3 genes have complete expressed sequence tags (ESTs) (Di Mario et al., 2016). Accordingly, inspection of RNASeq data in *Arabidopsis thaliana* either untreated or treated with the plant pathogen *Pseudomonas syringae* at 8 or 12 hpi (Jingjing Huang unpublished results) confirmed very low constitutive expression and expression upon treatment for six genes in this family (AtαCA3-8). Moreover, the AtαCA8 contains an early in-frame stop codon and is therefore considered as a pseudogene (DiMario et al., 2016). AtαCA1 was instead constitutively expressed in leaves at higher levels but its expression was strongly reduced by the pathogen treatment, while AtαCA2 was not constitutively expressed but was up-regulated significantly in response to avirulent bacteria, suggesting its possible involvement in hypersensitive defense response. Literature data are scarce about this gene family, and so far this specific protein (AtαCA2) was only shown to participate together with αCA4 in photosynthetic reactions (Zhurikova et al., 2016). Here, we aimed at enquiring then whether this protein could catalyze NO production, as shown for the bovine carbonic anhydrase II, being thus involved in plant defense.

Previous studies on AtαCA1 protein showed that this protein was targeted to chloroplast through a newly discovered secretory pathway, which is alternative to the traditional Toc/Tic complex that mediates delivery of nuclear proteins to the chloroplast, and that glycosylation was required for its folding, ER-export and carbonic anhydrase activity (Villarejo et al., 2005; Buren et al.,2011). AtαCA2 has a strong similarity with AtαCA1, sharing in particular a high similarity transit peptide and glycosylation sites according to *in silico* prediction. Thus, it is also likely to be targeted to chloroplast and to require glycosylation. Indeed, we found that its overexpression in *E.coli*, which lacks the N-glycosylation, leads to a protein which showed no carbonic anhydrase activity. Therefore, in order to produce a functional protein to be tested for its NO production activity we attempted to take advantage of

an alternative expression system, able to support protein glycosylation. We chose to express the protein transiently in plants. More in detail, we expressed AtαCA2 in *Nicotiana benthamiana* leaves by using two different binary vectors, one acting through a viral vector. However, the protein expression level was comparable in the two different systems. Endo H treatment of expressed proteins proved that AtαCA2 was a glycoprotein. According to our findings, AtαCA2, in its glycosylated form, was targeted to thylakoids or was associated to thylakoids membranes. Therefore, we evidenced a different targeting inside chloroplast for AtαCA2 compared to AtαCA1, which was instead targeted to chloroplast stroma. However, this finding is consistent with the finding reported in Zhurikova et al. 2016. Indeed, the authors characterized the photosynthetic yield of the *AtαCA2* knock-out Arabidopsis mutant, and, according to the results, proposed that this gene could be involved in photosynthetic electron transport chain functioning under illumination and in the protonation of PsbS, being therefore localized closed to photosystem II or PsbS in thylakoid membranes. Accordingly, a CA activity was indeed already reported in thylakoid membranes in several studies in higher plants (Ignatova et al., 2011, Rudenko et al., 2007, Khristin et al., 2004). However, the expression level of AtαCA2 by using the described transient systems was much lower compared to expected yield for these expression systems (Avesani et al., 2014), and not enough to justify to proceed further with purification, to reasonably evaluate any protein activity. Reasons for such low yield may include RNA silencing events in the agrobacterium-mediated transient gene expression system or complications related to the post-translational glycosylation modification or protein localization in thylakoids and targeting (Johansen and Carrington., 2001; Desai et al., 2010;).

Moreover, contrary to what was previously published (Aamand et al., 2009), it was recently reported by Andring et al., (2018) that the bovine carbonic anhydrase II does not exhibit nitrite reductase or nitrous anhydrase activity. These authors revisited previous findings from Aamand et al., 2009 and by measuring NO generation by two different methods did not observe the generation of NO upon the addition of $NaNO_2$

to bovine CA II in the presence or absence of the CA inhibitor dorzolamide. In addition, by a structural analysis of bovine CA II in complex with dorzolamide, they showed that the binding of sulphonamide based CA inhibitors to the catalytic zinc would exclude NO_2 binding in the active site.

To measure the NO generation, these authors relied on two methods, either mass spectrometry or electrode based NO measurement. The measurement of NO generation in the Aamand et al., 2009 work relied also on NO electrode, but produced a different result. Moreover, in the same work the NO generation was confirmed by using a chemiluminescence based NO sensor. In our hands, chemiluminescence based analysis of NO generation mediated by bovine CAII was in line with Aamand et al., 2009 results, and we used same commercial bovine CAII in this work. On the contrary, in Andring et al., the used bovine CA II was purified from red blood cells using affinity chromatography and then enzyme samples were extensively dialyzed against EDTA to remove extraneous metal ions. Thus, the reason for the discrepancy may lay in the different source for the enzyme used in the different works, as Aamand et al., 2009 used commercial bovine carbonic anhydrase II, as we did, while Andring et al., 2018 worked with purified carbonic anhydrase II. It is possible, for example, that the commercial carbonic anhydrase II may contain extraneous metal ions which could be a source of electron donation for nitrite reduction, or the purified bovine CAII could perform differently from the commercial one concerning its NO production activity for other unknown reasons. In any case, this obviously needs now to be further experimentally enquired, and bovine CAII-mediated NO generation validated, before putting new efforts in the attempt of providing a functional recombinant AtαCA2 protein as candidate to test the involvement of plant alpha carbonic anhydrases in NO generation from nitrite during the HR.

Plant βCAs are the most abundant CAs in plants and are also involved in carbon fixation. Their involvement in response to abiotic and biotic responses was previously demonstrated (Di Mario et al., 2017). Indeed, silencing of tobacco chloroplast

βCA1(SABP3, salicylic-acid-binding protein 3) expression suppressed the Pto:avrPto-mediated HR in leaves, suggesting tobacco βCA1 requirement for HR (Slaymaker et al., 2002). Therefore, we produced in *E.coli* the recombinant NtβCA1. This protein showed carbonic anhydrase activity, consistently with previous reports by Slaymaker et al., (2002). However, NtβCA1 was unable to convert nitrite to NO. βCA has significantly different amino acid sequence and dimensional structure compared to αCA. The zinc atom in the active site of αCAs, previously found to be able to convert nitrite to NO, is coordinated by three histidine residues and one water molecule (Tripp et al., 2001; Rudenko et al., 2015). Most αCAs are believed to be monomers, even if some evidences, in line with our results too, showed they could be also dimers (Moroney et al., 2011; Rudenko et al.,2015). Differently, the zinc ion in reaction center of the βCAs is coordinated by two cysteine residues and one histidine residue (Rowlett et al., 2010) and βCAs are multimers such as tetramer or octamers with a fundamental dimeric unit (Rowlett et al., 2010). Thus, even admitting αCAs, like bovine CAII, could indeed generate NO from nitrite, this doesn't imply a similar enzymatic function for βCAs. Thus, given the results, we can speculate that βCAs involvement in response to biotic responses is likely indirect and not directly due to a βCA NO generation activity. For example, it was proposed that CA may participate in lipid biosynthesis, so the βCA involvement in defense response may be related with the activation of the jasmonate-dependent pathway (Hoang and Chapman, 2002). Moreover, the finding that Arabidopsis βCA1 undergoes S-nitrosylation, which suppresses both CA and SA binding activities and abolishes the immune response, suggested that a negative feedback loop modulates βCA1 activity in plant defense (Wang et al., 2009). Additionally, under conditions such as high temperature, which can induce nitrosative stress, βCA activity was found to be inhibited by protein tyrosine nitration (Chaki et al.,2013). Therefore, a careful modulation of protein activity is likely required under different stresses, possibly through different NO mediated post-translational modification events, which eventually allows the fine-tuning of its activity.

Plant γCAs act as subunits essential for mitochondrial respiratory complex I assembly and participate in CO_2 translocation from mitochondria to chloroplasts during photorespiration (Braun and Zabaleta, 2007; Zabaleta et al., 2012). So far, no carbonic anhydrase activity of higher plant gamma carbonic anhydrase has been detected. In our study, the recombinant AtγCA2 protein overexpressed in *E. coli* showed also no carbonic anhydrase activity, even though sequence comparison and computer modeling suggested a possible carbonic anhydrase activity of AtγCA2 (Perales et al.,2005). Moreover, no NO signal was detected from the recombinant AtγCA2. The structural difference in the active domain between αCAs, possibly producing NO, and γ types of carbonic anhydrase likely justify the absence of this NO generation activity in γCAs which are possibly mainly having structural function (Kimber and Pai.,2000; Tripp et al., 2001).

After having worked on the NO production during the HR, in the last part of this thesis work, we focused on NO downstream signaling and wanted to enquire in details the NO-triggered modulation of gene expression during the HR. Our main purpose was to characterize the transcriptomic changes associated to the NO induced triggering of cell death during the HR.

Transcriptomic studies applied so far in plants to NO treatment mainly relied on the application of exogenous NO donors. However, as we already mentioned these data should be interpreted with caution. Here, we decide to exploit a fumigation system allowing the treatment of plants directly with NO gas, thus avoiding side effects associated to backbones of NO donors or additionally released compounds. We first experimentally identified conditions triggering an uniform cell death in plant tissue comparable to that occurring in response to an avirulent pathogen. In our hands, a treatment with NO at the concentration of 200 ppm for 8 hours triggered an uniform cell death in plant leaf tissue, which was confirmed either by visual symptoms inspection and release of ions from broken cell membranes. This condition was in line with previous findings in our lab, with younger plants (Zahra Imanifard, PhD thesis).

However, we have not quantified so far the NO content in plant cells under this condition, neither compared it to the NO content in plant cells upon infection under pathophysiological conditions triggering the HR. This would be definitely an interesting point to be further explored in the near future, in order to validate our experimental set-up, and confirm that it properly allows to carefully explore a special feature of HR, thus focusing specifically NO-modulated genes. On the other hand, the evaluation of the behavior of mutants impaired in NO homeostasis or signaling during the HR, would represent a complimentary approach to validate our setup. Unfortunately, few genes known to be specifically involved in NO signaling triggering HR are known so far and we are currently exploring the behavior of mutants affected in NO homeostasis/signaling in response to this treatment.

Transcriptome sequencing by the RNASeq approach on samples subjected to the established treatment was done to characterize the transcriptome modulation associated to cell death triggering and identify gene functional classes which expression is more affected by the treatment. First of all, the analysis of RNASeq data showed that a huge transcriptomic change was associated to the NO treatment triggering cell death. Indeed, complexively 10638 genes were significantly modulated with a $|Log_2FC|>1,5$. This modulation was much stronger than that found so far in literature associated to NO donor treatments. Indeed, in a recent RNASeq study in Arabidopsis roots and leaves, GSNO mediated transcriptome analysis triggered differential expression of 3263 genes (Begara Morales et al., 2014). More recently, the CysNO infiltration of Arabidopsis leaf samples caused the differential expression of 6436 genes among which 3448 were upregulated and 2879 downregulated (Hussain et al., 2016). Therefore, it is likely that the characterized transcriptomic changes induced by these NO donors do not fully reflect those triggered by an NO burst resembling that occurring endogenously upon infection by an avirulent pathogen, similarly leading to the activation of a PCD program.

In order to confirm sensing by plants of NO, the induction of genes which are

typically induced by NO was first explored. Among induced genes, the PR1 gene, a known marker induced by NO (Durner et al., 1998) was found.

A GO enrichment analysis was applied to identify functional classes which are more represented in differentially expressed genes (Figure 32). The emerging picture was a massive transcriptomic change associated to changes in cellular and metabolic processes. Both induced and down regulated genes were enriched in genes involved in signal transduction, in response to biotic and abiotic stresses as well as endogenous stimuli. The major class included indeed transcription factors. In a recent study, a comprehensive characterization of transcription factors modulated by CysNO was reported (Imran et al., 2017). Even though a large number of transcription factor classes were found to be modulated in this study, our results point to a more massive change in transcription factors expression. Moreover, several receptors like kinases and several phosphatases or receptors involved in hormones perception were also modulated according to our results. Interestingly, among these, NPR3/NPR4 working as salicylic acid receptors in immune signaling and modulating NPR1 turnover required for ETI, were found to be induced by NO (Fu et al., 2012).

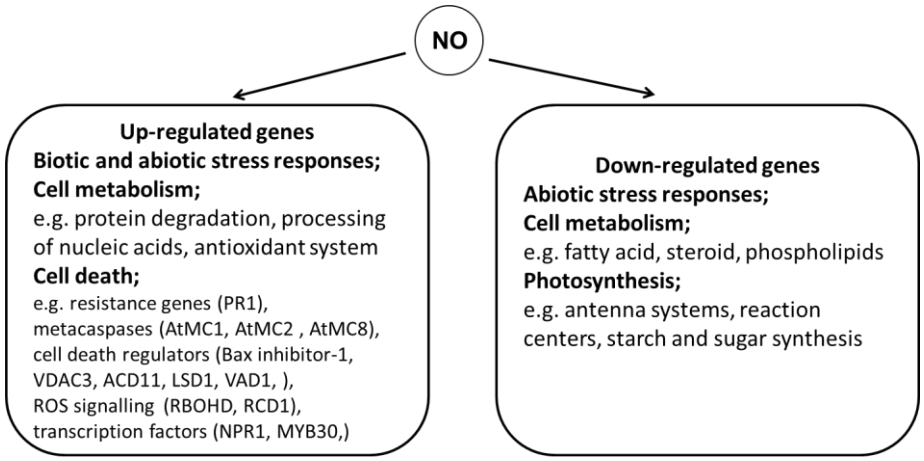

Figure 32. **A simplified schematic diagram of functional classification of differentially expressed genes regulated by NO treatment triggering cell death.**

Beside this huge transcriptomic modulation and changes affecting plant signal transduction, the GO enrichment analysis revealed also important changes in the plant cell metabolism. However, genes in this functional class differed in upregulated and downregulated genes. More careful inspection showed that upregulated genes in the

metabolic processes were mainly genes involved in protein activity modulation and degradation. Several ubiquitin ligases and genes involved in proteasome mediated protein degradation were found. Moreover, genes involved in the modulation of the antioxidant system were also strongly induced. Finally, we also observed induction of genes involved in processing of nucleic acids.

On the other hand, genes involved in anabolic processes were strongly downregulated. Indeed, genes encoding proteins involved in the photosynthetic reactions or working in producing energy precursors (e.g. antenna systems or reaction centers in photosystems), as well as genes for starch and sugar synthesis were switched off by the NO treatment. Interestingly, an important down regulation of genes involved in lipid metabolism, namely fatty acid synthesis, steroid metabolism and synthesis and metabolism of phospholipids was found. Genes involved in lipid metabolism were partially enriched also in upregulated genes by the NO treatment. This is in agreement with finding from a recent publication, in which the metabolic reprogramming induced by NO treatment was enquired in Arabidopsis by a metabolomics analysis. Authors found that content of compounds belonging to the lipid category underwent large changes in NO-treated plants likely connected to lipid trafficking, membrane remodeling or alteration in lipidic leaf structures, such as cuticles. An enhancement of membrane permeability by NO was clearly demonstrated in this study. Moreover, in lines with our findings, authors also found progressive genomic degradation processes and reduction in glycolysis intermediate and starch with a general rearrangement in carbon metabolism upon NO treatment (Leon et al., 2016).

Interestingly, the enrichment analysis of NO induced genes revealed also a significant enrichment in genes belonging to the functional class “cell death”. 93 genes related to cell death processes were found as significantly upregulated by NO, among which 57 genes with a Log_2FC higher than 1,5. Among these a large number (18) of R-genes and genes encoding for receptor like kinase or proteins strictly involved in pathogen perception were found. For example, the Arabidopsis R-genes RPP13, RPS4, RPW8,

RRS, RPS5 or MLO-like proteins, which recessive mutation confers broad spectrum and durable pathogen resistance (Consonni et al., 2006) were induced. Beside these, several proteins involved in basal resistance and pathogen MAMP/PAMP perception like SERK3, CRK13, CRK20 or BAK1 functioning as a co-receptor with the receptor kinase for bacterial flagellin FLAGELLIN-SENSING 2 (FLS2) or the EF-TU RECEPTOR (EFR) involved in immunity (Chinchilla et al., 2007) were also induced. Moreover, proteins associated to ETI and involved in immunity associated signaling through interaction/regulation of R-genes like RIN2/RIN3 E3 ubiquitin ligases (Kawasaki et al., 2005), other ubiquitin ligases (BOI related ubiquitin ligases AT4G19700 or AT5G45100), or the BON3 copin protein (Li et al., 2009) were also found among these induced genes.

Furthermore, marker genes previously known to be associated or involved in programmed cell death execution were also found, which demonstrates that our analysis successfully focused on transcriptomic changes induced by NO and related to the cell death triggering. The AtMC1 metacaspase, a positive regulator of cell death triggered by avirulent pathogens with a conserved caspase-like putative catalytic residues for its function, was found in this table (Coll et al., 2010). AtMC2 and AtMC8 metacaspases, also involved in modulating plant cell death were also found to be induced by NO during cell death (Coll et al., 2010, He et al., 2008). Among the most NO induced genes in the functional class “cell death”, we found then HSR4, a long known hypersensitive response and stress-induced ATPase encoding a protein located in the outer mitochondrial membrane, recently renamed AtOM66, which is known to be involved in cell death (Sugimoto et al., 2004, Zhang et al., 2014). The Bax inhibitor-1, an highly conserved cell death regulator recently found to interact with ATG6 to modulate autophagy and plant cell death (Xu et al., 2017), the Flavin-containing monooxygenase 1 (FMO1), and the mitochondrial outer membrane protein porin 3 (VDAC3) previously studied in apoptosis in the animal system and recently found to trigger cell death by a complex with PR10 in grapevine, were also among the most induced genes by NO (Bartsch et al., 2006, Ma et al., 2018). Finally,

also the accelerated cell death 11 (ACD11), phospholipase D, the zinc finger protein LSD1 negative regulator of PCD, the mitogen activated protein kinase 6 (MPK6) activated in ETI associated PCD, the vascular associated cell death 1 (VAD1) and the nudix hydrolase 7 (NUDT7), all previously found to be involved in plant programmed cell death, were among induced genes (Petersen et al., 2008, Dietrich et al., 1997, Lorrain et al., 2004, Bartsch et al., 2006).

It is also interesting to mention here that among the NO induced genes belonging to this functional class "cell death", we found also genes involved in ROS production and signalling, like the RBOHD protein which is involved in superoxide production during the hypersensitive response (Torres et al., 2005), or the radical induced cell death (RCD1) which is involved in ozone induced signalling leading to cell death (Overmyer et al., 2005). Importantly, RBOHD is one of the best know proteins targeted and modulated by NO during the immunity and the ozone sensitive *rcd1* mutant over accumulates NO, thus demonstrating that NO accumulation act also through a finely regulated cross-talk with ROS, acting on ROS producing/sensing proteins at different levels (Yun et al., 2011, Ahlfors et al., 2009).

Finally, we observed that several transcription factors related to plant cell death were induced by NO, which are thus possibly involved in the observed large transcriptomic rearrangement associated to NO and cell death triggering. Among these, the transcriptional regulator NPR1 was induced, as were induced genes involved in SA signalling and systemic acquired resistance (SAR) (just to name a few, the transcription factor TGA3 or the AZI1 protein which mediates SAR through mobilization of lipid signalling (Cecchini et al., 2015)). Transcription factors belonging to the NAC or MYB family (among which MYB30 a member of this family involved in cell death processes during the hypersensitive response (HR) of plants which is targeted and inhibited by NO (Tavares et al., 2014)) were found as well as transcription factors involved in the ethylene signalling, among which the ERF011 and the RAP2.3.

6. Conclusions

In the first part of this work, we enquired NO production mechanism in the plant HR. Based on literature reports, we enquired if plant carbonic anhydrases can directly produce NO from nitrite during HR. Indeed, it was reported that carbonic anhydrases could be involved in immunity in plants. Moreover, the Bovine carbonic anhydrase II, an alpha type carbonic anhydrase which catalyzes the conversion between carbon dioxide and bicarbonate, was shown to be able to convert nitrite to NO. We first focused on the plant alpha CA family aiming to verify their NO production activity. However, we found that this protein requires glycosylation for activity. Unfortunately, the transient expression in plant system, which could yield a properly glycosylated protein, led to low protein expression and we could therefore not finally use this protein to verify its NO production activity. However, meanwhile, the finding reporting its ability to produce NO from nitrite was questioned by a more recent publication. As conclusion, based on this new literature finding, and on the protein localization as observed in our study and previous literature about mutant characterization, appears currently less likely that this alpha CA protein is directly involved in NO production from nitrite in HR. Clarification of controversial literature reports about bovine CAII NO production activity would help to postulate alpha CAII function in HR. Meanwhile, we also cloned and expressed in an heterologous system CAs member belonging to beta and gamma families and demonstrated these were not able to catalyze the nitrite conversion to NO. The documented involvement of beta type CA in immunity is thus likely to occur indirectly. Recently, in *Chlamydomonas reinhardtii*, the Amidoxime Reducing Component (ARC) protein was shown to complex with NR to constitute a dual enzymatic system which can reduce nitrite to NO in the presence of high NO_3^- concentrations and in normoxia (Chamizo-Ampudia et al 2016, 2017). Interestingly, the *A. thaliana* genome contains two genes for ARC protein, one presenting an NO-producing activity *in vitro* (Yang et al., 2015). The determination of the existence of an NR:NOFNiR complex in higher plants, similar to what was found in *C. reinhardtii*, represents now a very promising research field.

In the second part of this work, we enquired the NO downstream signaling, focusing on transcriptomic changes associated to NO induced cell death. A massive transcriptomic rearrangement was found to be associated to the NO induced plant cell death. The functional class “response to stimuli” was strongly enriched in the differentially expressed genes modulated by NO. Moreover, we found a large modulation in signaling and transcription factors. Genes encoding for proteins involved in protein degradation or metabolism of nucleic acids were induced, while genes involved in anabolic processes were down-regulated. Importantly, we confirmed that NO treatment leads to a massive metabolic reprogramming which specially affects lipid metabolism. Finally, the enrichment among induced genes of several genes previously found to be involved/associated to the cell death confirmed that conditions we have selected were adequate to our aim. The comparison of this dataset with transcriptomic modulation induced by NO at low concentration not triggering cell death (Jingjing Huang PhD thesis, RNASeq with 3h NO at 100ppm) or with avirulent pathogen induced transcriptomic modulation will allow to carefully select among all NO modulated genes the most relevant, specifically involved in the cell death activation and execution during the HR.

7. References

Aamand, R., Dalsgaard, T., Jensen, F.B., Simonsen, U., Roepstorff, A., Fago, A. (2009). Generation of nitric oxide from nitrite by carbonic anhydrase: a possible link between metabolic activity and vasodilation. Am J Physiol Heart Circ Physiol 297, H2068-H2074.

Aarts, N., Metz, M., Holub, E., Staskawicz, B.J., Daniels, M.J., Parker, J.E. (1998). Different requirements for EDS1 and NDR1 by disease resistance genes define at least two R gene-mediated signaling pathways in Arabidopsis. Proc Natl Acad Sci USA 95, 10306-10311.

Abat, J.K., and Deswal, R. (2009). Differential modulation of S-nitrosoproteome of Brassica juncea by low temperature: change in S-nitrosylation of Rubisco is responsible for the inactivation of its carboxylase activity. Proteomics 9, 4368-4380.

Abat, J.K., Mattoo, A.K., and Deswal, R. (2008). S-nitrosylated proteins of a medicinal CAM plant Kalanchoe pinnata-ribulose-1,5-bisphosphate carboxylase/oxygenase activity targeted for inhibition. FEBS J 275, 2862-2872.

Ahlfors, R., Brosche, M., Kollist, H., Kangasjarvi, J. (2009). Nitric oxide modulates ozone-induced cell death, hormone biosynthesis and gene expression in Arabidopsis thaliana. Plant J 58, 1-12.

Ali, R., Ma, W., Lemtiri-Chlieh, F., Tsaltas, D., Leng, Q., von Bodman, S., and Berkowitz, G.A. (2007). Death don't have no mercy and neither does calcium: Arabidopsis CYCLIC NUCLEOTIDE GATED CHANNEL2 and innate immunity. Plant Cell 19, 1081-1095.

Anders, S., Huber, W. (2010). Differential expression analysis for sequence count data. Genome Biol 11, R106.

Angell, S.M., Baulcombe, D.C.(1997). Consistent gene silencing in transgenic plants expressing a replicating potato virus X RNA. The EMBO J 16, 3675-3684.

Andring, J.T., Lomelino, C.L., Tu, C., Silverman, D.N., McKenna, R., Swenson, E.R. (2018). Carbonic anhydrase II does not exhibit Nitrite reductase or Nitrous Anhydrase Activity. Free Radic Biol Med 117, 1-5.

Asai. S. and Yoshioka, H. (2009). Nitric oxide as a partner of reactive oxygen species participates in disease resistance to necrotrophic pathogen Botryis cinerea in Nicotiana benthamiana. Mol Plant Microbe Interact 22, 619-629.

Astier, J., Gross, I., Durner, J. (2017). Nitric oxide production in plants: an update. J Exp Bot, 10.1093/jxb/erx420

Astier, J., Kulik, A., Koen, E., Besson-Bard, A., Bourque, S., Jeandroz, S., Lamotte, O., Wendehenne. (2012). Protein S-nitrosylation: What’s going on in plants? Free Radic Biol Med 53, 1101-1110.

Avesani, L., Merlin, M., Gecchele, E., Capaldi, S., Brozzetti, A., Falorni, A., Pezzotti, M. (2014). Comparative analysis of different biofactories for the production of a major diabetes autoantigen. Transgenic Res 23, 281-291.

Axtell, M.J., Staskawicz, B.J. (2003). Initiation of RPS2-specified disease resistance in

Arabidopsis is coupled to the AvrRpt2-directed elimination of RIN4. Cell 112, 369-377.

Badger, M.R., Price, G.D. (1994). The role of carbonic anhydrase in photosynthesis. Annu Rev Plant Physiol Plant Mol Biol 45, 369-392.

Bartsch, M., Gobbato, E., Bednarek, P., Debey, S., Schultze, J.L., Bautor, J., Parker, J.E. (2006). Salicylic acid-independent ENHANCED DISEASE SUSCEPTIBILITY1 signaling in Arabidopsis immunity and cell death is regulated by the monooxygenase FMO1and the Nudix hydrolase NUDT7. Plant Cell 18, 1038-1051.

Begara-Morales, J. C., Sanchez-Calvo, B., Chaki, M., Mata-Perez, C., Valderrama, R.,Padilla, M. N., Lopez-Jaramillo, J., Luque, F., Corpas, F.J., Barroso, J.B. (2015). Differential molecular response of monodehydroascorbate reductase and glutathione reductase by nitration and S-nitrosylation. J Exp Bot 66, 5983-5996.

Begara-Morales, J.C, Sánchez-Calvo, B., Luque, F., Leyva-Pérez, M.O., Leterrier, M., Corpas, F.J., Barroso, J.B. (2014). Differential transcriptomic analysis by RNA-Seq of GSNO-responsive genes between Arabidopsis roots and leaves. Plant Cell Physiol 55, 1080-1095.

Bethke, P.C., Badger, M.R., Jones, R.L. (2004). Apoplastic synthesis of nitric oxide by plant tissues. Plant Cell 16, 332-341.

Bellin, D., Asai, S., Delledonne, M., Yoshioka, H. (2013). Nitric oxide as a mediator for defense responses. Mol Plant Microbe Interact 26, 271-277.

Besson-Bard, A., Astier, J., Rasul, S., Wawer, I., Dubreuil-Maurizi, C., Jeandroz, S., Wendehenne, D. (2009). Current view of nitric oxide-responsive genes in plants. Plant Sci 177, 302-309.

Besson-Bard, A., Pugin, A., Wendehenne, D. (2008). New insights into nitric oxide signaling in plants. Annu Rev Plant Biol 59, 21-39.

Besson-Bard, A., Wendehenne, D. (2009). Nitric oxide contributes to cadmium toxicity in Arabidopsis by promoting cadmium accumulation in roots and by up-regulating genes related to iron uptake. Plant Physiol 149, 1302-1315.

Bigeard, J., Colcombet, J., Hirt, H. (2015). Signaling mechanisms in pattern-triggered immunity (PTI). Mol Plant 8, 521-539.

Boccara, M., Mills, C.E., Zeier, J., Anzi, C., Lamb, C., Poole, R.K., Delledonne, M. (2005). Flavohaemoglobin HmpX from *Erwinia chrysanthemi* confers nitrosative stress tolerance and affects the plant hypersensitive reaction by intercepting nitric oxide produced by the host. Plant J 43, 226-237.

Boller, T., and Felix, G. (2009). A renaissance of elicitors: perception of microbe-associated molecular patterns and danger signals by pattern-recognition receptors. Annu Rev Plant Biol 60, 379-406.

Bolwell, G.P., Buti, V.S., Davies, D.R., Zimmerlin, A. (1995). The origin of the oxidative burst in plants. Free Radic Res Commun 23, 517-532.

Bolwell, G.P., Wojtaszek, P. (1997). Mechanisms for the generation of reactive oxygen species in plant defense: a broad perspective. Physiol Mol Plant Pathol 51, 347-366.

Braun, H.P., Zabaleta, E. (2007). Carbonic anhydrase subunits of the mitochondrial NADH dehydrogenase complex (complex I) in plants. Physiologia Plantarum 129, 114-122.

Butt, Y.K., Lum, J.H., Lo, S.C. (2003) Proteomic identification of plant proteins probed by mammalian nitric oxide synthase antibodies. Planta 216, 762-771.

Buren, S., Ortega-Villasante, C., Blanco-Rivero, A., Martinez-Bernardini, A., Shutova, Tatiana., Shevela, D., Johannes, M., Bako, L., Villarejo, A., Samuwlsson, G. (2011). Importance of post-translational modifications for functionality of a chloroplast-localized carbonic anhydrase (CAH1) in Arabidopsis thaliana. PLoS ONE 6, e21021.

Castillo, M. C., Lozano-Juste, J., Gonzalez-Guzman,M., Rodriguez, L., Rodriguez, P. L., Leon, J. (2015). Inactivation of PYR/PYL/RCAR ABA receptors by tyrosine nitration may enable rapid inhibition of ABA signaling by nitric oxide in plants. Science Signaling 8, ra89.

Cecchini, N.M., Steffes, K., Schlappi, M.R., Gifford, A.N., Greenberg, J.T. (2015). Arabidopsis AZI1 family proteins mediate signal mobilization for systemic defence priming. Nat Commun 6.

Cerovska, N., Pecenkova, T., Moravec T., Veleminsky, J.(2004). Transient expression of heterologous model gene in plants using Potato virusX-based vector. Plant Cell Tissue Organ Cult 79,147-152.

Chaki, M., Carreras, A., Lopez-Jaramillo, J., Begara-Morales, J. C., Sanchez-Calvo, B.,Valderrama, R., Corpas, F.J., Barroso, J.B. (2013). Tyrosine nitration provokes inhibition of sunflower carbonic anhydrase (beta-CA) activity under high temperature stress. Nitric Oxide 29, 30-33.

Chamizo-Ampudia, A., Sanz-Luque, E., Llamas, A., Ocana-Calahorro, F., Mariscal, V., Carreras, A., Barroso, J.B., Galvan, A., Fernandez, E. (2016). A dual system formed by the ARC and NR molybdoenzymes mediates nitrite-dependent NO production in Chlamydomonas. Plant Cell Environ 39, 2097-2107.

Chamizo-Ampudia, A., Sanz-Luque, E., Llamas, A., Galvan, A., Fernandez, E. (2017). Nitrate reductase regulates plant nitric oxide homeostasis. Trends Plant Sci 22, 163-174.

Chandok, M.R., Ytterberg, A.J., van Wijk, K.J., Klessig, D.F. (2003). The pathogen-inducible nitric oxide synthase (iNOS) in plants is a variant of the P protein of the glycine decarboxylase complex. Cell 113, 469-482.

Chen, J., Vandelle, E., Bellin, D., Delledonne, M. (2014). Detection and function of nitric oxide during the hypersensitive response in Arabidopsis thaliana: Where there's a will there's a way. Nitric Oxide 43, 81-88.

Chisholm, S. T., Coaker, G., Day, B. Staskawicz, B. J. (2006). Host-microbe interactions: shaping the evolution of the plant immune response. Cell 124, 803-814.

Chinchilla, D., Zipfel, C., Robatzek, S., Kemmerling, B., Nu ¨rnberger, T., Jones, J.D., Felix,

G., and Boller, T. (2007). A flagellin-induced complex of the receptor FLS2 and BAK1 initiates plant defence. Nature 448, 497-500.

Christopher-Kozjan, R., Heath, M.C. 2003. Cytological and pharmacological evidence that biotrophic fungi trigger different cell death execution processes in host and nonhost cells during the hypersensitive response. Physiol Mol Plant Pathol 62, 265-275.

Clough, S.J., Fengler, K.A., Yu, I.C., Lippok, B., Smith Jr, R.K., Bent, A.F. (2000). The Arabidopsis dnd1 'defense, no death' gene encodes a mutated cyclic nucleotide-gated ion channel. Proc Natl Acad Sci USA 97, 9323-9328.

Collins, R.M., Afzal, M., Ward, D.A., Prescott, M.C., Sait, S.M., Rees, H.H., and Tomsett, A.B. (2010). Differential proteomic analysis of Arabidopsis thaliana genotypes exhibiting resistance or susceptibility to the insect herbivore, Plutella xylostella. PLoS One 5:e10103.

Coll, N.S., Epple, P., Dangl, J.L. (2011). Programmed cell death in the plant immune system. Cell Death Differ 18, 1247-1256.

Coll, N.S., Vercammen, D., Smidler, A., Clover, C., van Breusegem, F., Dangl, J.L., Epple, P. (2010). Arabidopsis Type I metacaspases control cell death. Science 330, 1393-1397.

Consonni, C., Humphry, M.E., Hartmann, H.A., Livaja, M., Durner, J., Westphal, L., Vogel, J., Lipka, V., Kemmerling, B., Schulze-Lefert, P., Somerville, S.C., Panstruga, R. (2006). Conserved requirement for a plant host cell protein in powdery mildew pathogenesis. Nat Genet 38, 716-720.

Corpas, F.J. Barroso, J.B. (2015). Nitric oxide from a "green" perspective. Nitric Oxide 45,15-19.

Corpas, F.J., Barroso, J.B., Carreras, A., Quirós, M., León, A.M., Romero-Puertas, M.C., Esteban, F.J., Valderrama, R., Palma, J.M., Sandalio, L.M, et al. (2004). Cellular and subcellular localization of endogenous nitric oxide in young and senescent pea plants. Plant Physiol 136, 2722-2733.

Corpas, F.J., Palma, J.M., del Río L.A., Barroso, J.B. (2009). Evidence supporting the existence of L-arginine-dependent nitric oxide synthase activity in plants, New Phytol 184, 9-14.

Corpas, F.J., Barroso, J.B., Carreras, A., Valderrama, R., Palma, J.M., Leon, A.M., Sandalio, L.M., del Rio, L.A. (2006). Constitutive arginine-dependent nitric oxide synthase activity in different organs of pea seedlings during plant development. Planta 224, 246-254.

Cui, H., Tsuda,K., and Parker, J.E. (2015). Effector-triggered immunity: from pathogen perception to robust defense. Annu Rev Plant Biol 66, 487-511.

Dangl, J.L., Jones, J.D. (2001). Plant pathogens and integrated defence responses to infection. Nature 411, 826-833.

Dat, J., Vandenabeele, S., Vranová, E., Van Montagu, M., Inzé, D., Van Breusegem, F. (2000). Dual action of the active oxygen species during plant stress responses. Cell Mol Life Sci 57, 779-795.

DellaPenna, D., Pogson, B.J. (2006). Vitamin synthesis in plants: tocopherols and carotenoids. Annu Rev Plant Biol 57, 711-738.

Delledonne, M. (2005). NO news is good news for plants. Curr Opin Plant Biol 8, 390-396.

Delledonne, M., Xia, Y., Dixon, R.A., Lamb, C. (1998). Nitric oxide functions as a signal in plant disease resistance. Nature 394, 585-588.

Delledonne, M., Zeier, J., Marocco, A., Lamb C.(2001). Signal interactions between nitric oxide and reactive oxygen intermediates in the plant hypersensitive disease resistance response. Proc Natl Acad Sci USA 98, 13454-13459.

De Pinto MC, Tommasi F, De Gara L. (2002). Changes in the antioxidant systems as part of the signaling pathway responsible for the programmed cell death activated by nitric oxide and reactive oxygen species in tobacco Bright-Yellow 2 cells. Plant Physiol 130, 698-708.

De Michele, R., Vurro, E., Rigo, C., Costa, A., Elviri, L., Di Valentin, M., Careri, M., Zottini, M., Sanità di Toppi, L., Lo Schiavo, F. (2009). Nitric oxide is involved in cadmium induced programmed cell death in Arabidopsis suspension cultures. Plant Physiol 150, 217-228.

De Pinto, M.C., Tommasi, F., De Gara, L. 2002. Changes in the antioxidant systems as part of the signaling pathway responsible for the programmed cell death activated by nitric oxide and reactive oxygen species in tobacco Bright-Yellow 2 cells. Plant Physiol 130, 698-708.

Desai, P.N., Shrivastava, N., Padh, H. (2010). Production of heterologous proteins in plants: Strategies for optimal expression. Biotechnol Adv 28, 427-435.

Dietrich, R.A., Richberg, M.H., Schmidt, R., Dean, C., Dangl, J.L. (1997). A novel zinc-finger protein is encoded by the Arabidopsis lsd1 gene and functions as a negative regulator of plant cell death. Cell 88, 685-694.

Di Mario, R.J., Quebedeaux, J.C., Longstreth, D.J., Dassanayake, M., Hartman, M.M., Moroney, J.V. (2016). The cytoplasmic carbonic anhydrases CA2 and CA4 are required for optimal plant growth at low CO_2. Plant Physiol 171, 280-293.

Di Mario, R.J., Clayton, H., Mukherjee, A., Ludwig, M., Moroney, J.V. (2017). Plant Carbonic Anhydrases: Structures, Locations, Evolution, and Physiological Roles. Mol. Plant. 10, 30-46.

Dixon, R.A. (2001). Natural products and plant disease resistance. Nature 411, 843-847.

Dodds, P.N., and Rathjen, J.P. (2010). Plant immunity: towards an integrated view of plant-pathogen interactions. Nat Rev Genet 11, 539-548.

Du, Z., Zhou, X., Ling, Y., Zhang, Z.H., Su, Z. (2010). agriGO: a GO analysis toolkit for the agricultural community. Nucleic Acids Res 38, W64–W70.

Durner, J., Wendehenne, D., Klessig, D.F. (1998). Defense gene induction in tobacco by nitric oxide, cyclic GMP, and cyclic ADP-ribose. Proc Natl Acad Sci USA 95, 10328-10333.

Elmore, J.M., Lin, Z.J., Coaker. G. (2011). Plant NB-LRR signaling: upstreams and downstreams. Curr Opin Plant Biol 14, 65-371.

Engineer, C.B., Ghassemian, M., Anderson, J.C., Peck, S.C., Hu, H., Schroeder, J.I. (2014). Carbonic anhydrases, EPF2 and a novel protease mediate CO_2 control of stomatal development. Nature 513, 246-250.

Eriksson, A.E., Jones,T.A., Liljas, A. (1988). Refined structure of human carbonic anhydrase II at 2.0 Å resolution. Proteins 4, 274-282.

Everson, R.G. (1970). Carbonic anhydrase and CO_2 fixation in isolated chloroplasts. Phytochemistry 9, 2

Fabre, N., Reiter, I.M., Becuwe-Linka, N., Genty, B., and Rumeau, D. (2007). Characterization and expression analysis of genes encoding alpha and beta carbonic anhydrases in Arabidopsis. Plant Cell Environ 30, 617-629.

Feechan, A., Kwon, E., Yun, B.W., Wang, Y., Pallas, J.A., Loake, G.J. (2005). A central role for S-nitrosothiols in plant disease resistance. Proc Natl Acad Sci USA 102: 8054-8059.

Ferreira, F.J., Guo, C., and Coleman, J.R. (2008). Reduction of plastid-localized carbonic anhydrase results in reduced Arabidopsis seedling survivorship. Plant Physiol 147, 585-594.

Ferry, J.G. (2010). The γ class of carbonic anhydrases. Biochim Biophys Acta 1804, 374-381.

Feys, B.J., and Parker, J.E. (2000). Interplay of signaling pathways in plant disease resistance. Trends Genet 16, 449-455.

Flores, T., Todd, C.D., Tovar-Mendez, A., Dhanoa, P.K., Correa-Aragunde, N., Hoyos, M.E., Brownfield, D.M., Mullen, R.T., Lamattina, Lorenzo., Polacco, J.C. (2008) Arginase-negative mutants of Arabidopsis exhibit increased nitric oxide signaling in root development. Plant Physiol 147, 1936-1946.

Floryszak-Wieczorek J, Arasimowicz-Jelonek M. (2017) The effects of pharmacological carbonic anhydrase suppression on defence responses of potato leaves to phytophthora infestans. J Plant Sci Phytopathol 1, 011-025.

Foresi, N., Mayta, M.L., Lodeyro, A.F., Scuffi, D., Correa-Aragunde, N., Garc á-Mata, C., Casalongue, C., Carrillo, N., Lamattina, L. (2015). Expression of the tetrahydrofolate-dependent nitric oxide synthase from the green alga Ostreococcus tauri increases tolerance to abiotic stresses and influences stomatal development in Arabidopsis, Plant J 82, 806-821.

Foresi, N., Correa-Aragunde, N., Parisi, G., Calo, G., Salerno, G., Lamattina, L. (2010). Characterization of a nitric oxide synthase from the plant kingdom: NO generation from the green alga Ostreococcus tauri is light irradiance and growth phase dependent. Plant Cell 22, 3816-3830.

Forstermann, U.and Swssa. W.C. (2012). Nitric oxide synthases: regulation and function. Eur Heart J 33, 829-837.

Friso, G.,Giacomelli, L., Ytterberg, A.J., Peltier, J.-B., Rudella, A., Sun, Q., and van Wijk, K.J. (2004). In-depth analysis of the thylakoid membrane proteome of Arabidopsis thaliana chloroplasts: new proteins, new functions, and a plastid proteome database. Plant Cell 16,

478-499.

Fromm, S., Braun, H.P., Peterhansel, C. (2016a). Mitochondrial gamma carbonic anhydrases are required for complex I assembly and plant reproductive development. New Phytol 211, 194-207.

Fromm, S., Going, J., Lorenz, C., Peterhansel, C., Braun, H.-P. (2016b). Depletion of the ‘‘gamma-type carbonic anhydrase-like’’ subunits of complex I affects central mitochondrial metabolism in Arabidopsis thaliana. Biochim Biophys Acta 1857, 60-71.

Frungillo, L., Skelly, M. J., Loake, G. J., Spoel, S. H., Salgado, I. (2014). S-nitrosothiols regulate nitric oxide production and storage in plants through the nitrogen assimilation pathway. Nature Communications, 5. http://dx.doi.org/10.1038/ncomms6401.

Fujiwara, S., Fukuzawa, H., Tachiki, A., Miyachi, S. (1990). Structure and differential expression of two genes encoding carbonic anhydrase in Chlamydomonas reinhardtii. Proc Natl Acad Sci USA 87, 9779-9783.

Fu, Z.Q., Yan, S., Saleh, A., Wang, W., Ruble, J., Oka, N., Mohan, R., Spoel, S.H., Tada, Y., Zheng, N, et al. (2012). NPR3 and NPR4 are receptors for the immune signal salicylic acid in plants. Nature 486, 228-232.

Fukuzawa, H., Fujiwara, S., Tachiki, A., Miyachi, S. (1990). Nucleotide sequences of two genes CAH1 and CAH2 which encode carbonic anhydrase polypeptides in Chlamydomonas reinhardtii. Nucleic Acids Res 18, 6441-6442.

Gay, N.J. Gangloff, M. (2007). Structure and function of toll receptors and their ligands. Annu Rev Biochem 76, 141-65.

Gas, E., Flores-Pe ́rez, U., Sauret-Gu¨eto, S., Rodrı´guez-Concepcio ́n, M. (2009). Hunting for plant nitric oxide synthase provides new evidence of a central role for plastids in nitric oxide metabolism. Plant Cell 21, 18-23.

Gehring, C., Turek, I.S. (2017). Cyclic nucleotide monophosphates and their cyclases in plant signaling. Front Plant Sci 8, 1704.

Glazebrook, J. (2005). Contrasting mechanisms of defense against biotrophic and necrotrophic pathogens. Annu Rev Phytopathol 43, 205-227.

Glazener, J. A., Orlandi, E. W., Baker, J. C. (1996). The active oxygen response of cell suspensions to incompatible bacteria is not sufficient to cause hypersensitive cell death. Plant Physiol 110, 759-763.

Gohre, V. Robatzek, S. 2008. Breaking the barriers: microbial effector molecules subvert plant immunity. Annu Rev Phytopathol 46, 189-215.

Grant, M., Brown, I., Adams, S., Knight, M., Ainslie, A., Mansfield, J. (2000). The RPM1 plant disease resistance gene facilitates a rapid and sustained increase in cytosolic calcium that is necessary for the oxidative burst and hypersensitive cell death. Plant J 23, 441-450.

Gross, F., Rudolf, E.E., Thiele, B., Durner, J., Astier, J. (2017). Copper amine oxidase 8

regulates arginine-dependent nitric oxide production in Arabidopsis thaliana. J Exp Bot 68, 2149-2162.

Grun, S., Lindermayr, C., Sell, S., Durner, J. (2006). Nitric oxide and gene regulation in plants. J Exp Bot 57, 507-516.

Guo, F.Q., Okamoto, M., Crawford, N. (2003). Identification of a plant nitric oxide synthase gene involved in hormonal signaling. Science 302, 100-103.

Gupta, K.J., Fernie, A.R., Kaiser, W.M., van Dongen, J.T. (2011). On the origins of nitric oxide. Trends Plant Sci 16, 160-168.

Gupta, K.J., Brotman, Y., Segu, S., Zeier, T., Zeier, J., Persijn, S.T., Cristescu, S.M., Harren, F.J.M., Bauwe, H., Fernie, A.R., Kaiser, W.M., Mur, L.A.J. (2013). The form of nitrogen nutrition affects resistance against Pseudomonas syringae pv. phaseolicola in tobacco. J Exp Bot 64, 553-568.

Hatsugai, N., Kuroyanagi, M,. Yamada, K., Meshi, T., Tsuda, S., Kondo, M. Nishimura, M., Hara-Nishimura, I. (2004). A plant vacuolar protease, VPE, mediates virus-induced hypersensitive cell death. Science 305, 855-858.

He, R., Drury, G.E., Rotari, V.I., Gordon, A., Willer, M., Farzaneh, T., Woltering, E.J., Gallois, P. (2008). Metacaspase-8 modulates programmed cell death induced by ultraviolet light and H_2O_2 in Arabidopsis. J Biol Chem 283, 774-783.

Heath, M.C. (2000). Hypersensitive response-related death. Plant Mol Biol 44, 321-334.

Hebenstreit, D., Fang, M., Gu, M., Charoensawan, V., van Oudenaarden, A., and Teichmann, S.A. (2011). RNA sequencing reveals two major classes of gene expression levels in metazoan cells. Mol Syst Biol 7, 497.

Hewett-Emmett, D., Tashian, R.E. (1996). Functional diversity, conservation, and convergence in the evolution of the -α, -β, and γ-carbonic anhydrase gene families. Mol Phylogenet Evol 5, 50-77.

Hoang, C.V., Chapman, K.D. (2002b). Biochemical and molecular inhibition of plastidial carbonic anhydrase reduces the incorporation of acetate into lipids in cotton embryos and tobacco cell suspensions and leaves. Plant Physiol 128, 1417-1427.

Holzmeister, C., Frohlich, A., Sarioglu, H., Bauer, N., Durner, J., Lindermayr, C. (2011). Proteomic analysis of defense response of wildtype Arabidopsis thaliana and plants with impaired NO-homeostasis. Proteomics 11, 1664-1683.

Holzmeister, C., Gaupels, F., Geerlof, A., Sarioglu, H., Sattler, M., Durner, J., Lindermayr, C. (2015). Differential inhibition of Arabidopsis superoxide dismutases by peroxynitrite-mediated tyrosine nitration. Journal of Experimental Botany 66, 989-999.

Hofius, D., Schultz-Larsen, T., Joensen, J., Tsitsigiannis, D.I., Petersen, N.H., Mattsson, O., Jorgensen, L.B., Jones, J.D., Mundy, J., Petersen, M. (2009). Autophagic components contribute to hypersensitive cell death in Arabidopsis. Cell 137, 773-783.

Holub, E.B., Beynon, J.L., Crute, I.R. (1994). Phenotypic and genotypic characterization of interactions between isolates of Peronospora parasitica and accessions of Arabidopsis thaliana. Mol Plant Microbe Interact 7, 223-239.

Hu, H., Boisson-Dernier, A., Israelsson-Nordstrom, M., Bohmer, M., Xue, S., Ries, A., Godoski, J., Kuhn, J.M., and Schroeder, J.I. (2010). Carbonic anhydrases are upstream regulators of CO_2-controlled stomatal movements in guard cells. Nat Cell Biol 12, 87-93.

Hu, H.H., Rappel, W.J., Occhipinti, R., Ries, A., Bohmer, M., You, L., Xiao, C.L., Engineer, C.B., Boron, W.F., and Schroeder, J.I. (2015). Distinct cellular locations of carbonic anhydrases mediate carbon dioxide control of stomatal movements. Plant Physiol 169, 1168-1178.

Huang, X., von Rad, U., Durner, J. (2002). Nitric oxide induces the nitric oxidetolerant alternative oxidase in Arabidopsis suspension cells. Planta 215, 914-923.

Hussain, J., Chen, J., Locato, V., Sabetta W., Behera, S., Cimini, S., Griggio, F., Mart ńez-Jaime, S., Graf, A., Bouneb, M. et al. (2016). Constitutive cyclic GMP accumulation in Arabidopsis thaliana compromises systemic acquired resistance induced by an avirulent pathogen by modulating local signals. Scientific Reports 6, p. 36423

Hussain, A., Mun, B., Imran, Q.M., Lee,S., Adamu, T.A., Shahid, M.,Kim, K., Yun, B. (2016). Nitric oxide mediated transcriptome profiling reveals activation of multiple regulatory pathways in Arabidopsis thaliana. Front Plant Sci 7, 957.

Ignatova, L.K., Rudenko, N.N., Mudrik, V.A., Fedorchuk, T.P., Ivanov, B.N. (2011). Carbonic anhydrase activity in Arabidopsis thaliana thylakoid membrane and fragments enriched with PSI or PSII. Photosynth Res 110, 89-98.

Imran, Q.M., Hussain, A., Lee, S-U, Mun, B-G, Falak, N., Loake, G.j., Yun, B-W. (2017). Transcriptome profile of NO-induced Arabidopsis transcription factor genes suggests their putative regulatory role in multiple biological processes. Scientific Reports 8, 771

Jeandroz, S., Wipf, D., Stuehr, D.J., Lamattina, L., Melkonian, M., Tian, Z., Zhu, Y., Carpenter, E.J., Wong, G.K., Wendehenne, D. (2016). Occurrence, structure, and evolution of nitric oxide synthase-like proteins in the plant kingdom. Sci Signal 9, re2.

Jiang, C.Y., Tholen, D., Xu, J.M., Xin, C.P., Zhang, H., Zhu, X.G., and Zhao, Y.X. (2014). Increased expression of mitochondria-localized carbonic anhydrase activity resulted in an increased biomass accumulation in Arabidopsis thaliana. J Plant Biol. 57, 366-374.

Johansen, L.K., Carrington, J.C. (2001). Silencing on the spot. Induction and suppression of RNA silencing in the agrobacterium-mediated transient expression system. Plant Physiol 126, 930-938.

Jones, J.D., Dangl, J.L. (2006). The plant immune system. Nature 444, 323-329.

Jung, H.W., Lim, C.W., Lee, S.C., Choi, H.W., Hwang, C.H., Hwang, B.K. (2008). Distinct roles of the pepper hypersensitive induced reaction protein gene CaHIR1 in disease and osmotic stress, as determined by comparative transcriptome and proteome analyses. Planta

227, 409-425.

Karimi, M., Inze, D. Depicker, A. (2002). GATEWAY vectors for Agrobacterium-mediated plant transformation. Trends Plant Sci 7, 193-195.

Karlsson, J., Clarke, A.K., Chen, Z.Y., Hugghins, S.Y., Park, Y.I., Husic, H.D., Moroney, J.V., Samuelsson, G. (1998). A novel alpha-type carbonic anhydrase associated with the thylakoid membrane in Chlamydomonas reinhardtii is required for growth at ambient CO_2. EMBO J 17, 1208-1216.

Kawasaki, T., Nam, J., Boyes, D.C., Holt III, B.F., Hubert, D.A., Wiig, A., Dangl, J.L. (2005). A duplicated pair of Arabidopsis RINGfinger E3 ligases contribute to the RPM1- and RPS2-mediated hypersensitive response. Plant J 44, 258-270.

Khristin, M.S., Ignatova, L.K., Rudenko, N.N., Ivanov, B.N., Klimov, V.V. (2004). Photosystem II associated carbonic anhydrase activity in higher plant is situated in core complex. FEBS Lett 577, 305-308.

Kim, D., Langmead, B. Salzberg, S.L. (2015). HISAT: a fast spliced aligner with low memory requirements. Nature Methods 12, 357-360.

Kimber, M.S., Pai, E.F. (2000). The active site architecture of Pisum sativum β-carbonic anhydrase is a mirror image of that of α-carbonic anhydrases. The EMBO J 19, 1407-1418.

Kisker, C., Schindelin, H., Alber, B.E., Ferry, J.G., Rees, D.C. (1996). A left-handed beta-helix revealed by the crystal structure of a carbonic anhydrase from the archaeon Methanosarcina thermophila. EMBO J 15, 2323-2330.

Kitajima, A., Asatsuma, S., Okada, H., Hamada, Y., Kaneko, K., Nanjo, Y., Kawagoe, Y., Toyooka, K., Matsuoka, K., Takeuchi, M., Nakano, A., Mitsui, T. (2009). The rice a-Amylase glycoprotein is targeted from the Golgi apparatus through the secretory pathway to the plastids. Plant Cell 21, 2844-2858.

Kourelis, J.,van der Hoorn, R.A.L. (2018). Defended to the nines: 25 years of resistance gene cloning identifies nine mechanisms for R protein function. Plant Cell, DOI 10.1105/tpc.17.00579

Krzymowska, M., Konopka-Postupolska, D., Sobczak, M., Macioszek, V., Ellis, B.E., Hennig, J. (2007). Infection of tobacco with different Pseudomonas syringae pathovars leads to distinct morphotypes of programmed cell death. Plant J 50, 253-264.

Laloi, C., Przybyla, D., Apel, K. (2006). A genetic approach towards elucidating the biological activity of different reactive oxygen species in Arabidopsis thaliana. J Exp Bot 57, 1719-1724.

Lam, E., del Pozo, O. (2000). Caspase-like protease involvement in the control of plant cell death. Plant Mol Biol 44, 417-428.

Lamb, C. Dixon, R.A. (1997). The oxidative burst in plant disease resistance. Annu Rev Plant Physiol Plant Mol Biol 48, 251-275.

Leitner, M., Vandelle,E., Gaupels,F., Bellin,D., Delledonne,M. (2009). NO signals in the haze: Nitric oxide signalling in plant defence. Curr Opin Plant Biol 12, 451-458.

León, J., Costa, Á., Castillo, M.C. (2016). Nitric oxide triggers a transient metabolic reprogramming in Arabidopsis. Sci Rep 6, 37945.

Levine, A., Pennell, R.I., Alvarez, M.E., Palmer, R., Lamb, C. (1996). Calcium-mediated apoptosis in plant hypersensitive disease resistance response. Curr Bio 6, 427-437.

Levine, A., Tenhaken, R., Dixon, R. A. Lamb, C. (1994). H_2O_2 from the oxidative burst orchestrates the plant hypersensitive response. Cell 79, 583-593.

Lillo, C., Christian, M., Lea, U.S., Provan, F., Oltedal, S. (2004). Mechanism and importance of post-translational regulation of nitrate reductase. J Exp Bot 55, 1275-1282.

Li, M., Ma, X., Chiang, Y-H., Yadeta, K.A., Ding, P., Dong, L., et al. (2014). Proline isomerization of the immunereceptor-interacting protein RIN4 by a cyclophilin inhibits effector-triggered immunity in Arabidopsis. Cell Host Microbe 16, 473-83.

Li, Y., Pennington, B.O., Hua, J. (2009). Multiple R-like genes are negatively regulated by BON1 and BON3 in Arabidopsis. Mol Plant Microbe Interact 22, 840-848.

Lindermayr, C., Saalbach, G., Durner, J. (2005). Proteomic identification of S-nitrosylated proteins in Arabidopsis. Plant Physiol 137, 921-930.

Ling, T., Bellin, D., Vandelle, E., Imanifard, Z., Delledonne, M. (2017). Host-mediated S-nitrosylation disarms the bacterial effector HopAI1 to reestablish immunity. Plant Cell 29: 2871–2881

Liu, J., Elmore, J.M., Lin, Z-J.D. Coaker. G. (2011). A receptor-like cytoplasmic kinase phosphorylates the host target RIN4, leading to the activation of a plant innate immune receptor. Cell Host Microbe 9, 137-146.

Liu, L. M., Hausladen, A., Zeng, M., Que, L., Heitman, J., Stamler, J. S. (2001). A metabolic enzyme for S-nitrosothiol conserved from bacteria to humans. Nature 410,
490-494.

Liu, Z.Z., Wang, J.L., Huang, X., Xu, W.H., Liu, Z.M., Fang, R.X. (2003). The promoter of a rice glycine-rich protein gene, Osgrp-2, confers vascular-specific expression in transgenic plants. Planta 216, 824-833.

Lorrain, S., Lin, B., Auriac, M.C., Kroj, T., Saindrenan, P., Nicole, M., Balague ´, C., Roby, D. (2004). VASCULAR ASSOCIATED DEATH1, a novel GRAM domain-containing protein, is a regulator of cell death and defense responses in vascular tissues. Plant Cell 16, 2217-2232.

Lorrain, S., Vailleau, F., Balague, C., Roby, D. (2003). Lesion mimic mutants: keys for deciphering cell death and defense pathways in plants? Trends Plant Sci 8, 263-271.

Ludwig, M. (2012). Carbonic anhydrase and the molecular evolution of C4 photosynthesis. Plant Cell Environ 35, 22-37.

Ma, H., Xiang, G., Li, Z., Wang, Y., Dou, M., Su, L., Yin, X., Liu, R., Wang, Y., Xu, Y. (2018).

Grapevine VpPR10.1 functions in resistance to Plasmopara viticola through triggering a cell death‐like defence response by interacting with VpVDAC3. Plant Biotechnol J, doi: 10.1111/pbi.12891.

Macho, A. P., Zipfel, C. (2014). Plant PRRs and the activation of innate immune signaling. Mol Cell 54, 263-272.

Mackey, D., Holt III, B.F., Wiig, A., Dangl, J.L. (2002). RIN4 Interacts with Pseudomonas syringae Type III Effector Molecules and Is Required for RPM1-Mediated Resistance in Arabidopsis. Cell 108, 743-754.

Mackey, D., Belkhadir, Y., Alonso, J.M., Ecker, J.R., Dangl, J.L. (2003). Arabidopsis RIN4 is a target of the type III virulence effector AvrRpt2 and modulates RPS2-mediated resistance. Cell 112, 379-389.

Majeau, N., Arnoldo, M., Coleman, J.R. (1994). Modification of carbonic anhydrase activity by antisense and over-expression constructs in transgenic tobacco. Plant Mol Biol 25, 377-385.

Martinez-Ruiz, A., Cadenas, S., Lamas, S. (2011). Nitric oxide signaling: classical, less classical, and nonclassical mechanisms. Free Radic Biol Med, 17-29.

Maia, L.B. Moura, J.J.G. (2015). Nitrite reduction by molybdoenzymes: a new class of nitric oxide-forming nitrite reductases. J. Biol. Inorg. Chem 20, 403-433.

McDowell, J.M., Dangl, J.L. (2000). Signal transduction in the plant immune response. Trends Biochem Sci 25, 79-82.

Melotto, M., Underwood, W., He, S.Y. (2008). Role of stoma in plant innate immunity and foliar bacterial diseases. Annu Rev Phytopathol 46, 101-22.

Meier, S., Madeo, L., Ederli, L., Donaldson, L., Pasqualini, S., Gehring, C. (2009). Deciphering cGMP signatures and cGMP-dependent pathways in plant defence. Plant Signal Behav 4, 307-309.

Meyer, C., Lea, U.S., Provan, F., Kaiser, W.M., Lillo, C. (2005). Is nitrate reductase a major player in the plant NO (nitric oxide) game? Photosynth Res 83, 181-189.

Moreau, M., Lee, G.I., Wang, Y,, Crane, B.R., Klessig, D.F. (2008). AtNOS/AtNOA1 is a functional Arabidopsis thaliana cGTPase and not a nitric-oxide synthase. J Biol Chem 283, 32957-32967.

Moreau, M., Lindermayr, C., Durner, J., Klessig, D.F. (2010). NO synthesis and signaling in plants –where do we stand? Physiol Plant 138, 372-383.

Moroney, J.V., Bartlett, S.G., Samuelsson, G. (2001). Carbonic anhydrases in plants and algae. Plant Cell Environ 241, 41-153.

Moroney, J.V., Ma, Y., Frey,W.D., Fusilier, K., Pham, T.T., Simms, T.A., DiMario, R.J., Yang, J., Mukherjee, B. (2011). The carbonic anhydrase isoforms of Chlamydomonas reinhardtii: expression, intracellular location and physiological roles. Photosynth Res 109, 1331-49.

Morot Gaudry-Talarmain, Y., Rockel, P., Moureaux, I., Quillere, I., Leydecker, M.T., Kaiser, W.M., Morot-Gaudry, J.F. (2002). Nitrite accumulation and nitric oxide emission in relation to cellular signaling in nitrite reductase antisense tobacco. Planta 215, 708-715.

Montillet, J-L., Chamnongpol, S,, Rusterucci, C., Dat, J., van de Cotte, B., Agnel, J-P., Battesti, C., Inze, D., Van Breusegem, F., Triantaphylides, C. (2005). Fatty acid hydroperoxides and H_2O_2 in the execution of hypersensitive cell death in tobacco leaves. Plant Physiol 138, 1516-1526.

Mou, Z., Fan, W., Dong, X. (2003). Inducers of plant systemic acquired resistance regulate NPR1 function through redox changes. Cell 113, 935-944.

Mur, L.A., Kenton, P., Lloyd, A.J., Ougham, H., Prats, E. (2008). The hypersensitive response; the centenary is upon us but how much do we know? J Exp Bot 59, 501-520.

Mur, L. A. J., Sivakumaran, A., Mandon, J., Cristescu, S. M., Harren, F. J. M., Hebelstrup, K. H. (2012). Haemoglobin modulates salicylate and jasmonate/ethylene-mediated resistance mechanisms against pathogens. Journal of Experimental Botany 63, 4375-4387.

Nagaraj, N., Wisniewski, J. R., Geiger, T., Cox, J., Kircher, M., Kelso, J., Paabo, S., Mann, M. (2011). Deep proteome and transcriptome mapping of a human cancer cell line. Mol Syst Biol 7, 548.

Nicaise, V., Roux, M., Zipfel, C. (2009). Recent Advances in PAMP-Triggered Immunity against Bacteria: Pattern Recognition Receptors Watch over and Raise the Alarm. Plant physiol 150, 1638-1647.

O'Brien, J.A., Daudi, A., Finch, P., Butt, V.S., Whitelegge, J.P., Souda, P., Ausubel, F.M, Bolwell, G.P. (2012). A peroxidase-dependent apoplastic oxidative burst in cultured Arabidopsis cells functions in MAMP-elicited defense. Plant Physiol 158, 2013-2027.

Overmyer, K., Brosche, M., Pellinen, R., Kuittinen, T., Tuominen, H., Ahlfors, R., Keina ̈nen, M., Saarma, M., Scheel, D., Kangasja ̈rvi, J. (2005). Ozone-induced programmed cell death in the Arabidopsis radical-induced cell death1 mutant. Plant Physiol 137, 1092-1104.

Palmieri, M.C., Sell, S., Huang, X., Scherf, M., Werner, T., Durner, J., Lindermayr, C. (2008). Nitric oxide-responsive genes and promoters in Arabidopsis thaliana: a bioinformatics approach. J Exp Bot 59, 177-186.

Parani, M., Rudrabhatla, S., Myers, R., Weirich, H., Smith, B., Leaman, D.W., and Goldman, S.L. (2004). Microarray analysis of nitric oxide responsive transcripts in Arabidopsis. Plant Biotechnol J 2, 359-366.

Peng, M., Kuc, J.A. (1992). Peroxidase generated hydrogen peroxide as a source of antifungal activity in vitro and on tobacco leaf disks. Phytopathol 82, 696-699.

Perales, M., Eubel, H., Heinemeyer, J., Colaneri, A., Zabaleta, E., Braun, H.P. (2005). Disruption of a nuclear gene encoding a mitochondrial gamma carbonic anhydrase reduces complex I and supercomplex I+III2 levels and alters mitochondrial physiology in Arabidopsis. J Mol Biol 350, 263-277.

Perazzolli, M., Dominici, P., Romero-Puertas, M. C., Zago, E., Zeier, J., Sonoda, M., Lamb, C., Delledonne, M. (2004). Arabidopsis nonsymbiotic hemoglobin AHb1 modulates nitric oxide bioactivity. Plant Cell, 16, 2785-2794.

Petersen, N.H., McKinney, L.V., Pike, H., Hofius, D., Zakaria, A., Brodersen, P., Petersen, M., Brown, R.E., Mundy, J. (2008). Human GLTP and mutant forms of ACD11 suppress cell death in the Arabidopsis acd11 mutant. FEBS J 275, 4378-4388.

Planchet, E., Gupta, K.J., Sonoda, M., Kaiser., W.M. (2005). Nitric oxide emission from tobacco leaves and cell suspensions: rate limiting factors and evidence for the involvement of mitochondrial electron transport. Plant J 41, 732-743.

Polverari, A., Molesini, B., Pezzotti, M., Buonaurio, R., Marte, M., Delledonne, M. (2003). Nitric oxide-mediated transcriptional changes in Arabidopsis thaliana. Mol Plant Microbe Interact 16, 1094-1105.

Poincelot, R.P. (1972). Intracellular distribution of carbonic anhydrase in spinach leaves. Biochim Biophys Acta 258, 637-642.

Porra, R.J., Thompson, W.A., Kriedemann, P.E. (1989). Determination of accurate extinction coefficients and simultaneous equations for assaying chlorophylls a and b extracted with four different solvents: verification of the concentration of chlorophyll standards by atomic absorption spectroscopy. Biochim Biophys Acta 975, 384-394.

Price, G.D., von Caemmerer, S., Evans, J.R., Yu, J.W., Lloyd, J., Oja, V., Kell, P., Harrison, K., Gallagher, A., Badger, M.R. (1994). Specific reduction of chloroplast carbonic anhydrase activity by antisense RNA in transgenic tobacco plants has a minor effect on photosynthesis. Planta 193, 331-340.

Pugin, A., Frachisse, J.M., Tavernier, E., Bligny, R., Gout, E., Douce, R., Guern, J. (1997). Early events induced by the elicitor cryptogein in tobacco cells: involvement of a plasma membrane NADPH oxidase and activation of glycolysis and the pentose phosphate pathway. Plant Cell 9, 2077-2091.

Quirino, B.F Bent, A.F. (2003). Deciphering host resistance and pathogen virulence: the Arabidopsis/Pseudomonas interaction as a model. Mol Plant Pathol 4, 517-530.

Radi, R. (2004). Nitric oxide, oxidants, and protein tyrosine nitration. Proc Natl Acad Sci USA 101, 4003-4008.

Restrepo, S., Myers, K.L., del Pozo, O., Martin, G.B., Hart, A.L., Buell, C.R., Fry,W.E., Smart, C.D. (2005). Gene profiling of a compatible interaction between Phytophthora infestans and Solanum tuberosum suggests a role for carbonic anhydrase. Mol Plant Microbe Interact 18, 913-922.

Roberts, A., Pimentel, H., Trapnell, C. Pachter, L. (2011). Identification of novel transcripts in annotated genomes using RNA-seq. Bioinformatics 27, 2325-2329.

Rockel, P., Strube, F., Rockel, A., Wildt, J., Kaiser, W.M. (2002). Regulation of nitric oxide (NO) production by plant nitrate reductase in vivo and in vitro. J Exp Bot 53, 103-110.

Rodriguez-Serrano, M., Romero-Puertas, M.C., Zabalza, A., Corpas, F.J., Gomez, M., Del Rio, L.A., Sandalio, L.M. (2006). Cadmium effect on oxidative metabolism of pea (Pisum sativum L.) roots. Imaging of reactive oxygen species and nitric oxide accumulation in vivo. Plant Cell Environ 29, 1532-1544.

Rojo, E., Martin, R., Carter, C., Zouhar, J., Pan, S., Plotnikova, J., Jin, H., Paneque,M., Sánchez-Serrano, J.J., Baker, B., Ausubel, F.M., Raikhel, N.V. (2004). VPEgamma exhibits a caspase-like activity that contributes to defense against pathogens. Curr Biol 14, 1897-1906.

Romero-Puertas, M.C., Campostrini, N., Matte, A., Righetti, P.G., Perazzolli, M., Zolla, L.,Roepstorff, P., Delledonne, M. (2008). Proteomic analysis of S-nitrosylated proteins in Arabidopsis thaliana undergoing hypersensitive response. Proteomics 8, 1459-1469.

Romero-Puertas,M. C., Laxa,M.,Matte, A., Zaninotto, F., Finkemeier, I., Jones, A.M., Perrazzolli, M., Vandelle, E., Dietz, K., Delledonne, M. (2007). S-nitrosylation of peroxiredoxin II E promotes peroxynitrite-mediated tyrosine nitration. Plant Cell, 19(12), 4120-4130.

Rowlett, R.S. (2010). Structure and catalytic mechanism of the β-carbonic anhydrases. Biochim Biophys Acta 1804, 362-373.

Rudenko, N.N., Ignatova, L.K., Ivanov, B.N. (2007). Multiple sources ofcarbonic anhydrase activity in pea thylakoids: soluble and membrane-bound forms. Photosynth Res 91,81-89.

Rudenko, N.N., Ignatova, L.K., Fedorchuk, T.P., Ivanov, B.N. (2015). Carbonic anhydrases in photosynthetic cells of higher plants. Biochemistry (Moscow) 80, 674-687.

Rumer, S. Gupta, K.J., Kaiser, W.M. (2009). Oxidation of hydroxylamines to NO by plant cells. Plant Signal Behav 4, 853-855.

Rusterucci, C., Espunya, M. C., Diaz, M., Chabannes, M., Martinez, M. C. (2007). S-nitrosoglutathione reductase affords protection against pathogens in Arabidopsis, both locally and systemically. Plant Physiology 143, 1282-1292.

Ryals, J.A., Neuenschwander, U.H., Willits, M.G., Molina, A., Steiner, H-Y, Hunt, M.D. (1996). Systemic acquired resistance. Plant Cell 8, 1809-1819.

Santolini, J., Andre, F., Jeandroz, S., Wendehenne, D. (2017). Nitric oxide synthase in plants: where do we stand? Nitric Oxide 63, 30-38.

Slaymaker, D.H., Navarre, D.A., Clark, D., del Pozo, O., Martin, G.B., Klessig, D.F. (2002). The tobacco salicylic acid-binding protein 3 (SABP3) is the chloroplast carbonic anhydrase, which exhibits antioxidant activity and plays a role in the hypersensitive defense response. Proc Natl Acad Sci USA 99, 11640-11645.

Shao, F., Golstein, C., Ade, J., Stoutemyer, M., Dixon, J.E., Innes, R.W. (2003). Cleavage of Arabidopsis PBS1 by a Bacterial Type III Effector. Science 301, 1230-1233.

Shi, H., Ye, T., Zhu, J., Chan Z. (2014). Constitutive production of nitric oxide leads to enhanced drought stress resistance and extensive transcriptional reprogramming in Arabidopsis. J Exp Bot 65, 4119-4131.

Simon-Plas, F., Elmayan, T., Blein, J-P. (2002). The plasma membrane oxidase NtrbohD is responsible for AOS production in elicited tobacco cells. Plant J 31, 137-148.

Stamler, J.S., Lamas, S., Fang, F.C. (2001). Nitrosylation: the prototypic redox-based signaling mechanism. Cell 106, 675-683.

Stohr, C., Strube, F., Marx, G., Ullrich, W.R. Rockel, P. (2001). A plasma membrane-bound enzyme of tobacco roots catalyses the formation of nitric oxide from nitrite. Planta 212, 835-841.

Stohr, C., Stremlau, S. (2006). Formation and possible roles of nitric oxide in plant roots. J Exp Bot 57, 463-470.

Sugimoto, M., Yamaguchi, Y., Nakamura, K., Tatsumi, Y., Sano, H. (2004). A hypersensitive response-induced ATPase associated with various cellular activities (AAA) protein from tobacco plants. Plant Mol Biol 56, 973-985.

Sunderhaus, S., Dudkina, N.V., Jansch, L., Klodmann, J., Heinemeyer, J., Perales, M., Zabaleta, E., Boekema, E.J., Braun, H.P. (2006). Carbonic anhydrase subunits form a matrix-exposed domain attached to the membrane arm of mitochondrial complex I in plants. J Biol Chem 281, 6482-6488

Sudhamsu, J., Lee, G.I., Klessig, D.F., Crane, B.R. (2008). The structure of YqeH. An AtNOS1/AtNOA1 ortholog that couples GTP hydrolysis to molecular recognition. J Biol Chem 283, 32968-32976.

Supuran, C.T. (2008). Carbonic anhydrases: novel therapeutic applications for inhibitors and activators. Nat Rev Drug Discov 7, 168-181.

Supuran, C.T. (2016). Structure and function of carbonic anhydrases. Biochem J 473, 2023-2032.

Tada, Y., Spoel, S. H., Pajerowska-Mukhtar, K., Mou, Z., Song, J., Wang, C., Zuo, J., Dong, X. (2008). Plant immunity requires conformational changes of NPR1 via S-nitrosylation and thioredoxins. Science 321, 952-956.

Tavares, C.P., Vernal, J., Delena, R.A., Lamattina, L., Cassia, R., Terenzi, H. (2014). S-nitrosylation influences the structure and DNA binding activity of AtMYB30 transcription factor from Arabidopsis thaliana. Biochim Biophys Acta 1844, 810-817.

Thomma, B.P., Nurnberger, T., Joosten, M.H. (2011). Of PAMPs and effectors: the blurred PTI-ETI dichotomy. Plant Cell 23, 4-15.

Tian, T., Liu, Y., Yan, H., You, Q., Yi, X., Du, Z., Xu, W., Su, Z. (2017). agriGO v2.0: a GO analysis toolkit for the agricultural community, 2017 update. Nucleic Acids Res 45, W122-W129.

Tischner, R., Galli, M., Heimer, Y.M., Bielefeld, S., Okamoto, M., Mack, A., Crawford, N.M. (2007) Interference with the citrulline-based nitric oxide synthase assay by argininosuccinate lyase activity in Arabidopsis extracts. FEBS J 274, 4238-4245.

Torres, M.A., Dangl, J.L. (2005). Functions of the respiratory burst oxidase in biotic interactions, abiotic stress and development. Curr Opin Plant Biol 8, 397-403.

Torres, M.A., Dangl, J.L., Jones, J.D. (2002). Arabidopsis gp91phox homologues AtrbohD and AtrbohF are required for accumulation of reactive oxygen intermediates in the plant defense response. Proc Natl Acad Sci USA 99, 517-522.

Trapnell, C., Roberts, A., Goff, L., Pertea, G., Kim, D., Kelley, D.R., Pimentel, H., Salzberg, S.L., Rinn, J.L., Pachter, L. (2012). Differential gene and transcript expression analysis of RNA-seq experiments with TopHat and Cufflinks. Nat Protoc. 7, 562-578.

Tripp, B.C., Smith, K., Ferry, J.G. (2001). Carbonic anhydrase: new insights for an ancient enzyme. J Biol Chem 276, 48615-48618

Truman, W., de Zabala, M.T., Grant, M. (2006). Type III effectors orchestrate a complex interplay between transcriptional networks to modify basal defence responses during pathogenesis and resistance. Plant J 46, 14-33.

Tsuda, K., Katagiri, F. (2010). Comparing signaling mechanisms engaged in pattern-triggered and effector-triggered immunity. Curr Opin Plant Biol 13, 459-465.

Tun, N.N., Santa-Catarina, C., Begum, T., Silveira, V., Handro, W., Floh, EIS., Scherer, GFE. (2006). Polyamines induce rapid biosynthesis of nitric oxide (NO) in Arabidopsis thaliana seedlings. Plant Cell Physiol 47, 346-354.

Turek, I., Gehring, C. (2016). The plant natriuretic peptide receptor is a guanylyl cyclase and enables cGMP-dependent signaling. Plant Mol Biol 91, 275-286.

Van Breusegem, F., Dat, J.F. (2006). Reactive oxygen species in plant cell death. Plant Physiol 141, 384-390.

Vandelle, E., Delledonne, M. (2011). Peroxynitrite formation and function in plants. Plant Science 181, 534-539.

Vandelle, E., Ling, T., Imanifard, Z., Liu, R., Delledonne, M., Bellin, D. (2016). Chapter Eleven-Nitric Oxide Signaling during the Hypersensitive Disease Resistance Response. In Advances in Botanical Research 77, 219-243.

Villarejo, A., Buren, S., Larsson, S.,Dejardin, A.,Monne,M., Rudhe, C., Karlsson, J., Jansson, S., Lerouge, P., Rolland, N., von Heijne, G., Grebe, M., Bako, L., Samuelsson, G. (2005). Evidence for a protein transported through the secretory pathway en route to the higher plant chloroplast. Nat Cell Biol 7, 1224-1231.

Villarreal, F., Martín, V., Colaneri, A., González-Schain, N., Perales, M., Martín, M., Lombardo, C., Braun, H.P., Bartoli, C., Zabaleta, E. (2009). Ectopic expression of mitochondrial gamma carbonic anhydrase 2 causes male sterility by anther indehiscence. Plant Mol Biol 70, 471-485.

Wang, C., El-Shetehy, M., Shine, M.B., Yu, K., Navarre, D., Wendehenne, D., Kachroo, A., Kachroo, P. (2014). Free radicals mediate systemic acquired resistance. Cell Reports 7, 348-355.

Wang, J., Krizowski, S., Fischer, K., Niks, D., Tejero, J., Sparacino-Watkins, C., et al., (2014). Sulfite oxidase catalyzes single electron transfer at molybdenum domain to reduce nitrite to nitric oxide. Antioxidants and Redox Signaling 23, 283-294.

Wang Q, Fristedt R, Yu X, Chen Z, Liu H, Lee Y, Guo H, Merchant SS, Lin C.(2012). The gamma-carbonic anhydrase subcomplex of mitochondrial complex I is essential for development and important for photomorphogenesis of Arabidopsis. Plant Physiol 160, 1373-1383.

Wang, Y.H., Chen,T., Zhang, C.Y., Hao, H.Q., Liu, P., Zheng, M.Z., Baluska, F., Samaj, J., Lin, J.X. (2009). Nitric oxide modulates the influx of extracellular Ca^{2+} and actin filament organization during cell wall construction in Pinus bungeana pollen tubes. New Phytologist 182, 851-862.

Wang, Y.Q., Feechan, A., Yun, B.W., Shafiei, R., Hofmann, A., Taylor, P., Xue, P., Yang, F.Q., Xie, Z.S., Pallas, J.A., Chu, C.C., Loake, G.J. (2009). S-nitrosylation of AtSABP3 antagonizes the expression of plant immunity. J Biol Chem 284, 2131-2137.

Watanabe, N., Lam, E. (2011). Arabidopsis metacaspase 2d is a positive mediator of cell death induced during biotic and abiotic stresses. Plant J 66, 969-982.

Werdan, K., Heldt, H.W. (1972). Accumulation of bicarbonate in intact chloroplasts following a pH gradient. Biochim Biophys Acta 283, 430-441.

Wilbur, K.M., Anderson, N.G. (1948). Electrometric and colorimetric determination of carbonic anhydrase. J Biol Chem 176, 147-154.

Wilkinson, J.Q. Crawford, N.M. (1993). Identification and characterization of a chlorate-resistant mutant of Arabidopsis thaliana with mutations in both nitrate reductase structural genes NIA1 and NIA2. Mol Gen Genet 239, 289-297.

Xin, X.F., He, S.Y. (2013). Pseudomonas syringae pv. tomato DC3000: A model pathogen for probing disease susceptibility and hormone signaling in plants. Annu Rev Phytopathol 51, 473-98.

Xu, G., Wang, S., Han, S., Xie, K., Wang, Y., Li, J. Liu, Y. (2017). Plant Bax Inhibitor - 1 interacts with ATG6 to regulate autophagy and programmed cell death. Autophagy 13, 1161-1175.

Xu, H., Heath, M.C. (1998). Role of calcium in signal transduction during the hypersensitive response caused by basidiospore-derived infection of the cowpea rust fungus. Plant Cell 10, 585-598.

Yang. J., Giles. L.J., Ruppelt. C., Mendel. R.R., Bittner. F., Kirk. M.L. (2015). Oxyl and hydroxyl radical transfer in mitochondrial amidoxime reducing component catalyzed nitrite reduction. J Am Chem Soc 137, 5276-5279.

Yamasaki, H., Cohen, M.F. (2006). NO signal at the crossroads: polyamine-induced nitric oxide synthesis in plants? Trends Plant Sci 11, 522-524.

Yamasaki, H., Sakihama, Y. (2000). Simultaneous production of nitric oxide and peroxynitrite

by plant nitrate reductase: in vitro evidence for the NR-dependent formation of active nitrogen species. FEBS Lett 468, 89-92.

Yeats, T.H., Rose, J.K.C. (2013). The formation and function of plant Cuticles. Plant Physiol 163, 5-20.

Yu, M., Lamattina, L., Spoel, S.H., Loake, G.J. (2014). Nitric oxide in plant biology: a redox cue in deconvolution. New Phytol 202, 1142-1156.

Yun, B.W., Feechan, A., Yin,M., Saidi, N.B., Le Bihan, T., Yu, M., Moore, J.W., Kang, J.G., Kwon, E., Spoel, S.H., Pallas, J.A., Loake, G.J. (2011). S-nitrosylation of NADPH oxidase regulates cell death in plant immunity. Nature 478, 264-268.

Zabaleta, E., Martin, M.V., and Braun, H.P. (2012). A basal carbon concentrating mechanism in plants? Plant Sci 187, 97-104.

Zhang, B., Van Aken, O., Thatcher, L., De Clercq, I., Duncan, O., Law, S.R., Murcha ,M.W., van der Merwe, M., Seifi, H.S., Carrie, C., et al. (2014). The mitochondrial outer membrane AAA ATPase AtOM66 affects cell deathand pathogen resistance in Arabidopsis thaliana. Plant J 80, 709-727.

Zhurikova, E.M., Ignatova, L.K., Rudenko, N.N., Mudrik, V.A., Vetoshkina, D.V., Ivanov, B.N. (2016). Participation of two carbonic anhydrases of the alpha family in photosynthetic reactions in Arabidopsis thaliana. Biochemistry (*Moscow*) 81, 1182-1187.

Zeier, J., Delledonne, M., Mishina, T., Severi, E., Sonoda, M., Lamb, C. (2004). Genetic elucidation of nitric oxide signaling in incompatible plant-pathogen interactions. Plant Physiol 136, 2875-2886.

Zhurikova, E.M., Ignatova, L.K., Rudenko, N.N., Mudrik, V.A., Vetoshkina, D.V., Ivanov, B.N., 2016. Participation of two carbonic anhydrases of the alpha family in photosynthetic reactions in Arabidopsis thaliana. Biochem. (Mosc) 81, 1182-1187.

Zipfel, C. (2008). Pattern-recognition receptors in plant innate immunity. Curr Opin Immunol 20, 10-16.

8. Appendix

Supplemental Table 1. List of genes in the functional class "cell death" significantly differentially expressed following treatment for 8 hour with NO at 200 ppm.

Gene ID	FDR	P-value	logFC	Alias	Description
AT4G12470	2,94E-182	2,09E-184	9,92	AZI1	pEARLI1-like lipid transfer protein 1 [Uniprot/SWISSPROT Acc. Q9SU35]
AT2G44110	6,00E-08	3,04E-08	6,99	MLO15	MLO-like protein [Uniprot/SPTREMBL Acc. F4IT46]; MLO-like protein 15 [Uniprot/SWISSPROT Acc. O80580]
AT3G13610	4,31E-34	6,67E-35	6,78	F6'H1	F6'H1 [Uniprot/SPTREMBL Acc. A0A178V671]; Feruloyl CoA ortho-hydroxylase 1 [Uniprot/SWISSPROT Acc. Q9LHN8]
AT1G16420	6,92E-92	2,31E-93	6,27	AMC8	Metacaspase-8 [Uniprot/SWISSPROT Acc. Q9SA41]
AT2G26560	1,58E-113	3,41E-115	6,20	PLP2	Patatin-like protein 2 [Uniprot/SWISSPROT Acc. O48723]
AT3G50930	3,51E-107	8,43E-109	6,08	HSR4	Protein HYPER-SENSITIVITY-RELATED 4 [Uniprot/SWISSPROT Acc. Q8VZG2]
AT5G47130	7,45E-104	1,91E-105	5,74		Bax inhibitor-1 family protein [Uniprot/SPTREMBL Acc. Q9LTB6]
AT1G19250	1,60E-31	2,72E-32	5,73	FMO1	Probable flavin-containing monooxygenase 1 [Uniprot/SWISSPROT Acc. Q9LMA1]
AT3G01420	9,70E-06	5,77E-06	5,63	DOX1	Alpha-dioxygenase 1 [Uniprot/SWISSPROT Acc. Q9SGH6]
AT5G65600	6,83E-62	4,56E-63	4,81	LECRK92	Uncharacterized protein [Uniprot/SPTREMBL Acc. A0A178UB11]; L-type lectin-domain containing receptor kinase IX.2 [Uniprot/SWISSPROT Acc. Q9LSL5]
AT1G08860	1,41E-32	2,30E-33	4,76	BON3	Protein BONZAI 3 [Uniprot/SWISSPROT Acc. Q5XQC7]
AT5G15090	3,54E-111	8,05E-113	4,38	VDAC3	Mitochondrial outer membrane protein porin 3 [Uniprot/SWISSPROT Acc. Q9SMX3]
AT1G32230	1,25E-70	6,74E-72	3,90	RCD1	Poly [ADP-ribose] polymerase [Uniprot/SPTREMBL Acc. F4ICM3]; Poly [ADP-ribose] polymerase [Uniprot/SPTREMBL Acc. M5BF30]; Inactive poly [ADP-ribose] polymerase RCD1 [Uniprot/SWISSPROT Acc. Q8RY59]
AT4G23210	1,83E-22	4,35E-23	3,70	CRK13	Cysteine-rich receptor-like protein kinase 13 [Uniprot/SWISSPROT Acc. Q0PW40]
AT4G36480	7,84E-106	1,93E-107	3,50	LCB1	LCB1 [Uniprot/SPTREMBL Acc. A0A178UY56]; Long chain base biosynthesis protein 1 [Uniprot/SWISSPROT Acc. Q94IB8]
AT3G46530	7,03E-45	7,58E-46	3,43	RPP13	Disease resistance protein RPP13 [Uniprot/SWISSPROT Acc. Q9M667]
AT3G52400	2,95E-52	2,53E-53	3,39	SYP122	SYP122 [Uniprot/SPTREMBL Acc. A0A178VEE7]; Syntaxin-122 [Uniprot/SWISSPROT Acc. Q9SVC2]
AT4G37990	2,82E-15	9,23E-16	3,33	CAD8	ELI3-2 [Uniprot/SPTREMBL Acc. A0A178UVK9]; Cinnamyl alcohol dehydrogenase 8 [Uniprot/SWISSPROT Acc. Q02972]
AT4G23280	1,62E-13	5,81E-14	3,26	CRK20	Putative cysteine-rich receptor-like protein kinase 20 [Uniprot/SWISSPROT Acc. O65479]
AT5G45100	9,33E-52	8,13E-53	3,19	BRG1	BOI-related E3 ubiquitin-protein ligase 1 [Uniprot/SWISSPROT

					Acc. Q9FHE4]
AT5G44870	1,92E-47	1,91E-48	3,13	LAZ5	TTR1 [Uniprot/SPTREMBL Acc. A0A178ULB4]; Disease resistance protein LAZ5 [Uniprot/SWISSPROT Acc. O48573]
AT2G46240	3,42E-21	8,58E-22	3,09	BAG6	BAG family molecular chaperone regulator 6 [Uniprot/SWISSPROT Acc. O82345]
AT5G45250	2,50E-50	2,28E-51	3,00	RPS4	Disease resistance protein RPS4 [Uniprot/SWISSPROT Acc. Q9XGM3]
AT1G61560	5,27E-34	8,18E-35	2,90	MLO6	MLO-like protein [Uniprot/SPTREMBL Acc. F4HVC3]; MLO-like protein 6 [Uniprot/SWISSPROT Acc. Q94KB7]
AT3G50480	3,96E-54	3,23E-55	2,87	HR4	RPW8-like protein 4 [Uniprot/SWISSPROT Acc. Q9SCS6]
AT1G02170	3,52E-93	1,14E-94	2,87	AMC1	Metacaspase-1 [Uniprot/SWISSPROT Acc. Q7XJE6]
AT5G26920	2,25E-27	4,41E-28	2,71	CBP60G	Calmodulin-binding protein 60 G [Uniprot/SWISSPROT Acc. F4K2R6]
AT5G39610	3,11E-07	1,66E-07	2,68	NAC92	NAC domain-containing protein 92 [Uniprot/SWISSPROT Acc. Q9FKA0]
AT4G34180	4,46E-61	3,03E-62	2,66		AT4g34180/F28A23_60 [Uniprot/SPTREMBL Acc. Q93V74]
AT2G17430	2,33E-08	1,15E-08	2,62	MLO7	MLO-like protein 7 [Uniprot/SWISSPROT Acc. O22752]
AT2G01290	1,58E-29	2,87E-30	2,60	RPI2	Probable ribose-5-phosphate isomerase 2 [Uniprot/SWISSPROT Acc. Q9ZU38]
AT5G51290	5,58E-31	9,72E-32	2,58	CERK	Ceramide kinase [Uniprot/SWISSPROT Acc. Q6USK2]
AT5G51450	2,10E-48	2,02E-49	2,47	RIN3	E3 ubiquitin protein ligase RIN3 [Uniprot/SPTREMBL Acc. F4KD92]; E3 ubiquitin protein ligase RIN3 [Uniprot/SWISSPROT Acc. Q8W4Q5]
AT1G29690	5,79E-20	1,53E-20	2,29	CAD1	MACPF domain-containing protein CAD1 [Uniprot/SWISSPROT Acc. Q9C7N2]
AT1G11310	9,52E-54	7,85E-55	2,27	MLO2	MLO-like protein [Uniprot/SPTREMBL Acc. B3H6R0]; MLO-like protein [Uniprot/SPTREMBL Acc. Q0WWA7]; MLO-like protein 2 [Uniprot/SWISSPROT Acc. Q9SXB6]
AT3G54420	1,43E-11	5,75E-12	2,23	EP3	EP3 [Uniprot/SPTREMBL Acc. A0A178VE44]; Endochitinase EP3 [Uniprot/SWISSPROT Acc. Q9M2U5]
AT4G33430	1,46E-46	1,49E-47	2,18	BAK1	SERK3 [Uniprot/SPTREMBL Acc. A0A178UUK2]; Leu-rich receptor Serine/threonine protein kinase BAK1 [Uniprot/SPTREMBL Acc. F4JIX9]; BRASSINOSTEROID INSENSITIVE 1-associated receptor kinase 1 [Uniprot/SWISSPROT Acc. Q94F62]
AT4G25230	1,54E-47	1,52E-48	2,15	RIN2	E3 ubiquitin protein ligase RIN2 [Uniprot/SWISSPROT Acc. Q8VYC8]
AT4G03110	3,12E-31	5,37E-32	2,15	BRN1	RNA-binding protein BRN1 [Uniprot/SWISSPROT Acc. Q8LFS6]
AT1G77300	2,13E-17	6,31E-18	2,12		Histone-lysine N-methyltransferase ASHH2 [Uniprot/SPTREMBL Acc. F4I6Z9]
AT4G02640	1,83E-20	4,73E-21	2,00	BZIP10	Basic leucine zipper 10 [Uniprot/SWISSPROT Acc. O22763]
AT5G22290	5,82E-12	2,29E-12	2,00	NAC089	NAC089 [Uniprot/SPTREMBL Acc. A0A178UI96]; NAC

					domain-containing protein 89 [Uniprot/SWISSPROT Acc. Q94F58]
AT3G11820	5,86E-33	9,41E-34	1,95	SYP121	SYR1 [Uniprot/SPTREMBL Acc. A0A178VIM4]; Syntaxin-121 [Uniprot/SWISSPROT Acc. Q9ZSD4]
AT3G28910	1,93E-08	9,46E-09	1,94	MYB30	Transcription factor MYB30 [Uniprot/SWISSPROT Acc. Q9SCU7]
AT2G01180	9,12E-15	3,06E-15	1,92	LPP1	PAP1 [Uniprot/SPTREMBL Acc. A0A178VSS9]; Lipid phosphate phosphatase 1 [Uniprot/SWISSPROT Acc. Q9ZU49]
AT4G25110	3,00E-10	1,31E-10	1,83	AMC2	Metacaspase-2 [Uniprot/SWISSPROT Acc. Q7XJE5]
AT3G57330	1,04E-20	2,67E-21	1,83	ACA11	Calcium-transporting ATPase [Uniprot/SPTREMBL Acc. A0A178VG68]; Putative calcium-transporting ATPase 11, plasma membrane-type [Uniprot/SWISSPROT Acc. Q9M2L4]
AT5G13190	6,44E-22	1,57E-22	1,83		GILP [Uniprot/SPTREMBL Acc. Q94CD4]
AT1G22070	2,89E-18	8,22E-19	1,82	TGA3	At1g22070 [Uniprot/SPTREMBL Acc. Q147Q9]; Transcription factor TGA3 [Uniprot/SWISSPROT Acc. Q39234]
AT3G50260	4,31E-13	1,58E-13	1,81	ERF011	DEAR1 [Uniprot/SPTREMBL Acc. A0A178VN80]; Ethylene-responsive transcription factor ERF011 [Uniprot/SWISSPROT Acc. Q9SNE1]
AT2G34690	6,68E-24	1,50E-24	1,68	ACD11	Accelerated cell death 11 [Uniprot/SWISSPROT Acc. O64587]
AT3G15010	1,37E-16	4,22E-17	1,58	UBA2C	Uncharacterized protein [Uniprot/SPTREMBL Acc. A0A178V7K4]; UBP1-associated protein 2C [Uniprot/SWISSPROT Acc. Q9LKA4]
AT5G13320	5,07E-06	2,95E-06	1,56	GH3.12	4-substituted benzoates-glutamate ligase GH3.12 [Uniprot/SWISSPROT Acc. Q9LYU4]
AT1G28380	1,51E-13	5,42E-14	1,55	NSL1	MACPF domain-containing protein NSL1 [Uniprot/SWISSPROT Acc. Q9SGN6]
AT4G35790	2,55E-28	4,85E-29	1,54	PLDDELTA	Phospholipase D [Uniprot/SPTREMBL Acc. A0A178UUU1]; Phospholipase D [Uniprot/SPTREMBL Acc. F4JNU6]; Phospholipase D delta [Uniprot/SWISSPROT Acc. Q9C5Y0]
AT5G46180	6,25E-11	2,61E-11	1,52	DELTA-OAT	Ornithine aminotransferase, mitochondrial [Uniprot/SWISSPROT Acc. Q9FNK4]
AT2G39200	7,53E-06	4,44E-06	1,51	MLO12	MLO-like protein [Uniprot/SPTREMBL Acc. A0A178VNS1]; MLO-like protein 12 [Uniprot/SWISSPROT Acc. O80961]
AT4G20380	3,19E-18	9,10E-19	1,47	LSD1	Zinc finger protein LSD1 [Uniprot/SPTREMBL Acc. F4JUW0]; Protein LSD1 [Uniprot/SWISSPROT Acc. P94077]
AT2G34770	6,31E-20	1,67E-20	1,46	FAH1	FAH1 [Uniprot/SPTREMBL Acc. A0A178W0P1]; Dihydroceramide fatty acyl 2-hydroxylase FAH1 [Uniprot/SWISSPROT Acc. O48916]
AT4G19040	1,02E-13	3,61E-14	1,45	EDR2	Protein ENHANCED DISEASE RESISTANCE 2 [Uniprot/SWISSPROT Acc. F4JSE7]
AT3G50470	5,48E-06	3,20E-06	1,42	HR3	RPW8-like protein 3 [Uniprot/SWISSPROT Acc. Q9SCS7]
AT5G47910	1,28E-14	4,33E-15	1,42	RBOHD	Respiratory burst oxidase homolog protein D [Uniprot/SWISSPROT Acc. Q9FIJ0]

AT4G24290	1,21E-19	3,25E-20	1,41		MACPF domain-containing protein At4g24290 [Uniprot/SWISSPROT Acc. Q9STW5]
AT4G12720	1,85E-08	9,08E-09	1,40	NUDT7	NUDT7 [Uniprot/SPTREMBL Acc. A0A178V4N8]; Nudix hydrolase 7 [Uniprot/SPTREMBL Acc. F4JRE7]; Nudix hydrolase 7 [Uniprot/SWISSPROT Acc. Q9SU14]
AT4G19700	4,37E-08	2,19E-08	1,40	BOI	E3 ubiquitin-protein ligase BOI [Uniprot/SWISSPROT Acc. O81851]
AT3G45290	1,59E-05	9,63E-06	1,39	MLO3	MLO-like protein 3 [Uniprot/SWISSPROT Acc. Q94KB9]
AT1G64280	8,17E-19	2,27E-19	1,38	NPR1	Regulatory protein NPR1 [Uniprot/SWISSPROT Acc. P93002]
AT1G02860	1,46E-10	6,23E-11	1,33	BAH1	NLA [Uniprot/SPTREMBL Acc. A0A178WJE5]; E3 ubiquitin-protein ligase BAH1 [Uniprot/SWISSPROT Acc. Q9SRX9]
AT4G31300	1,03E-16	3,14E-17	1,28	PBA1	Proteasome subunit beta type [Uniprot/SPTREMBL Acc. A0A178V2B3]; Proteasome subunit beta type [Uniprot/SPTREMBL Acc. F4JRY2]; Proteasome subunit beta type-6 [Uniprot/SWISSPROT Acc. Q8LD27]
AT5G06100	1,00E-10	4,23E-11	1,28		Transcription factor [Uniprot/SPTREMBL Acc. Q8W1W6]; MYB family transcription factor-like [Uniprot/SPTREMBL Acc. Q9LHS6]
AT4G37980	1,56E-10	6,67E-11	1,20	CAD7	ELI3-1 [Uniprot/SPTREMBL Acc. A0A178V3X8]; Cinnamyl alcohol dehydrogenase 7 [Uniprot/SWISSPROT Acc. Q02971]
AT5G45260	5,94E-08	3,00E-08	1,19	RRS1	Disease resistance protein RRS1 [Uniprot/SWISSPROT Acc. P0DKH5]
AT1G29850	1,30E-11	5,21E-12	1,18		Double-stranded DNA-binding-like protein [Uniprot/SPTREMBL Acc. F4I355]; At1g29850/F1N18_19 [Uniprot/SPTREMBL Acc. Q9FXG0]
AT3G16770	3,63E-05	2,25E-05	1,18	RAP2-3	Ethylene-responsive transcription factor RAP2-3 [Uniprot/SWISSPROT Acc. P42736]
AT5G48030	3,18E-10	1,39E-10	1,12	GFA2	GFA2 [Uniprot/SPTREMBL Acc. A0A178UJR3]; Chaperone protein dnaJ GFA2, mitochondrial [Uniprot/SWISSPROT Acc. Q8GWW8]
AT1G12220	5,57E-09	2,63E-09	1,09	RPS5	Disease resistance protein RPS5 [Uniprot/SWISSPROT Acc. O64973]; Disease resistance protein [Uniprot/SPTREMBL Acc. Q56YM8]
AT1G30460	5,18E-07	2,80E-07	1,06	CPSF30	30-kDa cleavage and polyadenylation specificity factor 30 [Uniprot/SWISSPROT Acc. A9LNK9]
AT5G47120	2,72E-10	1,19E-10	1,05	BI-1	Bax inhibitor 1 [Uniprot/SWISSPROT Acc. Q9LD45]
AT3G46510	1,37E-08	6,63E-09	0,99	PUB13	U-box domain-containing protein 13 [Uniprot/SWISSPROT Acc. Q9SNC6]
AT5G23670	6,65E-08	3,38E-08	0,98	LCB2A	Long chain base biosynthesis protein 2a [Uniprot/SWISSPROT Acc. Q9LSZ9]
AT1G51660	2,90E-08	1,44E-08	0,98	MKK4	MKK4 [Uniprot/SPTREMBL Acc. A0A178WCC0]; Mitogen-activated protein kinase kinase 4 [Uniprot/SWISSPROT

					Acc. O80397]
AT2G43790	3,89E-09	1,82E-09	0,92	MPK6	Mitogen-activated protein kinase [Uniprot/SPTREMBL Acc. A0A178VTX8]; Mitogen-activated protein kinase 6 [Uniprot/SWISSPROT Acc. Q39026]
AT3G11440	0,0023217	0,00167909	0,89		Transcription factor [Uniprot/SPTREMBL Acc. Q9FR97]
AT1G02120	1,57E-05	9,47E-06	0,77	VAD1	VAD1 [Uniprot/SPTREMBL Acc. A0A178W223]; Protein VASCULAR ASSOCIATED DEATH 1, chloroplastic [Uniprot/SWISSPROT Acc. F4HVW5]
AT5G64930	4,76E-05	2,99E-05	0,76	CPR5	At5g64930 [Uniprot/SPTREMBL Acc. B4F7R3]; Protein CPR-5 [Uniprot/SWISSPROT Acc. Q9LV85]
AT5G54250	0,0085141	0,00648635	0,75	CNGC4	AT5G54250 protein [Uniprot/SPTREMBL Acc. B9DFK7]; Cyclic nucleotide-gated ion channel 4 [Uniprot/SPTREMBL Acc. F4K0A1]; Cyclic nucleotide-gated ion channel 4 [Uniprot/SWISSPROT Acc. Q94AS9]
AT2G47130	0,0021627	0,00156045	0,74	SDR3A	Short-chain dehydrogenase reductase 3a [Uniprot/SWISSPROT Acc. O80713]
AT3G56860	0,0003652	0,00024594	0,73	UBA2A	UBA2A [Uniprot/SPTREMBL Acc. A0A178VCS6]; UBP1-associated protein 2A [Uniprot/SWISSPROT Acc. Q9LES2]
AT5G17310	0,0033268	0,00243666	0,67	UGP1	UGP2 [Uniprot/SPTREMBL Acc. A0A178UCA6]; UTP--glucose-1-phosphate uridylyltransferase 1 [Uniprot/SPTREMBL Acc. F4KGY8]; UTP--glucose-1-phosphate uridylyltransferase 1 [Uniprot/SWISSPROT Acc. P57751]
AT2G17480	0,03248	0,02628418	0,61	MLO8	MLO-like protein 8 [Uniprot/SWISSPROT Acc. O22757]
AT2G26300	0,0026435	0,00192188	0,57	GPA1	GPA1 [Uniprot/SPTREMBL Acc. A0A178VY32]; Guanine nucleotide-binding protein alpha-1 subunit [Uniprot/SWISSPROT Acc. P18064]
AT4G36280	0,0023922	0,00173268	0,57	MORC2	Protein MICRORCHIDIA 2 [Uniprot/SWISSPROT Acc. Q5FV35]
AT3G25070	0,0354963	0,02884786	0,43	RIN4	RPM1-interacting protein 4 [Uniprot/SWISSPROT Acc. Q8GYN5]

Acknowledgements

My sincere gratitude and thanks are extended to my supervisor, Prof. Diana Bellin for her careful instruction, support, and supervision that she has delivered with much kindness and patience over the years.

I would like to thank Prof. Massimo Delledonne for his kind support of my Ph.D study, Dr. Elodie Vandelle for her discussion during my first year Ph.D study, Dr. Tengfang Ling for his instruct and care in life, Dr Jian Chen and Dr Jingjing Huang for their encouragement, Dr Zahra Imanifard for helping on ion leakage measurement, Pietro Delfino for helping me with the bioinformatics analysis, Xiaoyun lv for care in life.

I would also like to thank Prof. Luca Dall'Osto for sharing antibody with me, Dr. Linda Avesani for suggestion on agroinfiltration.

I would like to thank Dr. Alessandra Lanubile (Catholic University of the Sacred Heart) and Dr. Michela Zottini (University of Padova) for critically reading my thesis and for making many valuable suggestions.

Finally, I take this opportunity to thank my family members, my mother who always support me with her great and selfless love, my sisters for their great support and encouragement.